

Spring 2002

# Mechanism of activation of photoreceptor phosphodiesterase by transducin and by low molecular weight proteins

Angela W. Norton

*University of New Hampshire, Durham*

Follow this and additional works at: <https://scholars.unh.edu/dissertation>

---

## Recommended Citation

Norton, Angela W., "Mechanism of activation of photoreceptor phosphodiesterase by transducin and by low molecular weight proteins" (2002). *Doctoral Dissertations*. 76.  
<https://scholars.unh.edu/dissertation/76>

This Dissertation is brought to you for free and open access by the Student Scholarship at University of New Hampshire Scholars' Repository. It has been accepted for inclusion in Doctoral Dissertations by an authorized administrator of University of New Hampshire Scholars' Repository. For more information, please contact [nicole.hentz@unh.edu](mailto:nicole.hentz@unh.edu).

## INFORMATION TO USERS

This manuscript has been reproduced from the microfilm master. UMI films the text directly from the original or copy submitted. Thus, some thesis and dissertation copies are in typewriter face, while others may be from any type of computer printer.

**The quality of this reproduction is dependent upon the quality of the copy submitted.** Broken or indistinct print, colored or poor quality illustrations and photographs, print bleedthrough, substandard margins, and improper alignment can adversely affect reproduction.

In the unlikely event that the author did not send UMI a complete manuscript and there are missing pages, these will be noted. Also, if unauthorized copyright material had to be removed, a note will indicate the deletion.

Oversize materials (e.g., maps, drawings, charts) are reproduced by sectioning the original, beginning at the upper left-hand corner and continuing from left to right in equal sections with small overlaps.

Photographs included in the original manuscript have been reproduced xerographically in this copy. Higher quality 6" x 9" black and white photographic prints are available for any photographs or illustrations appearing in this copy for an additional charge. Contact UMI directly to order.

Bell & Howell Information and Learning  
300 North Zeeb Road, Ann Arbor, MI 48106-1346 USA  
800-521-0600

UMI<sup>®</sup>



**MECHANISM OF ACTIVATION OF PHOTORECEPTOR  
PHOSPHODIESTERASE BY TRANSDUCIN AND BY LOW MOLECULAR  
WEIGHT PROTEINS**

BY

ANGELA W. NORTON  
B.A., St. Olaf College, 1997

DISSERTATION

Submitted to the University of New Hampshire  
in Partial Fulfillment of  
the Requirements for the Degree of

Doctor of Philosophy  
in  
Biochemistry

May, 2002

UMI Number: 3045336

UMI<sup>®</sup>

---

UMI Microform 3045336

Copyright 2002 by ProQuest Information and Learning Company.  
All rights reserved. This microform edition is protected against  
unauthorized copying under Title 17, United States Code.

---

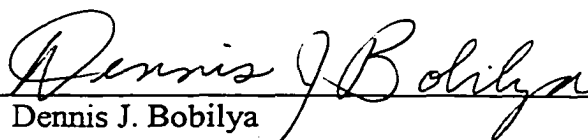
ProQuest Information and Learning Company  
300 North Zeeb Road  
P.O. Box 1346  
Ann Arbor, MI 48106-1346

This dissertation has been examined and approved.



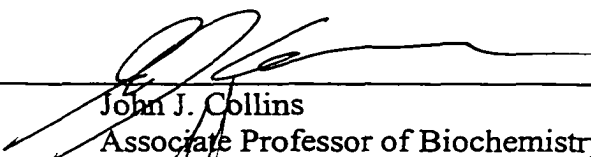
---

Dissertation Director, Dr. Richard H. Cote  
Associate Professor of Biochemistry



---

Dennis J. Bobilya  
Associate Professor of Animal and Nutritional Sciences



---

John J. Collins  
Associate Professor of Biochemistry



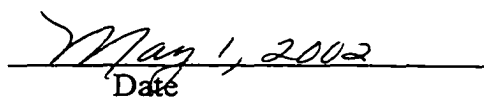
---

Thomas M. Laue  
Professor of Biochemistry



---

G. Eric Schaller  
Assistant Professor of Biochemistry



---

Date

## **DEDICATION**

I dedicate this thesis to my parents, Mary and Tom Norton. Their love, support, and encouragement throughout the years gave me the strength to fulfill this immense goal.

## ACKNOWLEDGEMENTS

I would like to thank all of my friends and family for being so understanding during the past five years while my life was dedicated to obtaining this degree.

I would like to thank my advisor, Rick Cote for his guidance throughout my graduate career. His thoroughness in completing each project has taught me to examine my work from many angles, allowing me to develop into a strong research scientist.

I would like to recognize my committee members, Dennis Bobilya, John Collins, Tom Laue and Eric Schaller for all of the research-stimulating ideas and constructive analysis of my thesis.

I would like to acknowledge each of the members of the lab who provided support and scientific discussions that aided in the completion of this research: Marc D'Amours, Rachel Collupy, Amy Daly, Tracy Hebert, Carmen Maftai, Hongmei Mou, Michael Paglia, Dana Pentia, Jen Terew, and Beverly Valeriani.

The work presented in this thesis was funded by a grant from the National Institute of Health (EY-05798), the New Hampshire Agricultural Experiments station, and the University of New Hampshire graduate summer teaching fellowship.



## TABLE OF CONTENTS

DEDICATION.....	iii
ACKNOWLEDGEMENTS.....	iv
LIST OF TABLES.....	vii
LIST OF FIGURES.....	viii
ABSTRACT.....	x

CHAPTER	PAGE
---------	------

### CHAPTER 1. INTRODUCTION

1. Retinal Diseases.....	1
2. Visual Transduction.....	2
3. Structure and Regulation of Photoreceptor Phosphodiesterase.....	9
4. Thesis Research Goals.....	16

### CHAPTER 2. MECHANISM OF TRANSDUCIN ACTIVATION OF FROG ROD PHOTORECEPTOR PHOSPHODIESTERASE: ALLOSTERIC INTERACTIONS BETWEEN THE INHIBITORY $\gamma$ SUBUNIT AND THE NONCATALYTIC cGMP BINDING SITES.

Summary .....	18
Introduction.....	19
Experimental Procedure.....	22

Results and Discussion.....	27
CHAPTER 3. ROLE OF THE 17 kDa $\delta$ PROTEIN AND IMMUNOLOGICALLY RELATED PROTEINS IN REGULATION OF PDE IN ROD PHOTORECEPTORS.	
Summary.....	53
Introduction.....	54
Experimental Procedure.....	57
Results and Discussion.....	63
Conclusions.....	79
CHAPTER 4. BINDING OF ROD OUTER SEGMENT PROTEINS TO PHOSPHODIESTERASE: POTENTIAL ROLES IN REGULATING VISUAL TRANSDUCTION.	
Summary.....	81
Introduction.....	82
Materials and Methods.....	88
Results and Discussion.....	94
Conclusions.....	110
SUMMARY.....	112
LIST OF REFERENCES.....	115

## LIST OF TABLES

CHAPTER 2		PAGE
Table 2.1	Equilibrium and Kinetic Parameters for High Affinity cGMP Binding to Frog PDE.....	29
Table 2.2	Summary of Maximal Activities for Various Preparations of Activated Frog PDE.....	45
CHAPTER 3		
Table 3.1	Content of $\delta$ and PDE in purified ROS.....	74
CHAPTER 4		
Table 4.1	Summary of $P\alpha\beta$ preparations.....	100

## LIST OF FIGURES

Figure	Title	Page
CHAPTER 1		
1.1	Excitation pathway for vision.....	3
1.2	Deactivation of rhodopsin.....	6
1.3	Structure of rod photoreceptor PDE.....	10
1.4	Proposed role of the $\delta$ protein.....	14
CHAPTER 2		
2.1	The kinetics of cGMP exchange at the noncatalytic sites of non-activated and transducin-activated PDE.....	31
2.2	Effects of exogenous $P\gamma$ on cGMP dissociation from noncatalytic sites and on the maximum extent of cGMP binding to nPDE and taPDE.....	34
2.3	$P\gamma$ content of membrane and supernatant fractions of frog ROS homogenates....	36
2.4	$P\gamma$ dissociation from transducin-activated PDE correlates with cGMP dissociation from noncatalytic binding sites.....	38
2.5	Endogenous $P\gamma$ binding to transducin-activated PDE correlates with titration of cGMP binding to the noncatalytic sites.....	40
2.6	The restoration of high affinity cGMP binding to PDE catalytic dimers by $P\gamma$ reveals two classes of binding sites.....	42
2.7	Stoichiometric $P\gamma$ inhibition of catalysis is observed with tPDE and $P\alpha\beta$ , but not with taPDE.....	48

2.8	Model for activation of rod photoreceptor PDE holoenzyme by transducin.....	50
-----	---	----

### CHAPTER 3

3.1	The frog $\delta$ sequence is homologous to other $\delta$ proteins.....	64
3.2	Frog $\delta$ releases PDE from ROS membranes.....	67
3.3	Frog $\delta$ binds to PDE upon releasing it from the disk membranes.....	68
3.4	$\delta$ decreases the ability of transducin to fully activate PDE.....	70
3.5	Little $\delta$ co-purifies with intact frog ROS.....	72
3.6	Localization of the $\delta$ protein in bovine retina .....	76
3.7	PDE does not associate tightly with the 36 kDa $\delta$ -immunoreactive protein.....	78

### CHAPTER 4

4.1	Time course of frog PDE trypsinization.....	92
4.2	Dilution of trypsinized PDE gives a higher maximum catalytic activity.....	96
4.3	Trypsinized PDE binds a fragment of $\gamma$ even after gel filtration chromatography purification.....	98
4.4	Extraction of endogenous $\gamma$ from frog ROS.....	102
4.5	Purification of recombinant $\gamma$ on reverse phase Sep Pak cartridges.....	103
4.6	Gel filtration of hypotonically extracted proteins from frog ROS membranes...	105
4.7	$\delta$ binding proteins from various ROS extracts.....	107
4.8	$\delta$ binding proteins in bovine ROS extracts.....	109

## **ABSTRACT**

### **MECHANISM OF ACTIVATION OF PHOTORECEPTOR PHOSPHODIESTERASE BY TRANSDUCIN AND BY LOW MOLECULAR WEIGHT PROTEINS**

by

Angela W. Norton

University of New Hampshire, May, 2002

Rod photoreceptor phosphodiesterase (PDE) is the central enzyme of visual transduction. PDE is a heterodimer ( $P\alpha\beta$ ) with two associated inhibitory  $\gamma$  subunits, and is bound to the disk membrane by isoprenyl groups. Each catalytic subunit contains a catalytic site and a high-affinity cGMP binding site. In this research, two independent mechanisms of PDE regulation are addressed. The first part examines transducin activation of PDE, focusing on the interactions between the  $\gamma$  subunits and  $P\alpha\beta$ . The second part examines the 17 kDa  $\delta$  protein believed to regulate bovine PDE. We found that transducin activation of PDE induces heterogeneity at the active sites as well as the cGMP binding sites, and that there is a strong correlation between cGMP binding and  $\gamma$  binding to PDE. The PDE activation induced by transducin is approximately half of the maximum rate of  $P\alpha\beta$  lacking bound  $\gamma$  inhibitory subunits. This research supports a model in which transducin interacts with  $\gamma$  bound to only one of the catalytic subunits. The relationship between cGMP and  $\gamma$  binding to PDE may play a role in light adaptation of rod photoreceptor cells.

The  $\delta$  protein is hypothesized to regulate adaptation of rod photoreceptor cells by  $\delta$  binding to the prenyl groups on PDE and releasing PDE from the disk membrane and thereby preventing activation by transducin. The frog homologue of the bovine 17 kDa  $\delta$  protein was identified in frog retina, but the amount of the  $\delta$  in rod cells was low ( $0.03 \pm 0.01$  mol  $\delta$  per mol PDE). This is consistent with frog PDE being >95% membrane-associated. Recombinant frog  $\delta$  bound to PDE and was able to release PDE from the membrane. The majority of the  $\delta$  in frog ROS is soluble, and the remainder does not co-purify with PDE when extracted from the membranes. Immunocytochemical evidence indicates that  $\delta$  localizes to the cone cells. We hypothesize that  $\delta$  may serve to direct the intracellular membrane trafficking for various prenylated proteins.

# CHAPTER 1

## INTRODUCTION

### 1. Retinal Diseases

#### Importance of vision research

A complete understanding of visual transduction is necessary to fight retinal diseases. Retinitis pigmentosa is the name given to a group of inherited retinopathies. Approximately 1 in 3500 people suffer from retinitis pigmentosa. The retina is the tissue at the back of the eye that includes the rod and cone photoreceptor cells. Rod photoreceptor cells are distributed across the retina. Cone photoreceptor cells are mostly located in the central region of the eye termed the macula. The majority of people with retinitis pigmentosa suffer from degeneration of their rod cells. This results in night-blindness as well as the loss of peripheral vision. As the disease progresses, cone cells are also affected, often leading to complete blindness (Phelan and Bok, 2000). It has been difficult to determine the exact cause of retinitis pigmentosa since several different factors can lead to the same symptoms. However, recent studies suggest that it is a genetic disease, but that environmental factors can influence the rate of progression of retinal degeneration.

Another common photoreceptor cell disease is macular degeneration. This is the degeneration of the macula, affecting mainly the cone cells. People suffering from macular degeneration gradually lose vision directly in front of them and loss of visual acuity occurs as the cone photoreceptors degenerate (Fong, 2000). For elderly



Americans, age-related macular degeneration is the major cause of non-treatable vision loss. The exact cause of age-related macular degeneration is still unknown. Loss of vision completely alters a persons lifestyle, prohibiting activities many people take for granted. For the elderly, the risk of losing independence and the inability to perform simple daily tasks is a severe concern. To combat the degeneration of photoreceptor cells seen in clinical studies, research must be done to understand the visual process. Once the mechanism of visual transduction in a healthy system is elucidated, the diseased state can be compared to see what occurred to cause the degeneration. This will allow the development of drugs to treat the specific problem that led to the loss of sight.

## **2. Visual Transduction**

### **Visual excitation**

Vertebrate photoreceptor cells are highly specialized neurons developed for visual transduction. There are two different types of photoreceptor cells: cones are for color detection and daylight vision, while rods are for vision in low levels of light. Although rod and cone photoreceptor cells have different roles, the cells are similar in their basic cellular function. Both consist of an inner segment containing the vegetative cellular machinery (nucleus, mitochondria, etc.) and an outer segment composed of an extensive membrane system. The large surface area of the outer segment membranes is the site for the protein components for the initial steps in vision. Though cellular morphology of rods and cones differs somewhat between the species, the central components of visual transduction are well conserved throughout the vertebrates. There are three main stages of the visual process: excitation, termination and adaptation.

Much is known about the excitation process of visual transduction, as it is the most well-studied of the G-protein coupled receptor pathways. A photon of light enters the cell and is absorbed by a chromophore located in the central region of the transmembrane receptor, rhodopsin (Figure 1.1). Upon light absorption, the chromophore, 11-cis retinal, undergoes a conformational change to all-trans retinal. This activates the receptor and catalyzes the exchange of GTP for GDP on the G-protein,

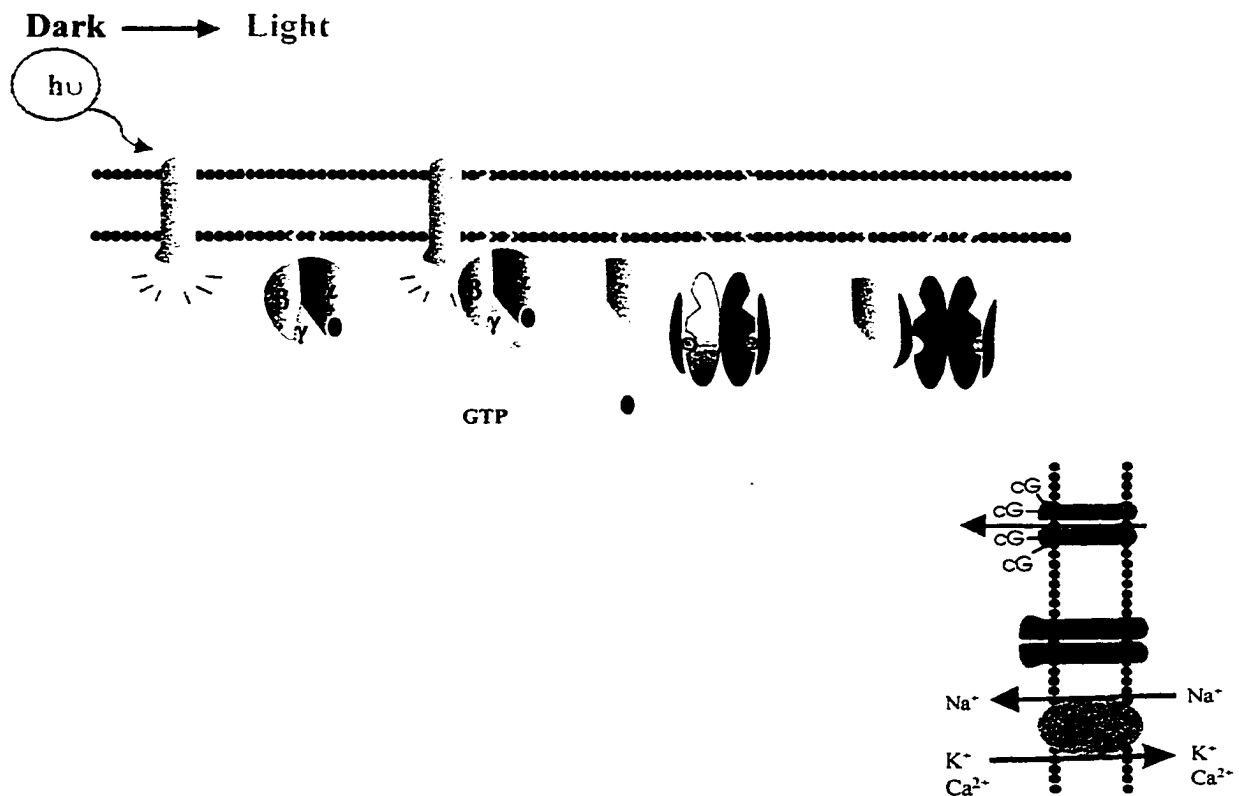


**Figure 1.1. Excitation pathway for vision.** The initial components for visual transduction are bound to the disk membranes of the outer segment of the cell. Light photoactivates rhodopsin, catalyzing the exchange of GTP for GDP on  $\text{T}\alpha$ .  $\text{T}\alpha$  dissociates and binds to PDE, leading to a drop in cGMP concentration in the cell. The cGMP-gated channels close and calcium levels drop, sending the light signal to the brain.

transducin. G-proteins are named for their high affinity interactions with guanine nucleotides and serve to transduce signals in many biochemical pathways. Transducin is composed of an  $\alpha$ ,  $\beta$ , and  $\gamma$  subunit, with the GTP binding site on the  $\alpha$  subunit (Arshavsky et al., 2002). The  $\alpha$ -subunit of transducin with bound GTP ( $T\alpha$ -GTP) dissociates from the transducin  $\beta\gamma$  subunits, then binds to and activates the effector enzyme, phosphodiesterase (PDE). PDE hydrolyzes guanosine 3', 5'-monophosphate (cGMP) to guanosine 5'-monophosphate (GMP), causing the total concentration of cGMP in the outer segment to drop. In response to the drop in cGMP, the cGMP bound to the cGMP-gated ion channels dissociates and the channels close (Mendez et al., 2001; Pugh, Jr. and Lamb, 2000).

The cGMP-gated ion channels allow for a steady influx of  $Na^+$  and  $Ca^{2+}$  into the outer segment of the photoreceptor cell. When photoreceptor cells are not exposed to light, there is a circulating current with  $Na^+$  and  $Ca^{2+}$  entering the outer segment of the cell through the cGMP-gated channel and exiting from the inner segment via a  $Na^+/K^+$ -ATPase pump. When the cGMP-gated channel closes due to light exposure,  $Ca^{2+}$ ,  $Na^+$ , and small amounts of  $Mg^{2+}$  are no longer able to enter the cell, but  $Ca^{2+}$  is still pumped out of the cell by the exchanger (Pugh, Jr. and Lamb, 2000). The decrease of positive ion influx into the cell causes the membrane potential to become more negative. This causes the cell to become hyperpolarized, transmitting the signal of light exposure to the synaptic terminal of the photoreceptor cell which communicates to many other classes of retinal neurons before passing to the optic nerve.

Rod photoreceptor cells are capable of detecting a single photon of light. This ability arises by two amplification steps that are intrinsically built into the visual

transduction pathway. The first amplification step occurs upon activation of rhodopsin. Once activated, rhodopsin catalyzes the activation of transducin and the G-protein is released, but rhodopsin remains active. Thus, a single activated rhodopsin can continue to activate ~100 transducin molecules until rhodopsin itself becomes deactivated. The second amplification step is the activation of PDE. A single  $T\alpha$ -GTP binds to PDE, allowing the hydrolysis of as many cGMP molecules as the enzyme encounters before  $T\alpha$  is deactivated and dissociates (Pugh, Jr. and Lamb, 2000; Mendez et al., 2001; Arshavsky et al., 2002). The amplification of the signal at these two steps allows for a very small stimulus to be reliably amplified and converted into a detectable signal to the nervous system.

### **Termination of the visual pathway**

As with many specialized pathways, termination of the activated signal of visual transduction is not merely the reverse of the activation mechanism. To turn off visual excitation, each of the two amplification steps must be separately blocked. The mechanism of deactivation of rhodopsin is very well known (Figure 1.2). The decrease in intracellular calcium levels upon light activation stimulates a  $Ca^{2+}$  feedback mechanism. Recoverin, a neuron-specific  $Ca^{2+}$ -binding protein with two bound  $Ca^{2+}$ , exists associated to rhodopsin kinase bound in the dark state. Light exposure greatly decreases the  $Ca^{2+}$  concentration, and the two  $Ca^{2+}$  bound to recoverin dissociate and release rhodopsin kinase from recoverin. Rhodopsin kinase is then available to phosphorylate distinct serine residues on rhodopsin. Phosphorylation of rhodopsin produces a binding site for arrestin, a 48 kDa protein that physically blocks the G-protein

activation site on rhodopsin to ensure transducin can no longer be activated (Pugh, Jr. and Lamb, 2000).

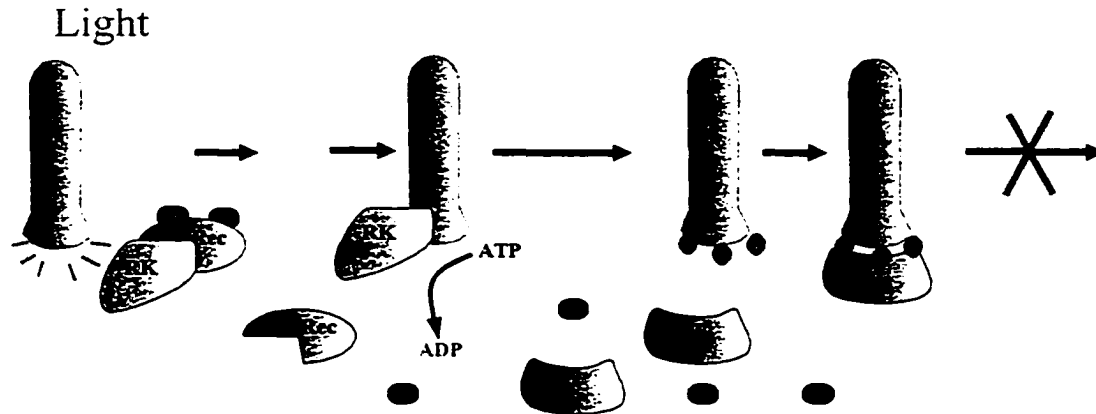


**Figure 1.2. Deactivation of rhodopsin.** The decrease in calcium levels induced by light exposure releases rhodopsin kinase from its association with recoverin. Rhodopsin kinase then phosphorylates distinct residues on the C-terminus of rhodopsin. Once the phosphorylation has taken place, arrestin will bind to rhodopsin, blocking the binding site of transducin and prohibiting further activation of the pathway.

After rhodopsin is deactivated, the chromophore dissociates from its ligand binding site on the rhodopsin receptor and is reduced to all-trans retinol. In this state, the pigment binds to an interphotoreceptor matrix retinoid binding protein (IRBP) which transports it to the retinal pigment epithelium. It can then be converted to 11-cis retinal and returned to the outer segment of the photoreceptors bound to IRBP to complete the cycle of pigment regeneration.

PDE activity must also be inhibited for termination of the visual response. PDE remains activated until hydrolysis of GTP to GDP on  $T\alpha$  occurs, allowing  $T\alpha$ -GDP to dissociate and rebind to  $T\beta\gamma$ . Recently it has been shown that GTPase activating proteins (GAP) work together to regulate the kinetics of transducin deactivation. To enhance hydrolysis of GTP, Regulator of G-protein Signaling 9 (RGS9) exists in a complex with type 5 G-protein  $\beta$  subunit ( $G\beta 5L$ ) and increases the intrinsic GTPase activity of

transducin (He et al., 1998). GAP proteins work by stabilizing the transition state of the G-protein (in this case  $T\alpha$ ) to favor GTP hydrolysis (Arshavsky et al., 2002).

Deactivation of  $T\alpha$  allows for the  $\gamma$  subunit to return to its tight association with PDE, blocking the catalytic site of the enzyme. *In vitro* studies have shown that  $\gamma$  released from  $P\alpha\beta$  further enhances the GTPase activity of transducin with RGS9 and  $G\beta 5L$  (Arshavsky and Bownds, 1992; He et al., 1998; Makino et al., 1999).

The final step to recovering the dark-adapted state of the cell is the production of cGMP. cGMP is formed by photoreceptor guanylate cyclase. In the dark, guanylate cyclase binds guanylate cyclase activating proteins (GCAPS). These are calcium binding proteins, that dissociate from guanylate cyclase when light activation decreases the  $Ca^{2+}$  in the cell. The release of the GCAPS from guanylate cyclase stimulates the production of cGMP, leading to recovery of the membrane potential.

### **Photoreceptor cell adaptation**

The final stage of the visual process is adaptation. Adaptation is the term used to describe how photoreceptor cells adjust their photoresponse based on the previous history of light exposure. When photoreceptor cells have been in the dark long enough for the transduction pathway to be completely turned off and the dark current restored, the dark-adapted state is reached. There are two types of light adaptation, background adaptation and bleaching adaptation. The photoreceptor cells must be able to recognize a change in light intensity when a background light exists, this is called light (or background) adaptation. Part of the adaptation mechanism is achieved by the two different types of photoreceptor cells. Rod photoreceptor cells are for the detection of very low levels of

light, down to a single photon. During the daytime, rod cells are completely saturated with light. Bleaching adaptation is a continuous activation of the pathway that is believed to be due to the presence of bleached pigment.

Background adaptation is composed of two phases; a rapid phase lasting only a few seconds, and a slow phase that occurs after tens of seconds of light exposure. The rapid phase of light adaptation is stimulated by the low  $\text{Ca}^{2+}$  levels in the outer segment arising from the closure of the cGMP-gated ion channels. This decrease in the  $\text{Ca}^{2+}$  levels stimulates guanylate cyclase-activating proteins, causing guanylate cyclase to produce cGMP which combats the drop in cGMP concentration due to PDE catalytic activity. Simultaneously, the low  $\text{Ca}^{2+}$  levels increase the affinity of cGMP for the cGMP-gated ion channels permitting them to open at lower cGMP concentrations. While the rapid phase of light adaptation occurs at all light intensities, the slow phase is observed only when the light intensity suppresses greater than 50% of the dark current. The actual cause of the slow phase of background adaptation is unknown, and the continued drop in  $\text{Ca}^{2+}$  could mean that this effect is also mediated by the overall  $\text{Ca}^{2+}$  in the outer segment of the photoreceptor cell, but not necessarily (Calvert et al., 2002; Burns and Baylor, 2001).

Bleaching adaptation is the ability of the rod photoreceptor cells to adjust to daytime saturation and recover for night vision. Rod photoreceptor cells exposed to bright light become desensitized, preventing them from further stimulation by light. It is well known that in order to recover from a bright flash of light, the cell must regenerate the visual pigment. However, throughout the time of the pigment regeneration, the cell behaves as though it is being continuously exposed to light, as the PDE remains active

and cGMP levels are low. The cause of this decrease in sensitivity is now believed to be due to the presence of bleached pigment in the cell. Rhodopsin is a protein containing a covalently bound chromophore, 11-cis-retinal. During the visual cycle of pigment regeneration, the light-activated all-trans-retinol must dissociate and be exported to the retinal pigment epithelium. Recent work suggests that the free opsin molecule (bleached pigment) is able to directly activate transducin, causing desensitization by maintaining the activated pathway (Melia, Jr. et al., 1997). The recovery of the sensitivity of the pathway occurs with the regeneration of the 11-cis-retinal, allowing dark adaptation, and the pathway is terminated until the next flash of light (Fain et al., 2001).

### **3. Structure and Regulation of Photoreceptor Phosphodiesterase**

#### **Structure and Function of PDE**

Due to its central role in the visual transduction pathway, PDE has been a major focus of research. There are eleven different members of the PDE superfamily that have been discovered thus far. All members of the PDE superfamily share sequence similarity in the region corresponding to the active site of the enzyme (SMART domain ID: HDc). The photoreceptor cell PDEs (both rod and cone) discussed here are designated as PDE6. Rod PDE is a heterodimeric protein composed of  $\alpha$  and  $\beta$  catalytic subunits ( $P\alpha\beta$ ). The catalytic subunits are tightly associated with inhibitory  $\gamma$  subunits (Figure 1.3). PDE6



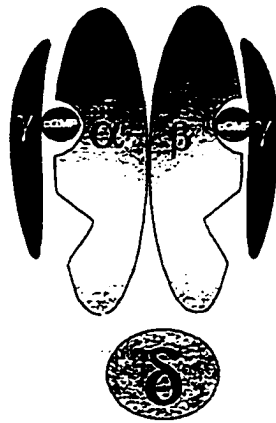


**Figure 1.3. Structure of rod photoreceptor PDE.** PDE is composed of two catalytic subunits,  $P\alpha\beta$ ; and two identical inhibitory subunits,  $\gamma$ .  $P\alpha$  and  $P\beta$  each contain a catalytic site for cGMP hydrolysis, as well as an N-terminal GAF domain that binds cGMP. PDE is attached to the membrane with isoprenyl groups. In mammalian ROS, 30% of the PDE exists in a soluble form bound with a bound  $\delta$  subunit.

subunits contain a C-terminal catalytic domain as well as a tandem pair of N-terminal GAF domains encoding for cGMP binding sites (Artemyev et al., 1998). PDE2, PDE5, PDE10 and PDE11 are members of the PDE superfamily that also contain GAF domains. PDE2 demonstrates cooperative behavior, such that cGMP binding at the noncatalytic sites stimulates cGMP hydrolysis at the catalytic site. Alternately, PDE5 shows allosteric regulation, where the cGMP binding sites control the accessibility of a phosphorylation site responsible for regulating the catalytic site (Martins et al., 1982; Yamamoto et al., 1983; Corbin et al., 2000). The exact role of the GAF domains on PDE10 and PDE11 are not well known.

Due to its importance in vision, research has focused largely on understanding how PDE6 is regulated. One mechanism of direct regulation that could occur is cooperation between the active sites and the noncatalytic cGMP binding sites as seen in

PDE2. However, up to this point no evidence has been found to show any direct control of photoreceptor PDE activity from cGMP binding to the noncatalytic sites (Arshavsky et al., 1992; Mou and Cote, 2001).

The C-terminal region of each of the catalytic subunits contains the consensus sequence (CaaX) for post translational modification by protein prenyltransferases. The  $\alpha$ -subunit is farnesylated and the  $\beta$  subunit is geranylgeranylated on the cysteine residue of the consensus sequence. Exposure of PDE6 to limited trypsin proteolysis cleaves off a portion of the C-terminus of the catalytic subunits, releasing them from their membrane-associated state. This suggests that prenylation of the catalytic dimer is necessary for membrane binding (Ong et al., 1989; Catty and Deterre, 1991), a mechanism that is often used in signal transduction pathways. In vision, the coupling of PDE6 to the membrane ensures that the PDE is localized near transducin and can be quickly activated by light exposure. In mammalian ROS up to 30% of the PDE is soluble with a bound  $\delta$  protein (Gillespie et al., 1989). It is believed that  $\delta$  may play a role in adaptation by uncoupling PDE from transducin activation (see below).

In a dark-adapted photoreceptor cell, PDE6 exists with two tightly associated  $\gamma$  subunits (Cote, 2000).  $\gamma$  binds to the catalytic dimer with very high affinity ( $K_d < 10$  pM) (Wensel and Stryer, 1986) and inhibits cGMP hydrolysis by physically blocking the active site (Takemoto et al., 1993; Artemyev et al., 1998). The high affinity interaction of  $\gamma$  is through the central region of the protein (residues 24–45) whereas the C-terminal region of the protein inhibits cGMP hydrolysis (Mou and Cote, 2001).

There are many fewer cone cells than rod cells in the majority of vertebrate retinas. Thus, less is known about cone PDE because it is difficult to obtain purified

biochemical amounts of the enzyme to study. Sequence analysis shows that cone PDE exists as a homodimer of  $\alpha'$  subunits. Each of these catalytic subunits contains an active site for cGMP hydrolysis and at least one noncatalytic cGMP binding site. Similar to rod PDE, the catalytic activity of cone PDE is regulated by the binding of two inhibitory  $\gamma'$  subunits. There is still a lot of work that needs to be done to characterize cone PDE and understand how it is regulated *in vivo*.

### **$\gamma$ release from $P\alpha\beta$ upon transducin activation**

There is some debate as to the interactions of the PDE subunits upon transducin activation of PDE. In bovine PDE,  $\gamma$  has such a high affinity for one of the catalytic subunits that cGMP is not readily exchanged from one of the noncatalytic binding sites. However, frog PDE contains two exchangeable cGMP binding sites at all times. It is well known that there is a highly cooperative relationship between occupation of the cGMP binding sites and  $\gamma$  binding affinity. Experimental manipulations can remove most  $\gamma$  from its association with  $P\alpha\beta$  when PDE is activated by  $T\alpha$ -GTP in the absence of cGMP. It remains to be seen whether cGMP levels in the outer segment drop low enough to allow  $\gamma$  to be released from  $P\alpha\beta$  during the visual process. The specifics of  $\gamma$  release from  $P\alpha\beta$  occurring *in vivo* are further examined in this thesis. If  $\gamma$  is released *in vivo*, it could serve an important function, since free  $\gamma$  binds to RGS9 to stimulate GTP hydrolysis on transducin, thereby causing  $T\alpha$ -GDP to dissociate from  $\gamma$  leading to termination of visual transduction (Arshavsky and Bownds, 1992; Calvert et al., 1998; Makino et al., 1999). Thus, one could envision the dissociation of  $\gamma$  being involved in

light or bleaching adaptation, by reducing cGMP hydrolysis and thus reducing expenditure of metabolic energy.

### **Regulation of PDE6 by phosphorylation**

One line of current research is looking at whether phosphorylation of the  $\gamma$  subunit of PDE serves to regulate PDE. When  $\gamma$  is free from association with  $P\alpha\beta$ , it can also serve as a substrate for phosphorylation *in vitro*. Previous research suggested that when  $\gamma$  is phosphorylated, it inhibits PDE catalysis stronger than the unphosphorylated form (Xu et al., 1998; Tsuboi et al., 1994; Hayashi et al., 2000; Udovichenko et al., 1994). However, more recent results contradict this finding. Instead, they propose that once phosphorylation of  $\gamma$  occurs, it is no longer capable of binding to  $T\alpha$ -GTP. Thus, the phosphorylated  $\gamma$  will reassociate with  $P\alpha\beta$  without binding to any alternative  $T\alpha$ -GTP molecules that may be present, thus speeding up the recovery phase of the pathway (Paglia et al., 2002). This would be important, as the stoichiometry of  $T\alpha$  to PDE is 12 to one, respectively in ROS (Arshavsky et al., 2002). Another hypothesis is that phosphorylation of  $\gamma$  actually serves to regulate an alternate pathway located in the rod outer segment. If  $\gamma$  does indeed get released from PDE due a large decrease in the cGMP concentration, it would then make an excellent substrate for phosphorylation. Since this soluble, phosphorylated  $\gamma$  cannot bind to  $T\alpha$ , it would be available for interacting with proteins from another signal transduction pathway. However, at this point it is still unclear as to whether or not significant levels of  $\gamma$  phosphorylation occur *in vivo*.

The phosphorylation of  $P\alpha\beta$  is also being examined as a mechanism of enzyme regulation, but the importance of this has not yet been completed. PDE5 has been shown

to be regulated by phosphorylation of its catalytic subunits such that when cGMP is bound to the noncatalytic sites, PDE5 is more likely to be phosphorylated (Corbin et al., 2000). The likelihood of PDE6 being phosphorylated *in vivo* and the effect of this phosphorylation are currently being examined.

### **A 17 kDa $\delta$ protein is a putative subunit of PDE6**

PDE is likely to be regulated by other proteins located in the outer segment. In bovine ROS, a 17 kDa  $\delta$  subunit solubilizes PDE from the membrane such that ~30% of bovine rod PDE exists off in the cytosol (Gillespie et al., 1989; Florio et al., 1996). This  $\delta$  protein is conserved among mammals showing a 96% sequence identity. Similar proteins have also been found in amphibians (80% identity) as well as *C. elegans* (70% identity) and *D. melanogaster* (60% identity) (Florio et al., 1996; Li and Baehr, 1998; Li et al., 1998; Lorenz et al., 1998; Adams et al., 2000). The proposed role of  $\delta$  is to regulate PDE by removing it from the rod disk membranes and away from membrane-bound association with transducin (Figure 1.4) (Cook et al., 2001).

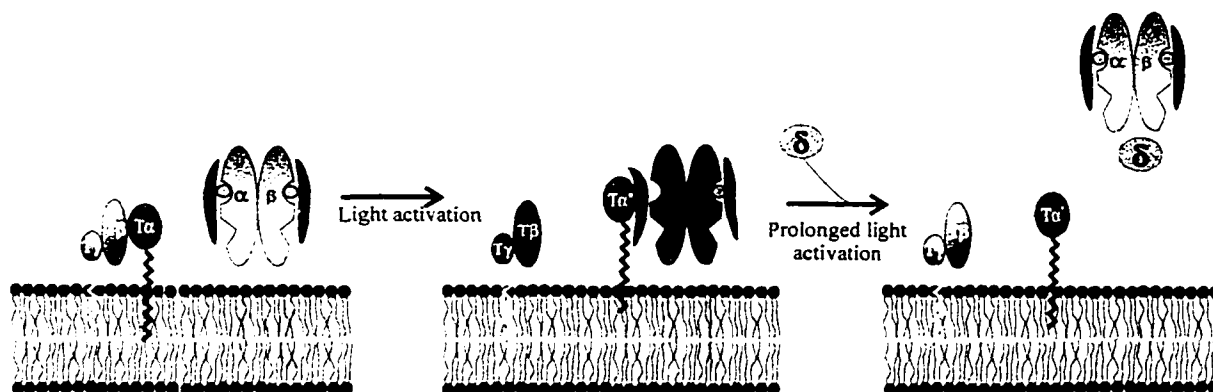


Figure 1.4. Proposed role of the  $\delta$  protein. Upon light exposure, T $\alpha$ -GTP dissociates from T $\beta\gamma$ , and binds to PDE causing activation. When light activation is prolonged,  $\delta$  binds to PDE at the C-terminus and releases it from the membrane, leaving T $\alpha$ -GTP bound by its myristoyl group to the disk membrane.

The interaction between PDE and  $\delta$  is believed to occur at the C-terminus of the catalytic subunits, and to involve the isoprenyl groups which attach PDE to the membrane. Trypsinized PDE, lacking the C-terminus of the catalytic subunits, does not bind to  $\delta$ . In addition, release of PDE from the disk membranes can be blocked by peptides containing a small sequence from the PDE C-terminus. PDE solubilized by  $\delta$  contains a higher level of carboxymethylation than the PDE that remains membrane-bound (Cook et al., 2000).

Besides altering membrane association,  $\delta$  also regulates PDE by altering cGMP binding to the noncatalytic sites (Mou et al., 1999). In bovine PDE, the interaction of the  $\gamma$  subunit with one of the catalytic subunits is so tight that the cGMP is not released. Addition of  $\delta$  to this membrane-associated PDE both releases the enzyme from the membrane and allows cGMP to be exchanged from both of the noncatalytic cGMP binding sites. However, it is still unclear whether  $\delta$  plays a role in regulating PDE *in vivo*.

### **Regulation of PDE by GARP**

Another protein believed to interact with PDE and decrease its catalytic activity is GARP (glutamic acid-rich protein). Research suggests that GARP serves to prevent cGMP hydrolysis when rod photoreceptor cells are completely saturated with light (Körschen et al., 1999). GARP binds to PDE, and is hypothesized to compete with  $T\alpha$ -GTP thereby reversing transducin activation of PDE. The interaction of PDE with other photoreceptor proteins is currently being examined. It is possible that there exists a

signaling complex for proteins involved in visual transduction, similar to the inactivated complex found in *Drosophila*. As there are many proteins in the outer segment of rod photoreceptor cells, it is likely that some proteins regulating visual transduction have not yet been discovered.

#### **4. Thesis research goals**

##### **Model for vision research**

Due to the conservation of rod photoreceptor proteins in the visual pathway, the species used for research does not often matter. Most of the work done to date used bovine photoreceptor cells because they are available in large quantities from slaughterhouses. The concern arises in that bovine retinas obtained from the slaughterhouses are light-adapted, and the conditions of retinal isolation are not under the control of the investigator. Thus, in order to make a more physiological assessment of the visual transduction pathway, the common bullfrog (*Rana catesbeiana*), is often used. The animals are easy to maintain in a controlled light environment, and all aspects of retinal isolation and light exposure can be controlled. In this way, preparations of dark-adapted purified ROS can be isolated and used to compare the biochemical pathways of the rod outer segment to the well characterized electrical responses of the same cell preparation.

##### **Goal of thesis research**

This research focuses on the regulation of rod PDE through cGMP,  $P\gamma$ ,  $T\alpha$  or  $\delta$  binding. The first section of the thesis examines a complete characterization of frog

PDE, observing catalytic rates as well as cGMP association, dissociation and equilibrium binding to the noncatalytic sites. The correlation between cGMP binding to the noncatalytic sites and  $\gamma$  binding to PDE was studied in more detail as well. Each of these pieces combined to form a model describing transducin activation of PDE in physiologically competent frog ROS. The second section of the thesis deals with the regulation of PDE by the  $\delta$  protein in frog ROS. The *in vivo* levels of the  $\delta$  protein in frog ROS was measured under several illumination conditions. For comparison to previous studies in bovine ROS, the *in vitro* effect of frog  $\delta$  on PDE was also measured. Co-purification of  $\delta$  and PDE was examined to test the possibility that delta or delta-like proteins interact with PDE to regulate visual transduction. The final part of this thesis contains research that addresses PDE-binding proteins. Much of this section focuses on the  $\gamma$  subunit of PDE, but the existence of other PDE-binding proteins is also explored. These experiments were preliminary studies that evolved into projects studied by myself or other lab members. Some of these observations may be used for future research in the lab.



## CHAPTER 2

### MECHANISM OF TRANSDUCIN ACTIVATION OF FROG ROD PHOTORECEPTOR PHOSPHODIESTERASE: ALLOSTERIC INTERACTIONS BETWEEN THE INHIBITORY $\gamma$ SUBUNIT AND THE NONCATALYTIC cGMP BINDING SITES<sup>1</sup>

#### Summary

The rod photoreceptor phosphodiesterase (PDE)<sup>2</sup> is unique among all known vertebrate PDE families for several reasons: it is a catalytic heterodimer ( $\alpha\beta$ ), it is directly activated by a G-protein, transducin, and its active sites are regulated by inhibitory  $\gamma$  subunits. Rod PDE binds cGMP at two noncatalytic sites on the  $\alpha\beta$  dimer but their function is unclear. We show that transducin activation of frog rod PDE introduces functional heterogeneity to both the noncatalytic and catalytic sites. Upon PDE

---

<sup>1</sup> This paper was published in the Journal of Biological Chemistry: Norton, A. W., D'Amours, M. R., Grazio, H. J., Hebert, T. L., and Cote, R. H. (2000) *J.Biol.Chem.* **275**, 38611-38619. This work was supported by National Institute of Health Grant EY-05798 (to R. H. C.). This paper is scientific contribution 2058 from the New Hampshire Agricultural Experiment Station.

<sup>2</sup> The abbreviations used are: PDE, phosphodiesterase (EC 3.1.4.35); PDE6, retinal photoreceptor PDE;  $P\alpha\beta$ , catalytic heterodimer of PDE;  $P\gamma$ , inhibitory 10 kDa  $\gamma$  subunit of rod PDE;  $\alpha_t$ ,  $\alpha$ -subunit of the rod photoreceptor G-protein, transducin; ROS, rod outer segments; SDS-PAGE, sodium dodecyl sulfate polyacrylamide gel electrophoresis; nPDE, nonactivated PDE; tPDE, trypsin-activated PDE; taPDE, transducin-activated PDE;  $GTP\gamma S$ , guanosine 5'-O-[3-thiotriphosphate],  $\alpha_t$ - $GTP\gamma S$ , activated form of  $\alpha_t$ ;  $k_{cat}$ , turnover number for activated PDE (units: cGMP hydrolyzed per s) based on the  $P\alpha\beta$  dimer concentration; PDE1, calcium-calmodulin-dependent PDE.

activation, one noncatalytic site is converted from a high affinity to low affinity state, while the second binding site undergoes modest decreases in binding affinity. Addition of  $\gamma$  to transducin-activated PDE can restore high affinity binding as well as reducing cGMP exchange kinetics at both sites. A strong correlation exists between cGMP binding and  $\gamma$  binding to activated PDE: dissociation of bound cGMP accompanies  $\gamma$  dissociation from PDE, while addition of either cGMP or  $\gamma$  to  $\alpha\beta$  dimers can restore high affinity binding of the other molecule. At the active site, transducin can activate PDE to about one-half the turnover number for catalytic  $\alpha\beta$  dimers completely lacking bound  $\gamma$  subunit. These results suggest a mechanism in which transducin interacts primarily with one PDE catalytic subunit, releasing its full catalytic activity as well as inducing rapid cGMP dissociation from one noncatalytic site. The state of occupancy of the noncatalytic sites on PDE determines whether  $\gamma$  remains bound to activated PDE or dissociates from the holoenzyme, and may be relevant to light adaptation in photoreceptor cells.

### **Introduction**

Initiation of the phototransduction cascade in vertebrate rod photoreceptors by light results in the sequential activation of the visual pigment (rhodopsin), the photoreceptor G-protein (transducin), and the effector enzyme (cGMP phosphodiesterase, PDE)[for reviews, see ref. (Stryer, 1991; Pugh, Jr. and Lamb, 1993; Helmreich and Hofmann, 1996; Arshavsky and Pugh, Jr., 1998)]. The PDE present in rod and cone photoreceptors (classified as PDE6) differs in several ways from other classes of mammalian phosphodiesterases (Loughney et al., 1996; Manganiello and Degerman, 1999; Soderling and Beavo, 2000): rod photoreceptor PDE forms a catalytic dimer from

two closely related  $\alpha$  and  $\beta$  subunits ( $P\alpha\beta$ ); rod and cone PDE are directly regulated via heterotrimeric G-proteins; the catalytic constant ( $k_{cat}$ ) for rod PDE is ~1000-fold greater than for any other class of PDE; the catalytic activity of photoreceptor PDE is potently inhibited by binding of an inhibitory  $\gamma$  subunit ( $P\gamma$ ) [for reviews, see ref. (Takemoto et al., 1993; Artemyev et al., 1998)].

Transducin activation of PDE results from binding of the activated transducin  $\alpha_t$  subunit ( $\alpha_t$ -GTP) to one or more sites on the PDE holoenzyme. One result of this interaction is the displacement of the inhibitory  $P\gamma$  subunit from its binding site in the catalytic pocket of PDE. It is not clear, however, whether each PDE catalytic subunit binds  $P\gamma$  with equal affinity, whether  $\alpha_t$ -GTP can activate each catalytic site equally well, and under what conditions the  $\alpha_t$ -GTP- $P\gamma$  complex dissociates from  $P\alpha\beta$ . Conflicting results reported by different laboratories may reflect underlying differences in how the phototransduction components were isolated and studied, as well as species differences in the protein-protein interactions of transducin and PDE (Yamazaki et al., 1983; Wensel and Stryer, 1986; Bennett and Clerc, 1989; Bennett et al., 1989; Whalen and Bitensky, 1989; Yamazaki et al., 1990; Wensel and Stryer, 1990; Clerc and Bennett, 1992; Clerc et al., 1992; Otto-Bruc et al., 1993; Bruckert et al., 1994; Dumke et al., 1994; D'Amours and Cote, 1999; Berger et al., 1999; Melia et al., 2000).

Comparison of the amino acid sequence of photoreceptor PDE with PDE2, PDE5, PDE10 and PDE11 reveals the presence of GAF domains (Aravind and Ponting, 1997) in the N-terminal half of each PDE that encode noncatalytic cGMP binding sites (Charbonneau et al., 1990; McAllister-Lucas et al., 1993; Manganiello and Degerman, 1999; Soderling and Beavo, 2000; Fawcett et al., 2000; Yuasa et al., 2000). In the case of

PDE2, cGMP binding to these noncatalytic sites directly stimulates cyclic nucleotide hydrolysis at the active site (Martins et al., 1982; Yamamoto et al., 1983). For PDE5, the noncatalytic sites allosterically regulate accessibility of a phosphorylation site that alters catalytic activity (Burns et al., 1992; Turko et al., 1998; Corbin et al., 2000). The possible regulatory function for the low affinity, noncatalytic sites on PDE10 is not known, nor is it known whether the GAF domains in PDE 11 represent functional cGMP binding sites.

Since the initial findings by Yamazaki et al. (Yamazaki et al., 1980; Yamazaki et al., 1982) that cGMP bound with high affinity to rod photoreceptor PDE, several possible roles for the noncatalytic sites on rod PDE have been proposed. One hypothesis is that cGMP occupancy of the noncatalytic sites on PDE affects the strength of the interaction between the inhibitory  $P\gamma$  subunit and  $P\alpha\beta$  [reviewed in ref. (Artemyev et al., 1998)]. It has also been proposed that changes in cGMP binding affinity to the noncatalytic sites during visual transduction might permit the release of bound cGMP to accelerate the restoration of cGMP levels during the recovery phase of the photoresponse (Cote and Brunnock, 1993; Yamazaki et al., 1996a). Finally, the idea that the noncatalytic sites on photoreceptor PDE might directly regulate hydrolysis of cGMP at the active site (as is the case for PDE2) has not been supported by current evidence (Arshavsky et al., 1992; D'Amours and Cote, 1999).

In this paper, we characterize the properties of non-activated, transducin-activated, and catalytic dimers of PDE, all derived from suspensions of purified amphibian rod outer segments, in order to provide a detailed account of the changes that occur at the catalytic and noncatalytic domains of PDE upon light activation of the phototransduction cascade. We demonstrate a direct correlation between occupancy of

cGMP at the noncatalytic sites of PDE and the state of association of the inhibitory  $P\gamma$  subunit. Our results are consistent with transducin activation reducing cGMP binding affinity primarily at one of the two high-affinity, noncatalytic sites on PDE. Furthermore, transducin activation of PDE cannot achieve the maximum catalytic potential of PDE that is observed when the  $P\gamma$  subunits are completely removed from the  $P\alpha\beta$  catalytic dimer. These changes in the noncatalytic and catalytic sites upon transducin activation are mediated through changes in  $P\gamma$  interaction with  $P\alpha\beta$  upon binding of transducin to PDE. The coordinated, allosteric regulation of cGMP and  $P\gamma$  binding to  $P\alpha\beta$  upon transducin activation operate too slowly to play a role in the rapid events of rod phototransduction (i.e., excitation and recovery), but may be important in more slowly developing aspects of light adaptation.

### **Experimental Procedure**

*Materials.* Frogs (*Rana catesbeiana*) were obtained from Niles Biologicals. [ $^3\text{H}$ ]cGMP was from NEN Life Science Products. Membranes for filter binding assays were obtained from Millipore. Reagents, substrates and nitrocellulose membranes for immunoblotting were from Pierce Chemical Co. or from Bio-Rad. Silicone oils for centrifugal separation were obtained from the William F. Nye Co. All other chemicals were obtained from Sigma.

*Preparation of Frog Rod Outer Segments (ROS) and recombinant bovine rod PDE inhibitory  $\gamma$  subunit ( $P\gamma$ ).* Osmotically intact frog ROS were purified on a discontinuous Percoll density gradient exactly as described in ref. (Cote, 2000). Purified

ROS were homogenized in Buffer A [containing: 77 mM KCl, 35 mM NaCl, 2.0 mM MgCl<sub>2</sub>, 1.0 mM CaCl<sub>2</sub>, 10 mM HEPES (pH 7.5), 2 mM dithiothreitol, 1 mM 4-(2-aminoethyl)-benzenesulfonyl fluoride, 5 μM leupeptin, and 1 μg/ml pepstatin] following the method of Dumke et al. (Dumke et al., 1994). Homogenized ROS were incubated in the dark at room temperature for 20-30 min to allow endogenous nucleotide hydrolases to degrade cGMP and GTP levels prior to experimental manipulations. Following depletion of nucleotides and determination of the rhodopsin concentration by difference spectroscopy (Bownds et al., 1971), ROS samples were exposed to light for subsequent steps (unless otherwise noted). The PDE concentration in ROS homogenates was determined by its ability to bind a maximum of 2 mol cGMP per mol holoenzyme in its non-activated state when supplemented with stoichiometric amounts of exogenous Py (see (Cote, 2000) for details).

Subcellular fractionation of ROS homogenates was typically performed by centrifuging samples for 1-3 min at 30 psig (110,000 x g<sub>av</sub>) at room temperature using a Beckman Airfuge. We verified that the integral membrane protein, rhodopsin, was present in the supernatant at undetectable levels and that >95% of the total rhodopsin could be recovered in the membrane pellet under these conditions.

Recombinant bovine rod Py was expressed in *E. coli* and purified to >97% purity as described in ref. (Granovsky et al., 2000). The Py concentration was determined spectrophotometrically using an experimentally determined extinction coefficient of 7550 OD M<sup>-1</sup> (Cote, 2000). The inhibitory activity of purified Py was assayed by its ability to stoichiometrically inhibit trypsin-activated bovine rod PDE (Mou et al., 1999); the

spectrophotometric and activity estimates of  $P\gamma$  concentration agreed to within 10% for all  $P\gamma$  preparations used in this study.

*PDE preparations used in this study.* Since PDE6 is the only detectible isoform of phosphodiesterase in purified ROS, no additional purification of the rod PDE was required. Non-activated PDE (nPDE) was obtained directly from nucleotide-depleted ROS homogenates; in the absence of GTP, dark-adapted and light-exposed ROS homogenates show no difference in the rate of cGMP hydrolysis or in the extent of cGMP binding. The catalytic activity of nPDE was typically 1-3% of the activated rate at the concentrations used in this paper (D'Amours and Cote, 1999). Transducin-activated PDE (taPDE) was prepared by incubating nucleotide-depleted ROS homogenates ( $[PDE] \geq 12$  nM; see (Dumke et al., 1994)) with an excess of GTP $\gamma$ S relative to the transducin concentration [ $\sim 30$  transducins per PDE; (Hamm and Bownds, 1984)]. Trypsinized PDE (tPDE), in which the  $P\gamma$  subunits are proteolytically digested to relieve their inhibitory constraint (Hurley and Stryer, 1982), was prepared by incubating ROS homogenates with TPCK-treated trypsin, followed by addition of a 6-fold molar excess of soybean trypsin inhibitor. The time course and concentration dependence of activation was closely followed to determine the minimum exposure of PDE to the protease yielding full activation (see Results). Excessive proteolysis of PDE leads to a gradual loss in the maximal catalytic activity, as well as irreversible damage to the noncatalytic sites. We prepared PDE heterodimers ( $P\alpha\beta$ ) depleted of  $P\gamma$  by modifying the original method of Yamazaki et al. (Yamazaki et al., 1990): nPDE was incubated with GTP $\gamma$ S for 60 min at 4° to allow  $P\gamma$  to dissociate from  $P\alpha\beta$ , and then centrifuged in the Airfuge to pellet ROS

membranes. The supernatant was discarded and the ROS membrane treated with GTP $\gamma$ S once more to further release membrane-bound Py. Following the second centrifugation, ROS membranes retained all of the original P $\alpha\beta$  content, but only 10-35% of the original Py (depending on the individual preparation). [The content of  $\alpha_t$  in GTP $\gamma$ S-washed ROS membranes was also reduced to <30% of its concentration in ROS homogenates, as judged by immunoblot analysis with anti- $\alpha_t$  antibodies.] P $\alpha\beta$  was used immediately following its preparation, because the enzyme was unstable once most of the Py had been removed. Only preparations containing <25% of the original Py content (i.e., < 0.5 Py per PDE) were used in experiments employing P $\alpha\beta$ . Efforts to completely eliminate Py from our P $\alpha\beta$  preparations were unsuccessful.

*Binding of cGMP to noncatalytic sites on PDE.* Because PDE is the only rod photoreceptor protein that binds cGMP with high affinity ( $K_D < \mu\text{M}$ ) (Cote and Brunnock, 1993; Cote et al., 1994), we were able to measure changes in binding occupancy at the noncatalytic sites of PDE in unfractionated ROS homogenates. For most experiments, a cGMP filter binding assay (Cote, 2000) was used to quantify binding of [ $^3\text{H}$ ]cGMP to high affinity sites on PDE. Inclusion of zaprinast or E4021 (D'Amours et al., 1999) with the [ $^3\text{H}$ ]cGMP solution during the filter binding assay prevented cGMP breakdown during the incubation with nPDE or activated PDE. In some experiments, the cGMP binding reaction was halted by addition of ice-cold 95% saturated ammonium sulfate (Cote, 2000) prior to membrane filtration of the quenched samples.

In order to directly correlate cGMP binding with Py binding to activated PDE (shown in Figure 2.4), we employed a centrifugal separation assay through a silicone oil



layer that partitions free [<sup>3</sup>H]cGMP from bound nucleotide (Forget et al., 1993; Cote, 2000). Portions (10 µl) of ROS homogenates were layered on top of 100 µl of silicone oil (density, 1.020 g/ml) in a 5 x 20 mm centrifuge tube (Beckman) at 4°. The tubes were spun at room temperature for 3 min at 110,000 x g<sub>av</sub>. Supernatants remaining above the oil layer were removed and processed for immunoblot analysis of Pγ concentration. The pellets were resuspended and one portion analyzed for Pγ content, while the other portion was used to quantitate bound [<sup>3</sup>H]cGMP.

*Quantitative immunoblot analysis of Pγ concentration in ROS.* Samples for Pγ analysis were added to electrophoresis sample buffer, and then subjected to sodium dodecyl sulfate-polyacrylamide gel electrophoresis (SDS-PAGE). After electrophoretic transfer to a 0.45 µm nitrocellulose membrane, the presence of Pγ was detected with an affinity-purified rabbit polyclonal antibody (UNH9710-4P; 1:15,000 dilution) specific for amino acid residues 63-87 of bovine rod Pγ. [Frog (*Rana pipiens*) Pγ has an identical amino acid sequence to bovine Pγ in this region; Wolfgang Baehr, personal communication.] Binding of the Pγ antibody was determined using a goat anti-rabbit antibody coupled to horseradish peroxidase (1:4000 dilution), followed by incubation of the membrane with substrate (SuperSignal West Pico Chemiluminescent Substrate, Pierce) and luminescent detection on film (Kodak BioMax Light). The intensity of the Pγ immunoreactive bands was recorded using a scanner and analyzed using the image analysis program, Quantiscan (Biosoft). The concentration of Pγ in ROS samples was calculated by comparison to a standard curve generated with known amounts (0.5 – 15 ng) of recombinant Pγ on the same blot, as described in detail elsewhere (Cote, 2000).

*PDE activity assay.* The rate of cGMP hydrolysis catalyzed by non-activated and activated forms of PDE was measured by a coupled-enzyme phosphate release assay, as described in detail in ref. (Cote, 2000). Activity measurements were made in the following buffer: 100 mM Tris, 10 mM MgCl<sub>2</sub>, 0.5 mM EDTA, 2 mM dithiothreitol, 0.5 mg/ml bovine serum albumin, pH 7.5. In all cases, rate measurements were obtained from at least three individual time points at saturating cGMP concentrations (10 mM), during which time less than 30% of the substrate was consumed.

*Other methods.* SDS-PAGE was performed by the method of Laemmli in 15% acrylamide gels (Laemmli, 1970). The immunoblotting protocol closely followed standard procedures (Gallagher, 1998). Fitting of PDE activity data was carried out with nonlinear regression analysis using Sigmaplot. Equilibrium binding data as well as the kinetics of cGMP association and dissociation were analyzed as described in ref. (Cote, 2000); in all cases, statistical comparisons of one-site versus two-site fits were carried out using KELL (Biosoft) to determine whether PDE exhibited one or two distinct classes of cGMP binding sites.

## **Results and Discussion**

*Transducin activation of PDE converts one class of noncatalytic sites to a low affinity, rapidly exchanging state.* While it has been reported that transducin activation of photoreceptor PDE leads to changes in cGMP binding to the noncatalytic sites of the enzyme, the regulatory and physiological significance of this process is not well understood. A previous study reported that transducin activation of PDE accelerated

cGMP exchange and reduced the binding affinity of cGMP to the noncatalytic sites on the enzyme without a significant reduction in the stoichiometry of binding (Cote et al., 1994). However, this work was conducted with PDE preparations supplemented with exogenous P $\gamma$  subunit that markedly affects the interaction of cGMP with the noncatalytic sites (see below). Therefore, we chose to examine the cGMP binding properties of nonactivated and transducin-activated PDE in ROS homogenates containing only the endogenous P $\gamma$  that is present in rod photoreceptor cells. We carried out equilibrium and kinetic studies at 4° to slow the binding reactions for accurate measurements of the rate constants.

Non-activated, nucleotide-depleted PDE (nPDE) in frog ROS homogenates binds cGMP with high affinity and as a single class of noninteracting binding sites at 4° ( $K_D = 8.4$  nM,  $B_{max} = 1.7$  mol cGMP per mol PDE ; see Table 2.1). The measured  $K_D$  for cGMP binding to frog nPDE agrees with previous estimates when the temperature dependence of the binding reaction is accounted for (Cote and Brunnock, 1993). [The  $B_{max}$  of nPDE can be increased to 2.0 by addition of  $\leq 1$  P $\gamma$  per PDE (see Figure 2.2C), suggesting that a small amount of P $\gamma$  was lost during preparation of nPDE.] When transducin is activated by addition of GTP $\gamma$ S to illuminated ROS homogenates and then 10 – 400 nM [ $^3$ H]cGMP is added, transducin-activated PDE (taPDE) undergoes a 7-fold decrease in binding affinity ( $K_D = 57$  nM) and a substantial loss in the number of cGMP binding sites ( $B_{max} = 1.0$  mol cGMP per mol PDE; Table 2.1). At higher [ $^3$ H]cGMP concentrations up to 1.3  $\mu$ M, we detected an additional 0.3 mol cGMP bound per PDE, but could not resolve a distinct, second class of binding sites. To improve detection of low affinity cGMP binding sites, we prepared high specific activity [ $^{32}$ P]cGMP, and found that

**Table 2.1**

**Equilibrium and Kinetic Parameters for High Affinity cGMP Binding to Frog PDE<sup>a</sup>**

	$K_D$ (obs.) <sup>b</sup> (nM)	$k_{-1}$ <sup>c</sup> (sec <sup>-1</sup> )	$k_{+1}$ <sup>d</sup> (M <sup>-1</sup> sec <sup>-1</sup> )
nPDE	8.4 ± 1.8 (5)	3.4 ± 0.2 × 10 <sup>-4</sup> (7)	7.6 ± 0.8 × 10 <sup>4</sup> (6)
taPDE	slow: fast:	3.4 ± 1.2 × 10 <sup>-4</sup> ; 64% (8)	7.8 ± 0.8 × 10 <sup>4</sup> (7)
		2.9 ± 0.9 × 10 <sup>-3</sup> ; 36% (8)	

<sup>a</sup> Binding of [<sup>3</sup>H]cGMP to non-activated PDE (nPDE) and transducin-activated PDE (taPDE) were performed at 4° as described in the Experimental Procedures. ROS homogenates were depleted of nucleoside phosphates prior to use. Values represent the mean ± S.E.M for the number of determinations shown in parentheses.

<sup>b</sup> Equilibrium binding measurements of cGMP to nPDE were performed at 4° by mixing PDE (8-11 nM) with 1 – 400 nM [<sup>3</sup>H]cGMP and incubating for 30 min. Transducin-activated PDE (8-17 nM) was pre-incubated with GTPγS (added at a concentration equal to the rhodopsin concentration) for 1 min prior to addition of [<sup>3</sup>H]cGMP. The  $B_{max}$  obtained from these binding isotherms was 1.73 ± 0.11 and 0.98 ± 0.11 mol cGMP per mol PDE for nPDE and taPDE, respectively. A second class of low affinity sites on taPDE was not detected in these experiments (see text).

<sup>c</sup> Dissociation rate constants ( $k_{-1}$ ) were determined as described in Fig. 1. Percentage values represent the proportion of the total binding sites exhibiting rapid or slow cGMP dissociation with taPDE in a two-site fit of the dissociation kinetics.

<sup>d</sup> Association rate constants ( $k_{+1}$ ) were calculated from the  $k_{obs}$  values in Fig. 1 using the equation:  $k_{+1} = (k_{obs} - k_{-1})/[cGMP]$ , where [cGMP] is the total cGMP concentration and ligand depletion is not significant (Hulme and Birdsall, 1992).

increasing the [<sup>32</sup>P]cGMP concentration from 1 μM to 15 μM results in a progressive ( $K_{1/2} \sim 5 \mu M$ ) increase in total cGMP binding to taPDE from 1.2 to 1.9 cGMP bound per PDE (data not shown). Low affinity cGMP binding sites were not detected with nPDE.

Thus, activation of PDE by transducin induces heterogeneity in the noncatalytic sites on PDE, with a large decrease in binding affinity at one noncatalytic site, and a more modest change at the second site.

Measurements of the rate of cGMP association and dissociation were performed to better understand how transducin activation differentially affects cGMP binding to the two noncatalytic sites of PDE. When PDE is incubated with 1  $\mu\text{M}$  [ $^3\text{H}$ ]cGMP, a single class of cGMP binding sites is resolved (Figure 2.1A), and the association rate constant is identical for nPDE and taPDE (Table 2.1). [The low affinity cGMP binding sites on taPDE ( $\sim 0.2$  cGMP per PDE under these conditions) apparently did not contribute sufficiently to be resolved in Figure 2.1A.] Thus, transducin activation does not significantly alter the initial step of cGMP binding to the moderate affinity class of sites on taPDE. The association rate constant for cGMP binding ( $k_{+1} = 8 \times 10^4 \text{ M}^{-1} \text{ s}^{-1}$ ) is approximately 3 orders of magnitude below the diffusion-controlled limit for a simple bimolecular protein-ligand binding reaction (Gutfreund, 1995). Restricted diffusion of cGMP to the binding pocket of the noncatalytic sites may result from binding of  $\text{P}\gamma$  in proximity to the noncatalytic domains on  $\text{P}\alpha\beta$  (Natochin and Artemyev, 1996).

Heterogeneity in the noncatalytic cGMP binding sites was readily observed (Figure 2.1B) when bound [ $^3\text{H}$ ]cGMP dissociated from taPDE (but not nPDE), in agreement with previous observations (Cote et al., 1994; Yamazaki et al., 1996a; Calvert et al., 1998). PDE activation accelerates 9-fold the exchange rate of cGMP from approximately 0.4 cGMP per PDE, probably reflecting the low affinity sites that are not saturated under the conditions of this experiment. The remaining two-thirds of the binding sites (0.8 cGMP per PDE) dissociate bound [ $^3\text{H}$ ]cGMP at the same rate as does

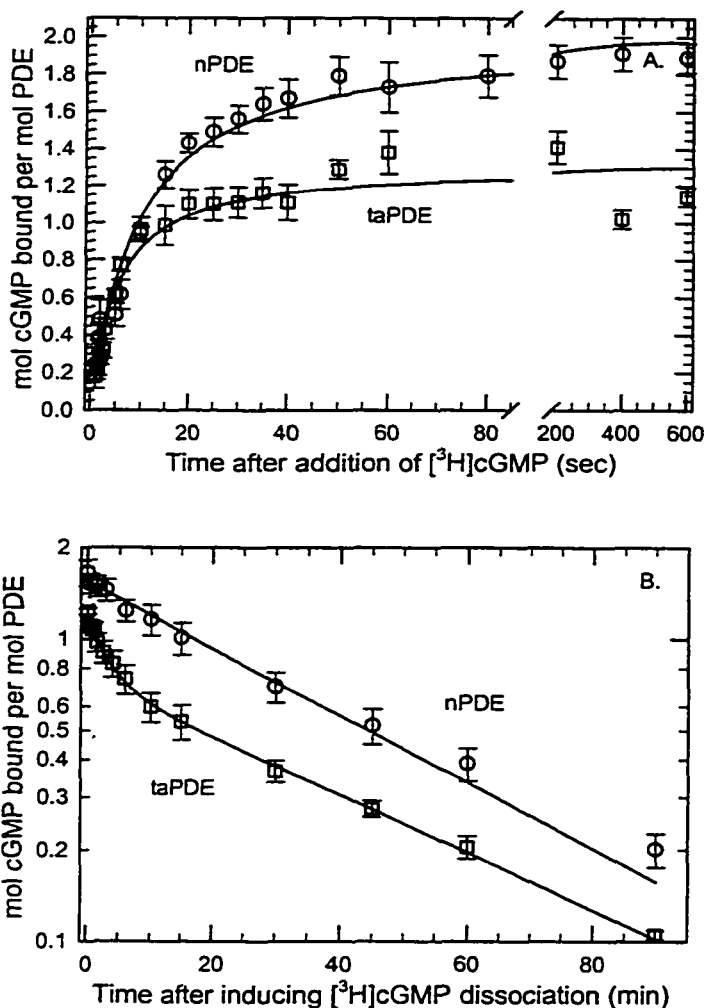


Figure 2.1. The kinetics of cGMP exchange at the noncatalytic sites of non-activated and transducin-activated PDE. A. For measuring the kinetics of cGMP association to nPDE, 25 nM PDE was mixed with 1  $\mu$ M [<sup>3</sup>H]cGMP at 4°, and the binding reaction quenched with ice-cold ammonium sulfate at the indicated times (see “Experimental Procedures”). Transducin-activated PDE (taPDE) was prepared from non-activated PDE (nPDE) by pre-incubating samples with 1 mM GTP $\gamma$ S for 1 min prior to cGMP addition. The nPDE data are the mean  $\pm$  S.E.M. for 6 experiments, and the curve is the fit of the data to a pseudo first-order reaction ( $k_{\text{obs}} = 7.7 \pm 0.8 \times 10^{-2} \text{ sec}^{-1}$ ;  $B_{\text{max}} = 1.83 \pm 0.07$  cGMP bound per PDE). For taPDE, the values are:  $k_{\text{obs}} = 7.9 \pm 0.8 \times 10^{-2} \text{ sec}^{-1}$ ;  $B_{\text{max}} = 1.25 \pm 0.08$  cGMP bound per PDE;  $n = 7$ ). Note that a two-site model was not statistically preferred to the one-site model in all experiments examined. B. To measure the kinetics of cGMP dissociation, 60 nM PDE (either non-activated or pre-incubated for 1 min with GTP $\gamma$ S as above) was first incubated with 1  $\mu$ M [<sup>3</sup>H]cGMP for 30 min at 4° to occupy the noncatalytic sites (nPDE: 1.7 cGMP bound per PDE; taPDE: 1.2 cGMP bound per PDE). At time zero, dissociation of [<sup>3</sup>H]cGMP was initiated by addition of 10 mM unlabeled

cGMP, and samples were directly filtered at the indicated times. The data points are the mean  $\pm$  SEM ( $n = 6$ ), and the curves represent the fit of the data to a single exponential for nPDE ( $k_{-1} = 3.4 \times 10^{-4} \text{ sec}^{-1}$ ) and a double exponential process for taPDE (36% fast sites,  $k_{-1} = 2.9 \times 10^{-3} \text{ sec}^{-1}$ ; 64% slow sites,  $k_{-1} = 3.4 \times 10^{-4} \text{ sec}^{-1}$ ). The dotted line demonstrates that the data for taPDE dissociation do not fit a single-site dissociation model.

nPDE. Thus, a 7-fold change in the  $K_D$  of the moderate affinity cGMP binding sites following transducin activation of PDE fails to significantly affect the dissociation rate constant from these sites. The approximately 1000-fold lowering of cGMP affinity to the second class of sites on taPDE has a relatively modest effect on the dissociation rate constant for this class of noncatalytic sites detected in Figure 2.1B.

We conclude that the nonactivated PDE holoenzyme consists of two identical, high affinity cGMP binding sites. Furthermore, the excellent agreement between the observed  $K_D$  and the kinetic  $K_D$  ( $k_{-1}/k_{+1} = 4.5 \text{ nM}$ ) indicates that the association and dissociation reaction steps measured in Fig. 2.1 represent the rate-limiting steps for cGMP interaction with the noncatalytic sites on nPDE. Upon transducin activation of PDE, heterogeneity in the noncatalytic sites becomes evident. The moderate affinity noncatalytic site on taPDE ( $K_D = 57 \text{ nM}$ ) retains the same kinetic rate constants for cGMP association and dissociation as observed for nPDE, indicating that some other rate-limiting process (e.g., conformational transition, protein-protein interaction, etc.) must contribute to destabilizing cGMP binding to this class of sites. The low affinity site can only be saturated at high cGMP concentrations (well above micromolar), and represents the small proportion of more rapidly dissociating sites in Figure 2.1B. The creation of two non-identical cGMP binding sites on upon PDE activation by transducin

is likely to result from differences in how  $\alpha_t$ -GTP $\gamma$ S interacts with the  $\alpha$  and  $\beta$  catalytic subunits.

*Exogenous P $\gamma$  regulates cGMP exchange rates at both low and high affinity noncatalytic sites on PDE.* To test the role of P $\gamma$  to regulate cGMP binding to the noncatalytic sites on nPDE and taPDE, we examined whether adding P $\gamma$  affected cGMP dissociation from nPDE and taPDE. Figure 2.2A shows that when nPDE is incubated with increasing amounts of P $\gamma$  and then 1  $\mu$ M [ $^3$ H]cGMP is added to occupy the noncatalytic sites, the half-time for [ $^3$ H]cGMP release is progressively slowed. The ability of P $\gamma$  to slow cGMP dissociation from nPDE is probably a consequence of reducing (by mass action) the number of PDE molecules lacking one or two bound P $\gamma$  at any moment in time. The sensitivity of cGMP exchange on nPDE to the free P $\gamma$  concentration suggests a strong allosteric linkage between P $\gamma$  binding to P $\alpha\beta$  and cGMP occupancy of the noncatalytic sites.

Pre-incubation of taPDE with increasing amounts of P $\gamma$  prior to transducin activation has two major effects on the noncatalytic cGMP binding sites. First, P $\gamma$  can convert low affinity cGMP binding sites on taPDE to high affinity sites (Figure 2.2C). Second, addition of increasing amounts of P $\gamma$  can reduce (1 P $\gamma$  added per taPDE) or abolish ( $\geq 2$  P $\gamma$  added per taPDE) the rapidly dissociating class of noncatalytic sites on taPDE, as well as slowing cGMP dissociation from the other class of sites to a similar extent as nPDE (Figure 2.2B). It is noteworthy that P $\gamma$  exerts these effects on the noncatalytic cGMP binding sites with greater potency than it can inhibit catalysis at the active site of taPDE (see Figure 2.7).



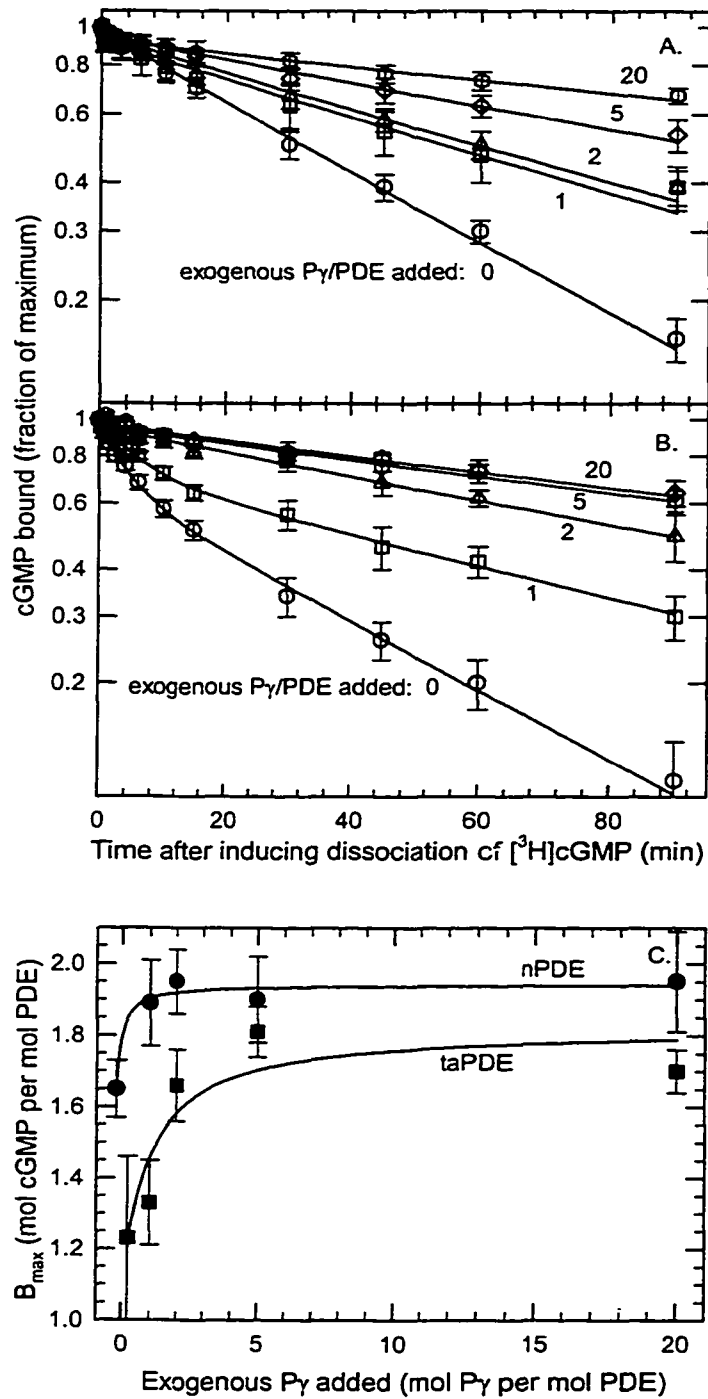


Figure 2.2. Effects of exogenous Py on cGMP dissociation from noncatalytic sites and on the maximum extent of cGMP binding to nPDE and taPDE. ROS homogenates (20 nM PDE, final concentration) were incubated at  $4^\circ$  for  $\sim 4$  min with the following concentrations of Py: 0 (circle), 1.0 (square), 2.0 (triangle), 5.0 (diamond) or 20 (upside-down triangle) mol Py per mol PDE. For transducin-activated PDE (panel B), the ROS were then incubated with 1 mM  $\text{GTP}\gamma\text{S}$  for 1 min. Following addition of  $1 \mu\text{M}$

[<sup>3</sup>H]cGMP for 30 min at 4°, samples were tested for the maximum extent of cGMP binding (panel C). [<sup>3</sup>H]cGMP dissociation was initiated upon addition of 10 mM unlabeled cGMP at time zero and then portions were directly filtered at the indicated times. For nPDE (panel A), the data were best fit to a single exponential decay with the dissociation rates progressively slowing from the control value of  $t_{1/2} = 34$  min to a  $t_{1/2} = 196$  min for the 20 P $\gamma$  per PDE condition. For taPDE, a two-site model for the dissociation kinetics was preferred for the 0 and 1 P $\gamma$  per PDE conditions, with the percentage of the total binding that can be attributed to the “fast” sites diminishing from 35% to <10% as the amount of added P $\gamma$  increased from 0 to 2 P $\gamma$  per PDE. The data are the mean  $\pm$  SEM for three to six determinations of the dissociation rates for each concentration of added P $\gamma$ .

*Quantitative analysis of the P $\gamma$  concentration and its subcellular location in purified frog ROS.* Because free P $\gamma$  greatly affects cGMP binding and exchange kinetics with PDE, we decided to measure the P $\gamma$  concentration in intact frog ROS as well as the stoichiometry of P $\gamma$  binding to frog P $\alpha\beta$ . Using a quantitative immunoblot procedure, we found that homogenates derived from Percoll-purified frog ROS contained  $1.81 \pm 0.13$  (mean  $\pm$  S.E.M.;  $n = 14$ ) mol of P $\gamma$  relative to the total concentration of PDE holoenzyme (Figure 2.3, “Homog.”). Upon fractionation of these ROS homogenates into membrane and soluble fractions by centrifugation, both dark-adapted and light-exposed ROS retain all P $\gamma$  (1.9 – 2.0 P $\gamma$  per P $\alpha\beta$ ) in a membrane-associated state, and  $< 0.1$  P $\gamma$  per P $\alpha\beta$  in the soluble fractions (Figure 2.3, “Control”). The membrane-associated P $\gamma$  was bound to PDE, because when frog PDE was released from ROS membranes by hypotonic extraction, a similar stoichiometry of P $\gamma$  binding to the released PDE was observed (data not shown).

Addition of cGMP to saturate the noncatalytic sites on PDE did not alter the membrane-associated state or stoichiometry of P $\gamma$  binding to dark-adapted or light-

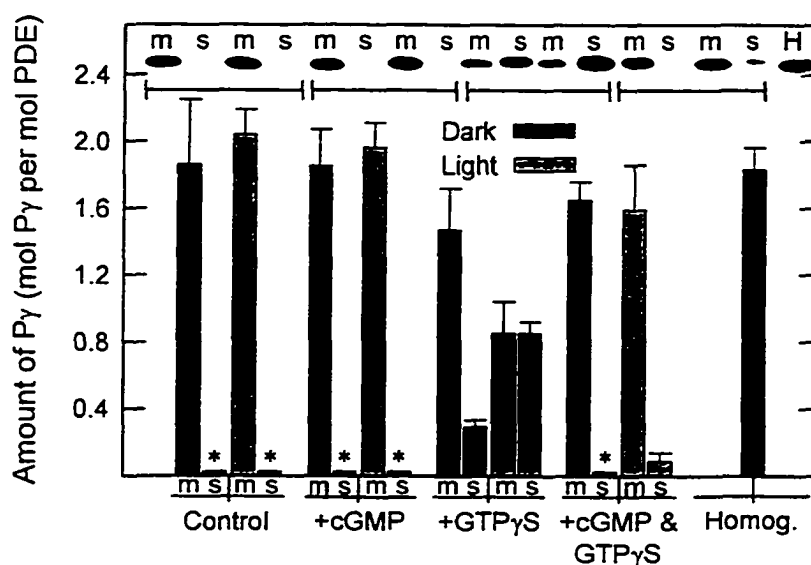


Figure 2.3. Py content of membrane and supernatant fractions of frog ROS homogenates. ROS homogenates (120 nM PDE holoenzyme) in Buffer A were incubated at 4° for 30 sec with: no additions (“Control”), 2.2 mM cGMP (“+cGMP”), 50  $\mu$ M GTP $\gamma$ S (“+GTP $\gamma$ S”), or both nucleotides supplemented with 50  $\mu$ M zaprinast (“+cG&GTP $\gamma$ S”). Identical portions were either kept dark-adapted (black bars) or exposed to room light (gray bars) during the incubation period, and then samples were centrifuged for 1 min at 110,000  $\times$  g at ambient temperature. Supernatant (s) and membrane (m) samples were processed on different gels, along with a set of Py standards on each gel, to quantitate the Py content (see “Experimental Procedures”). Unfractionated, dark-adapted ROS homogenates with no additions (“Homog.”) were also analyzed along with the membrane samples for the sake of comparison. In the representative immunoblot shown in the figure, the supernatant samples were exposed to film for longer times than the membrane samples to permit detection of lower amounts of immunoreactivity. The \* indicates that the amount of Py was below the level of detection. The data represent the mean  $\pm$  S.E.M. for three experiments with different ROS homogenates. This figure was done in collaboration with Tracy Hebert and Marc D’Amours.

exposed PDE (1.9 – 2.0 Py per P $\alpha\beta$ ; Figure 2.3, “+cGMP”). However, if light-exposed ROS homogenates are incubated with GTP $\gamma$ S to activate transducin, a substantial release of Py into the supernatant fraction occurs shortly after nucleotide addition (0.8  $\pm$  0.1 mol Py released per mol P $\alpha\beta$ ). This Py dissociation into the supernatant can be prevented if

millimolar levels of cGMP are included with GTP $\gamma$ S (0.1 P $\gamma$  released per P $\alpha\beta$ ; Figure 2.3). Our quantitative analysis of P $\gamma$  agrees with and extends the qualitative observations of Arshavsky et al. who first showed that occupancy of the noncatalytic sites by cGMP could prevent P $\gamma$  release from ROS membranes following transducin activation (Arshavsky et al., 1992).

We conclude that the frog rod PDE holoenzyme consists of a P $\alpha\beta$  catalytic dimer to which 2 P $\gamma$  subunits bind, identical to the  $\alpha\beta\gamma_2$  stoichiometry of membrane-associated bovine rod PDE holoenzyme (Deterre et al., 1988; Fung et al., 1990). The absence of P $\gamma$  in the ROS cytosol may reflect a tightly regulated, coordinated synthesis of catalytic and inhibitory subunits of PDE [as suggested by P $\gamma$  knockout experiments (Tsang et al., 1996)]. The fact that approximately 1 mol P $\gamma$  per mol P $\alpha\beta$  can be released within 1 min of light activation of PDE (Figure 2.3, "+GTP $\gamma$ S" condition) led us to hypothesize that the state of association of P $\gamma$  and cGMP with the PDE holoenzyme may be tightly coupled upon PDE activation by transducin.

*cGMP dissociation from noncatalytic sites correlates with P $\gamma$  release following transducin activation of PDE.* To test whether cGMP dissociation from noncatalytic sites is directly correlated with P $\gamma$  release from taPDE, we examined the time course of cGMP dissociation and of P $\gamma$  release following transducin activation of PDE under conditions where the free cGMP concentration was rapidly reduced from its "dark-adapted" concentration (2  $\mu$ M). To activate PDE and simultaneously lower the free cGMP concentration, we employed a "concentration jump" technique (Calvert et al., 1998) in which GTP $\gamma$ S was added (to activate frog rod PDE) along with activated PDE1 (to

rapidly hydrolyze free cGMP). Release of  $\text{P}\gamma$  and cGMP from PDE were determined by centrifugation of samples through silicone oil and analysis of the pellets for the amount of  $[^3\text{H}]\text{cGMP}$  or  $\text{P}\gamma$  bound to the membrane-associated PDE. We found that the time course of cGMP dissociation following transducin activation closely tracked the rate of  $\text{P}\gamma$  release (Figure 2.4). Both processes showed biphasic dissociation kinetics, with 20-30%

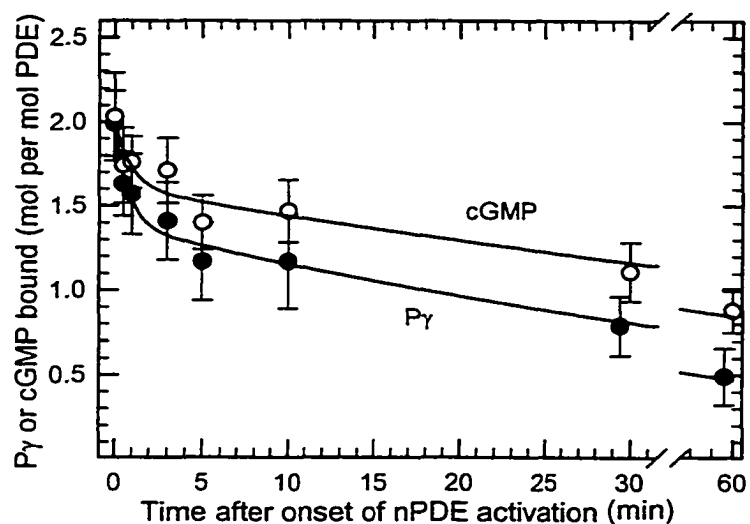


Figure 2.4.  $\text{P}\gamma$  dissociation from transducin-activated PDE correlates with cGMP dissociation from noncatalytic binding sites. ROS homogenates (30-120 nM PDE) were incubated with 2  $\mu\text{M}$  cGMP or  $[^3\text{H}]\text{cGMP}$  and 3  $\mu\text{M}$  E4021 for 10 min at 4°. Transducin activation of PDE and dissociation of its bound cGMP was initiated upon addition of 100  $\mu\text{M}$  GTP $\gamma$ S, 10<sup>3</sup> U/l PDE1, and 8x10<sup>4</sup> U/l calmodulin (final concentrations). [In control experiments similar to those of Calvert et al., Fig. 5A (Calvert et al., 1998), we determined that PDE1 activities ranging from 500 to 4000 U/l resulted in identical cGMP dissociation kinetics.] At the indicated times, portions were centrifuged for 1 min at 110,000 x g at room temperature. The membrane pellet was then analyzed for either  $\text{P}\gamma$  content (●) or  $[^3\text{H}]\text{cGMP}$  binding (○). The data points represent the mean  $\pm$  S.E.M. for four experiments where  $\text{P}\gamma$  and  $[^3\text{H}]\text{cGMP}$  were both measured on the same preparation. The curves represent the fit of the data to a 2-site binding model: for  $\text{P}\gamma$  release: 30  $\pm$  5% of the  $\text{P}\gamma$  rapidly dissociated ( $t_{1/2} = 0.6 \pm 0.2$  min) and 70  $\pm$  3% of the  $\text{P}\gamma$  slowly dissociated ( $t_{1/2} = 39 \pm 6$  min); for cGMP dissociation, 20  $\pm$  7% was rapidly released ( $t_{1/2} = 0.7 \pm 0.6$  min) while 80  $\pm$  5% slowly dissociated ( $t_{1/2} = 65 \pm 15$  min). This figure was done in collaboration with Tracy Hebert and Marc D'Amours.

of the reaction occurring rapidly ( $t_{1/2} = 0.6 - 0.7$  min), and the remainder of the dissociation reaction occurring much more slowly ( $t_{1/2} = 40-60$  min).

Experimental limitations prevented us from determining the temporal sequence of  $P\gamma$  and cGMP dissociation from  $P\alpha\beta$ . However, it is likely that interaction of  $\alpha_t$ -GTP $\gamma$ S with  $P\gamma$  bound to the PDE holoenzyme initially displaces  $P\gamma$  from its tight association with one catalytic subunit, thereby accelerating cGMP dissociation from the noncatalytic site. Loss of cGMP at this noncatalytic site would further lower the  $P\gamma$  binding affinity for  $P\alpha\beta$ , leading to dissociation of  $P\gamma$ - $\alpha_t$ -GTP $\gamma$ S from  $P\alpha\beta$ . The observation that cGMP and  $P\gamma$  dissociation from the other class of binding sites proceeds as slowly as for nPDE (Figure 2.1B) indicates that  $\alpha_t$ -GTP $\gamma$ S is much less effective in binding to the second  $P\gamma$  molecule and accelerating cGMP exchange at this noncatalytic site. This might be explained if the remaining  $P\gamma$  bound with higher intrinsic affinity to  $P\alpha\beta$  than the  $P\gamma$  that is rapidly released.

*cGMP occupancy of the noncatalytic sites induces stoichiometric binding of  $P\gamma$  to taPDE.* We next asked whether occupancy of the noncatalytic cGMP binding sites on taPDE was sufficient to reverse  $P\gamma$  dissociation from  $P\alpha\beta$ . We first prepared taPDE lacking bound cGMP, and then added increasing concentrations of [ $^3$ H]cGMP. After centrifuging the PDE-containing ROS membranes, we simultaneously assayed the extent of [ $^3$ H]cGMP binding and the stoichiometry of  $P\gamma$  binding to taPDE. Figure 2.5 demonstrates a one-to-one correlation between cGMP occupancy of the high affinity noncatalytic sites and  $P\gamma$  binding to  $P\alpha\beta$ . In the absence of cGMP, taPDE bound 0.2 mol  $P\gamma$  per mol PDE. As increasing concentrations of cGMP were added, taPDE displayed a n

= 4) and a single class of  $P\gamma$  binding sites ( $B_{\max} = 1.4 \pm 0.1$   $P\gamma$  bound per PDE;  $n = 4$ ).

When incubated with high concentrations of cGMP to occupy both high and low affinity cGMP binding sites on taPDE, the  $P\gamma$  binding stoichiometry approached the same value as for nPDE (Figure 2.3, “+cGMP & GTP $\gamma$ S”).

We conclude that cGMP occupancy of the noncatalytic sites must induce a conformational change in the  $P\alpha\beta$  catalytic dimer that enhances  $P\gamma$  binding to  $P\alpha\beta$ . This allosteric effect of cGMP to enhance  $P\gamma$  binding affinity does not act on the C-terminal inhibitory domain of  $P\gamma$  (Granovsky et al., 1997), because taPDE remains catalytically

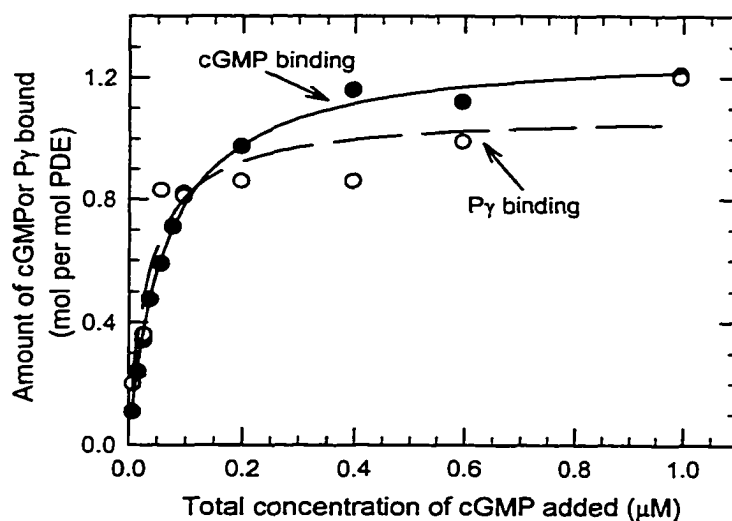


Figure 2.5. Endogenous  $P\gamma$  binding to transducin-activated PDE correlates with titration of cGMP binding to the noncatalytic sites. PDE (15 nM) was transducin-activated by the addition of 10  $\mu\text{M}$  GTP $\gamma$ S 1 minute prior to the addition of increasing amounts of [ $^3\text{H}$ ]cGMP (with 200  $\mu\text{M}$  zaprinast). After a 30 min incubation, two portions were quenched into ice-cold buffered ammonium sulfate (see Experimental Procedures) to determine the [ $^3\text{H}$ ]cGMP content (closed circle). The remaining portion was spun for 1 min at 110,000 x g. The supernatants were discarded, and the pellets were washed once and then analyzed for their  $P\gamma$  content (open circle). For the cGMP binding data, the curve is a 2-parameter hyperbolic fit with  $B_{\max} = 1.3$  cGMP bound per PDE and a  $K_d = 65$  nM, while the  $P\gamma$  binding curve parameters are:  $B_{\max} = 1.1$   $P\gamma$  per PDE and  $K_{1/2} = 34$  nM cGMP. The data shown are representative of 4 individual experiments.

single class of high affinity cGMP binding sites ( $B_{\max} = 1.3 \pm 0.1$  cGMP bound per PDE; activated (see Table 2.2). Rather, a distinct domain on  $P\gamma$  [e.g., the central polycationic domain; (Artemyev and Hamm, 1992)] must be involved in interacting with  $P\alpha\beta$  in a cGMP-dependent manner.

*Two distinct classes of  $P\gamma$  binding sites on  $P\alpha\beta$  restore high affinity cGMP binding to the noncatalytic sites.* To understand the basis of the heterogeneity in the noncatalytic sites of taPDE, we needed to study the binding of cGMP and  $P\gamma$  to catalytic dimers ( $P\alpha\beta$ ) from which  $P\gamma$  had been completely removed. Previous work had demonstrated that physical removal of  $P\gamma$  from frog rod PDE following transducin activation resulted in a loss of cGMP binding, and that addition of  $P\gamma$  restored high affinity cGMP binding to noncatalytic sites (Yamazaki et al., 1982; Cote et al., 1994; Yamazaki et al., 1996b). However, heterogeneity in  $P\gamma$  binding to frog  $P\alpha\beta$  has been reported in some cases (Yamazaki et al., 1996b; Yamazaki et al., 1996a) but not in others (Yamazaki et al., 1982; Cote et al., 1994).

Two independent approaches were used to prepare  $P\alpha\beta$  catalytic dimers from which  $P\gamma$  had been removed. The first method is based on the ability of activated transducin to release 50 – 70% of its  $P\gamma$  when the noncatalytic sites are empty (Yamazaki et al., 1990). [We further optimized the conditions for  $P\gamma$  removal from  $P\alpha\beta$  to further reduce the amount of  $P\gamma$  associated with  $P\alpha\beta$  to 10 – 25% of the original amount (see “Experimental Procedures” and Fig. 2.4).] The second approach to preparing  $P\alpha\beta$  dimers



relied on the ability of trypsin proteolysis to degrade P $\gamma$  without adversely affecting the functional properties of P $\alpha\beta$  at its catalytic or noncatalytic sites (Mou et al., 1999).

Figure 2.6 demonstrates that when we prepared P $\alpha\beta$  catalytic dimers by either method, addition of P $\gamma$  to P $\alpha\beta$  in the presence of 1  $\mu$ M [ $^3$ H]cGMP restores high affinity cGMP binding to the noncatalytic sites in a biphasic manner. Addition of  $\leq 1$  mol P $\gamma$  per P $\alpha\beta$  results in equimolar cGMP binding to high affinity sites on P $\alpha\beta$ . Thereafter, only a slight increase in cGMP binding is observed in the range of 1 – 2 P $\gamma$  added per P $\alpha\beta$ . It is

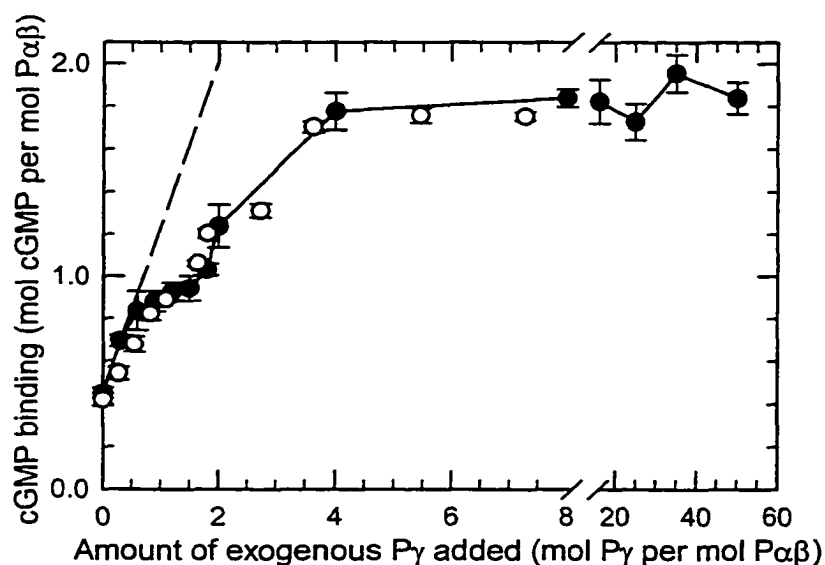


Figure 2.6. The restoration of high affinity cGMP binding to PDE catalytic dimers by P $\gamma$  reveals two classes of binding sites. Activated PDE was prepared either by extraction of P $\gamma$  from P $\alpha\beta$  by  $\alpha_i$ -GTP $\gamma$ S (closed circles, n = 5) or by trypsin proteolysis (2.5  $\mu$ g/ml trypsin for 5 min at 4 $^\circ$ ) to make tPDE (open circles, n = 3), as described in “Experimental Procedures”. The residual P $\gamma$  content was 16  $\pm$  2% for P $\alpha\beta$ , and 22  $\pm$  2% for tPDE. The indicated concentration of P $\gamma$  was incubated with 10 nM P $\alpha\beta$  (closed circles) or 17 nM tPDE (open circles) for 5 minutes before adding 1  $\mu$ M [ $^3$ H]cGMP plus 200  $\mu$ M zaprinast. The samples were incubated for 30 min at 4 $^\circ$ , then analyzed for the amount of [ $^3$ H]cGMP bound to the enzyme. The dashed line represents the results that would have been seen if the restoration of high affinity cGMP binding by P $\gamma$  occurred in a simple one-to-one stoichiometry.

noteworthy that adding exactly 2 mol exogenous  $P\gamma$  per mol  $P\alpha\beta$  in Figure 2.6 leads to the same extent of cGMP binding (1.2 cGMP per PDE) as is seen for taPDE samples (containing 2 mol endogenous  $P\gamma$  per mol PDE) under similar conditions (Table 2.1, Figure 2.2C, Fig. 2.5). Addition of  $\geq 4$   $P\gamma$  per  $P\alpha\beta$  fully restores cGMP binding to a second class of sites that were unoccupied at lower  $P\gamma$  concentrations (consistent with the results in Figure 2.2C for taPDE). The results shown in Figure 2.6 were also observed when  $P\alpha\beta$  was prepared by activating transducin with GTP instead of GTP $\gamma$ S (data not shown). The data in Figure 2.6 are in good agreement with previously published data (Cote et al., 1994); the more extensive data set and greater precision in determining PDE subunit concentrations in Figure 2.6 probably account for our ability to resolve the biphasic behavior that was overlooked in the earlier study.

The results in Figure 2.6 demonstrate that  $P\alpha\beta$  contains two distinct classes of  $P\gamma$  binding sites. One class of  $P\gamma$  binding sites has very high affinity for  $P\alpha\beta$  in the presence of 1  $\mu$ M cGMP, and can bind up to 1  $P\gamma$  per  $P\alpha\beta$  as a simple titration phenomenon. The noncatalytic cGMP binding sites that are restored by stoichiometric  $P\gamma$  addition correspond to the moderate affinity class of sites found in taPDE (Table 2.1, Figure 2.5). The second class of  $P\gamma$  binding sites on  $P\alpha\beta$  are of lower affinity and requires an excess of  $P\gamma$  (when the cGMP concentration is  $\leq 1$   $\mu$ M) in order to shift the equilibrium to the liganded state. This lower affinity class of  $P\gamma$  binding sites is very likely responsible for converting low affinity noncatalytic cGMP binding sites on taPDE to their high affinity state (Figure 2.2C). Although it is probable that the  $\alpha$  and  $\beta$  catalytic subunits of frog PDE have binding domains for  $P\gamma$  with intrinsically different binding affinities [as

reported for  $\text{P}\gamma$  binding to bovine rod PDE; (Berger et al., 1999)], we cannot rule out allosteric mechanisms that might induce heterogeneity in  $\text{P}\gamma$  binding to  $\text{P}\alpha\beta$ .

*Transducin activation fails to stimulate the maximum catalytic potential of the  $\text{P}\alpha\beta$  catalytic heterodimer.* Based on the above results, we hypothesized that heterogeneity in  $\text{P}\gamma$  binding to  $\text{P}\alpha\beta$  might also result in differences in catalysis at the two active sites on  $\text{P}\alpha\beta$ . While most previous work has assumed that each catalytic subunit contributes equally to catalysis upon activation of PDE by transducin, there is wide variation in the reported maximal hydrolytic rates for activated PDE [see Table V in (Pugh, Jr. and Lamb, 1993)] as well as uncertainty in the stoichiometry and cooperativity of transducin activation of PDE [see (Melia et al., 2000) and references cited therein].

We compared the rates of cGMP hydrolysis for various forms of activated PDE that differed in the method by which the inhibitory constraint of  $\text{P}\gamma$  was relieved. To determine the maximum hydrolytic rate of taPDE, we measured the enzyme activity in light-exposed ROS homogenates following addition of increasing concentrations of GTP $\gamma$ S. Complete activation of PDE by transducin required a concentration of GTP $\gamma$ S sufficient to activate the entire pool of transducin in ROS (data not shown). The  $k_{\text{cat}}$  for taPDE,  $4560 \pm 140$  cGMP per s (Table 2.2) is not significantly different from a previous estimate of 4400 cGMP per s (Dumke et al., 1994).

We used the same frog ROS homogenates to directly compare taPDE with PDE activated by trypsin proteolysis (tPDE). We found that the  $k_{\text{cat}}$  in the latter case was substantially higher, in contrast to previous comparisons using frog PDE (Whalen and Bitensky, 1989; Whalen et al., 1990). In one set of experiments where we added

increasing concentrations of trypsin to 2 nM PDE, we found a maximum catalytic rate of  $7640 \pm 140$  cGMP hydrolyzed per s ( $n = 5$ ; data not shown). In additional experiments where hydrolytic activity measurements were made at relatively low tPDE concentrations (0.5 to 3 nM PDE), we observed similarly high rates (Table 2.2). If hydrolytic activity of tPDE was assayed at substantially higher enzyme concentrations (15 – 30 nM tPDE), the maximal rate approached the  $k_{cat}$  for taPDE (Table 2.2). In a separate experiment,

**Table 2.2**  
**SUMMARY OF MAXIMAL ACTIVITIES FOR VARIOUS PREPARATIONS OF**  
**ACTIVATED FROG PDE**

PDE preparation <sup>a</sup>	[PDE] <sup>b</sup> (nM)	Maximum catalytic activity <sup>c</sup> (cGMP per s per PDE)	n
taPDE	$\geq 12$	4400	ref. (Dumke et al., 1994)
	12 – 20	$4560 \pm 140$	10
tPDE	0.02	$7870 \pm 150$	ref. (D'Amours and Cote, 1999)
	0.5 – 3.0	$7550 \pm 110$	23
	15 – 30	$4990 \pm 375$	5
P $\alpha\beta$	1 – 2	$7000 \pm 180^d$	8

<sup>a</sup>PDE activated by transducin (taPDE), trypsin proteolysis (tPDE), or P $\gamma$  extraction by  $\alpha_t$ -GTP $\gamma$ S (P $\alpha\beta$ ) was prepared as described in the “Experimental Procedures.”

<sup>b</sup>The concentration of PDE used to assay the hydrolytic rate.

<sup>c</sup>Determined by measuring catalysis in the presence of saturating levels of cGMP (~100 times the  $K_M$ ). The values are normalized to the concentration of PDE catalytic dimer in each instance.

<sup>d</sup>The maximal rate was calculated by correcting the observed rate in each experiment for the residual P $\gamma$  (15 – 25%) remaining bound to P $\alpha\beta$ , assuming a linear dependence of the observed rate with the P $\gamma$  content (see Fig. 2.7).

This table was done in collaboration with Marc D'Amours.

progressive dilution of tPDE from 3 nM to 0.5 nM caused the hydrolytic activity to increase from 6400 to 8100 cGMP per s per PDE; further dilution to 6 pM tPDE had no further effect on the apparent  $k_{cat}$ . We attribute this phenomenon to the presence of proteolytic fragments of P $\gamma$  in our tPDE preparations that retain the ability to bind to and inhibit P $\alpha\beta$  at high, but not low, PDE concentrations. A 4.6 kDa P $\gamma$ -immunoreactive band [corresponding to amino acids 46 to 87 of bovine P $\gamma$  (Artemyev and Hamm, 1992)] has been detected on immunoblots of tPDE preparations, and co-purifies with tPDE following gel filtration chromatography (data not shown).

We have also measured the maximal cGMP hydrolytic rates of P $\alpha\beta$  preparations in which 75 – 85% of the endogenous P $\gamma$  has been extracted by  $\alpha_t$ -GTP $\gamma$ S. We find catalytic rates substantially greater (range, 5000 – 6600 cGMP per s) than the  $k_{cat}$  for taPDE. When corrected for the residual P $\gamma$  content of these P $\alpha\beta$  preparations, the predicted  $k_{cat}$  of P $\alpha\beta$  dimer devoid of P $\gamma$  is  $7000 \pm 180$  cGMP per sec ( $n = 8$ ; Table 2.2). Trypsinization of these P $\alpha\beta$  preparations containing residual P $\gamma$  can further elevate the hydrolytic rate approximately 25%.

We conclude that the maximum catalytic potential of the P $\alpha\beta$  catalytic dimer approaches 8000 cGMP hydrolyzed per s per P $\alpha\beta$  when all P $\gamma$  is released from the enzyme. If we assume each catalytic subunit has the same turnover number (4000 cGMP per s per subunit) and the  $K_M$  for tPDE is 22  $\mu$ M (D'Amours and Cote, 1999), the specificity constant,  $k_{cat}/K_M$  is calculated to be  $1.8 \times 10^8 \text{ M}^{-1}\text{s}^{-1}$ . Thus, the catalysis of cGMP into 5'-GMP occurs with extremely high catalytic efficiency and very near the diffusion limit (Gutfreund, 1995). However, PDE never achieves this level of activation

*in vivo*, because transducin activation of the enzyme fails to fully relieve  $P\gamma$  inhibition at both active sites. Rather,  $\alpha_t$ -GTP $\gamma$ S acts to completely relieve inhibition at only one of the two active sites on  $P\alpha\beta$ , with perhaps a minor ( $\leq 10\%$ ) effect at the second catalytic site. Activation of PDE catalysis by one, not two, activated transducin molecules in frog ROS homogenates is consistent with the 1:1 stoichiometry of bovine rod PDE activation by transducin in a purified, reconstituted system (Melia et al., 2000).

*Exogenous  $P\gamma$  can stoichiometrically inhibit  $P\alpha\beta$  catalytic dimers, but not tPDE.*

To further probe how transducin binds to and activates the PDE holoenzyme, we examined the ability of exogenous  $P\gamma$  to inhibit the various forms of activated PDE used in this paper. Previous studies using tPDE or  $P\alpha\beta$  preparations offer conflicting views on the ability of  $P\gamma$  to inhibit activated frog PDE. In some reports, activated PDE can be inhibited by  $P\gamma$  as a single class of high affinity sites (Yamazaki et al., 1996b; Yamazaki et al., 1996a), exhibiting the same titration behavior observed with bovine tPDE [e.g., refs. (Wensel and Stryer, 1986; Brown and Stryer, 1989; Mou et al., 1999)]. Other studies with activated frog PDE show evidence for lower affinity  $P\gamma$  binding and/or complex inhibition of catalysis by added  $P\gamma$  (Yamazaki et al., 1982; Whalen and Bitensky, 1989; Yamazaki et al., 1990). These differing results may arise from a number of factors, including the concentration of PDE catalytic subunits used, residual  $P\gamma$  in the activated PDE preparations, and uncertainties in determining the active  $P\alpha\beta$  and/or  $P\gamma$  concentrations.

To resolve these discrepancies, we examined the ability of  $P\gamma$  to inhibit activated PDE under conditions where the catalytic and inhibitory subunit concentrations were

precisely determined. Figure 2.7 shows that PDE activated by transducin responds quite differently to the addition of  $P\gamma$  than do tPDE or  $P\alpha\beta$  preparations. Both tPDE and  $P\alpha\beta$  are stoichiometrically inhibited by 2 mol  $P\gamma$  per mol  $P\alpha\beta$ . The steep linear dependence of tPDE and  $P\alpha\beta$  activity on the  $P\gamma$  concentration reflects a titration phenomenon consistent with the sub-nanomolar binding affinity of  $P\gamma$  for frog PDE reported previously (D'Amours and Cote, 1999). The similar behavior for tPDE and  $P\alpha\beta$  in Figure 2.7 shows that trypsinization of PDE acts primarily on  $P\gamma$  and has no noticeable effect on the ability of  $P\alpha\beta$  subunits to be inhibited by added  $P\gamma$ . Although  $\alpha_t$ -GTP $\gamma$ S is present in our  $P\alpha\beta$  preparations (see "Experimental Procedures") and is capable of binding free  $P\gamma$

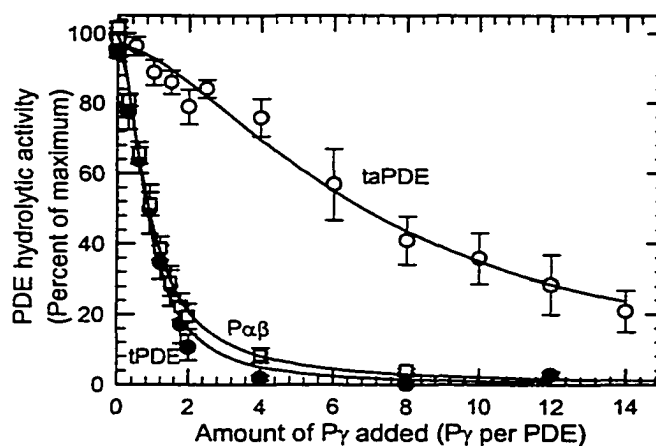


Figure 2.7. Stoichiometric  $P\gamma$  inhibition of catalysis is observed with tPDE and  $P\alpha\beta$ , but not with taPDE. tPDE (5 nM) was activated by trypsin treatment (200  $\mu$ g/ml trypsin for 10 min at 4 $^\circ$ ; see Experimental Procedures) and then incubated with the indicated amount of  $P\gamma$ . taPDE was prepared by first incubating nPDE (30 nM) with the indicated amounts of  $P\gamma$  for 2 min prior to addition of 1 mM GTP $\gamma$ S for 1 min at 22 $^\circ$ .  $P\alpha\beta$  dimers depleted of >70% of its endogenous  $P\gamma$  was prepared by two successive extractions of  $P\gamma$  with GTP $\gamma$ S followed by centrifugation (see Experimental Procedures).  $P\alpha\beta$  (1 nM) was then incubated with the indicated concentrations of exogenous  $P\gamma$ . PDE catalytic activity was measured with 10 mM cGMP as substrate, and the rates normalized to the maximum value obtained in the absence of added  $P\gamma$ . The curves represent a 3-parameter logistic curve fit to the data with  $IC_{50}$  values of 0.9, 0.9, and 7.1  $P\gamma$  per PDE for tPDE,  $P\alpha\beta$ , and taPDE, respectively.

(Yamazaki et al., 1990), the stoichiometric inhibition of  $P\alpha\beta$  by  $P\gamma$  demonstrates that  $\alpha_t$ -GTP $\gamma$ S cannot compete effectively with  $P\alpha\beta$  for binding to  $P\gamma$  under these conditions. Thus, in both instances where activated PDE has had its  $P\gamma$  physically removed from the catalytic dimer, exogenous  $P\gamma$  has free access to and high affinity for the catalytic sites and can stoichiometrically inhibit catalysis.

In contrast, the inhibition of taPDE by addition of  $P\gamma$  requires a greater than 15-fold molar excess of  $P\gamma$  to fully inhibit catalytic activity (Figure 2.7). The potency of  $P\gamma$  inhibition at the active site is several-fold weaker than its ability to convert low affinity noncatalytic binding sites on taPDE to higher affinity sites (Figure 2.2C). Note that in the presence of millimolar levels of cGMP in Figure 2.7, taPDE binds 2 mol endogenous  $P\gamma$  per mol PDE (Figure 2.3), and has a catalytic activity about one-half of the maximal rate of  $P\alpha\beta$  (Table 2.2). It is likely, therefore, that taPDE exists as a complex of  $\alpha_t$ -GTP $\gamma$ S with the PDE holoenzyme. We speculate that a molecule of  $\alpha_t$ -GTP $\gamma$ S, in a complex with  $P\gamma$  and a catalytic subunit, hinders the free diffusion of exogenous  $P\gamma$  to its inhibitory binding site, thereby reducing the effectiveness of free  $P\gamma$  to inhibit cGMP hydrolysis compared to tPDE or  $P\alpha\beta$  preparations.

*Role of the noncatalytic cGMP binding sites during transducin activation of PDE.*

Our results suggest that the noncatalytic sites on photoreceptor PDE detect changes in cytoplasmic cGMP concentration during phototransduction, and allosterically regulate the state of association of  $P\gamma$  with PDE and with activated transducin. In the dark-adapted state, cGMP levels in rod photoreceptors are much higher ( $> 1 \mu\text{M}$ ) than the  $K_D$  for cGMP binding to the noncatalytic sites of nPDE. Consequently,  $P\gamma$  remains bound to both



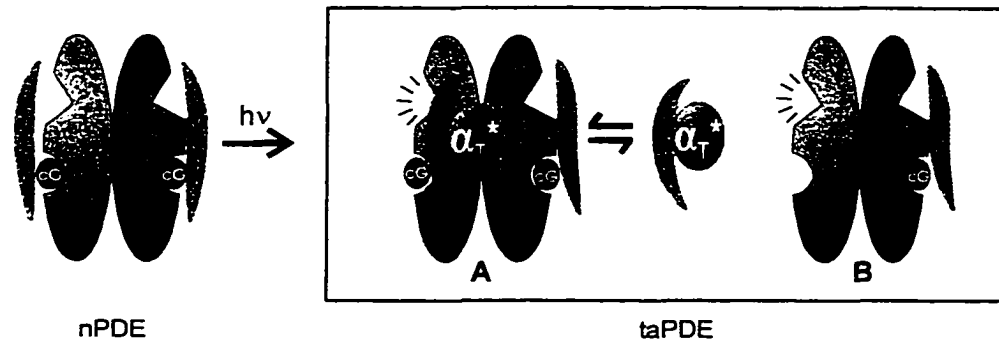


Figure 2.8. Model for activation of rod photoreceptor PDE holoenzyme by transducin. The nonactivated form of the PDE holoenzyme (nPDE) is depicted with the right-hand catalytic subunit having a higher affinity for Py. Following binding of activated transducin ( $\alpha_T^*$ ) to the PDE holoenzyme, the inhibitory constraint of Py is released at the active site (notch) on the left-hand catalytic subunit (lower Py binding affinity). In the presence of high cGMP concentrations, noncatalytic sites (semi-circles) remain occupied and Py remains bound to both subunits ("taPDE-A"). Lowering the cGMP concentrations causes a transition to taPDE-B in which cGMP dissociates from its low affinity noncatalytic site (left side), and Py dissociation accompanies cGMP release. The right-hand subunit of taPDE-B retains bound cGMP and Py because of its intrinsically higher binding affinity for both molecules, and little relief of inhibition occurs at this active site. See text for details.

catalytic subunits in its inhibitory conformation, and cGMP and Py exchange between the bound and free states is expected to be very slow (Figure 2.8, "nPDE").

Transient light activation of the visual excitation pathway causes activated  $\alpha_t$  to displace Py from its inhibitory conformation, and cGMP rapidly drops below micromolar levels. However, the recovery of the dark-adapted state in response to dim flashes (time scale, seconds) probably restores cGMP levels (via guanylate cyclase activation) more rapidly than cGMP can dissociate from noncatalytic sites. Under these conditions, activated PDE would consist of a complex of PDE holoenzyme (both noncatalytic sites occupied, both Py bound to  $P\alpha\beta$ , and one catalytic site fully active; Figure 2.8, "taPDE-

A”) and activated  $\alpha_t$ . PDE inactivation would depend upon the intrinsic GTPase rate of transducin converting activated  $\alpha_t$ -GTP to inactive  $\alpha_t$ -GDP.

Persistent activation of the phototransduction cascade by continuous illumination or bright flashes of light causes cytoplasmic cGMP levels to remain below the  $K_D$  for the low affinity sites on taPDE long enough for cGMP to dissociate from the low affinity noncatalytic sites. P $\gamma$  dissociation will occur at the same rate because of the highly cooperative nature of P $\gamma$  and cGMP binding to PDE (Figure 2.8, “taPDE-B”). The P $\gamma$  that is released is known to serve as a GTPase-accelerating factor for  $\alpha_t$ -GTP—in combination with the Regulator of G-protein Signaling-9 (RGS-9) and the G-protein  $\beta_{5L}$  subunit (Arshavsky and Bownds, 1992; He et al., 1998; Makino et al., 1999). This would speed up transducin inactivation, diminish the amplitude of the light response, and act as a feedback regulator for light adaptation.

Our model predicts that the second catalytic subunit of the PDE holoenzyme remains relatively unaffected by activation of the rod phototransduction cascade, in terms of catalytic activation, P $\gamma$  release, or cGMP dissociation (Figure 2.8, right-hand subunit). Only under certain *in vitro* conditions does this subunit undergo changes in ligand binding or catalytic activity. A higher intrinsic affinity of this catalytic subunit for P $\gamma$  may account for this phenomenon.

Additional experiments are needed to test the hypothesis that the noncatalytic sites on PDE serve as a detector of the cGMP concentration in rod photoreceptors during light adaptation. Future work will focus on better understanding the properties of the low affinity noncatalytic sites on activated PDE, identifying the structural basis for catalytic

subunit heterogeneity, and examining whether the homodimeric cone PDE employs similar regulatory mechanisms in cone photoreceptors.

## CHAPTER 3

### ROLE OF THE 17 kDa $\delta$ PROTEIN AND IMMUNOLOGICALLY RELATED PROTEINS IN REGULATION OF PDE IN ROD PHOTORECEPTORS

#### Summary

In rod photoreceptors, the disk membrane is the site where photo-isomerization of rhodopsin by light leads to activation of the photoreceptor phosphodiesterase (PDE) by the heterotrimeric G-protein, transducin. The PDE holoenzyme ( $\alpha\beta\gamma_2$ ) has been reported to exist in both a membrane-attached and soluble form. Isoprenylation of the catalytic subunit C-termini confers disk membrane association to PDE, while soluble PDE is found to bind a 17 kDa  $\delta$  "subunit." It has been proposed that  $\delta$  translocates PDE from the disk membrane, reducing its ability to be activated by transducin, and desensitizing the photoresponse. Using purified, intact amphibian rod outer segment (ROS) suspensions whose physiological and biochemical properties are well-characterized, we examined the occurrence, abundance, and regulatory significance of the 17 kDa  $\delta$  protein to regulate PDE in rod photoreceptors. The frog homologue of  $\delta$  was cloned and sequenced from a frog retinal cDNA library, and shows 83% amino acid identity to mammalian  $\delta$ . All of the PDE in frog ROS is membrane-associated, but addition of recombinant frog  $\delta$  can solubilize PDE and prevent its activation by transducin.

Antibodies to  $\delta$  detect several proteins present in frog retinal homogenates, but the abundance of the 17 kDa protein compared to PDE in purified frog ROS is low ( $< 0.1 \delta$  per PDE). Similarly low ratios of  $\delta$  to PDE are observed in purified bovine ROS. Immunocytochemical results show that  $\delta$  is localized to several retinal cell types, but not to rod outer segments. Higher molecular weight  $\delta$ -immunoreactive bands observed in frog and bovine ROS were analyzed for specific binding to PDE with negative results. We conclude that frog rod photoreceptors do not utilize the 17 kDa  $\delta$  protein or immunologically related proteins to regulate phototransduction. Although we cannot rule out species differences in regulation of phototransduction pathways by  $\delta$  in mammalian and amphibian photoreceptors, our results suggest that  $\delta$  is not involved in phototransduction in ROS and that its function in the retina remains to be determined.

### **Introduction**

The surface of the disk membranes of the outer segment is the initial site of visual transduction in rod photoreceptors. Light entering the cell is absorbed by the visual pigment, rhodopsin. The activation of rhodopsin allows it to catalyze the exchange of GDP for GTP on the  $\alpha$ -subunit of the heterotrimeric G-protein, transducin ( $T\alpha$ ).  $T\alpha$ -GTP dissociates from  $T\beta\gamma$  and activates the effector enzyme of the pathway, phosphodiesterase (PDE). PDE hydrolyzes cGMP, closing the cGMP-gated ion channels and causing hyperpolarization of the cell [for recent reviews, see Pugh, Jr. and Lamb, (2000); Burns and Baylor, (2001)].

Rod photoreceptor PDE is composed of a catalytic dimer of  $\alpha$  and  $\beta$  subunits ( $P\alpha\beta$ ) and two identical inhibitory  $\gamma$  subunits ( $P\gamma$ ). The catalytic subunits each have one

active site and one high-affinity noncatalytic cGMP binding site within the regulatory GAF domain. Each catalytic subunit is post-translationally modified at its C-terminus with an isoprenyl group that confers its ability to bind to the disk membrane [for review, see (Cote, 2002)].

In bovine rod photoreceptor cells, a fraction of the total PDE is found in a soluble form (Gillespie et al., 1989; Florio et al., 1996), and co-purifies with a 17 kDa protein that was named the  $\delta$  subunit of PDE. PDE derived from cone photoreceptors also binds  $\delta$  and is not membrane-associated (Gillespie and Beavo, 1988). The bovine  $\delta$  protein is highly conserved among mammals (99% sequence identity), and homologous proteins are found in *C. elegans* (65% identity) and *D. melanogaster* (62% identity) (Florio et al., 1996; Li et al., 1998; Lorenz et al., 1998; Adams et al., 2000). Interestingly, while the  $\delta$  protein is highly expressed in the retina, it is also found in many other tissues that do not express photoreceptor PDE (Florio et al., 1996; Lorenz et al., 1998; Marzesco et al., 1998; Wang et al., 1999). Furthermore,  $\delta$  can specifically interact with other proteins unrelated to known phototransduction proteins, such as Rab13 (Marzesco et al., 1998), the retinitis pigmentosa GTPase regulator (Linari et al., 1999b), and the Arf-like protein Arl3 (Linari et al., 1999a).

Biochemical studies have shown that exogenous  $\delta$  can bind to bovine rod PDE with high affinity, and cause release of PDE from the disk membrane (Florio et al., 1996). This solubilization of PDE correlates with a decrease in the ability of transducin to activate PDE (Cook et al., 2001). The primary site of interaction of  $\delta$  with PDE is with the prenylated, methylated C-terminus of the catalytic subunits (Cook et al., 2000). It has been proposed that the ability of  $\delta$  to solubilize disk membrane-associated PDE in vitro

may be physiologically important as a desensitization mechanism during light adaptation (Cook et al., 2001).

To date, all studies of the  $\delta$  protein's interaction with photoreceptor PDE have been carried out using light-exposed, frozen bovine retinas from which ROS were isolated. Thus, the light history, degree of ROS purity, and extent of loss of ROS soluble proteins is difficult to control. To address the physiological role of  $\delta$  in regulating PDE during phototransduction, we focused on amphibian ROS for several reasons: (1) ability to control illumination conditions (diurnal light-dark cycle, dark versus light-adapted conditions); (2) ease of purification of osmotically intact frog ROS retaining the full complement of soluble and membrane proteins (Cote et al., 1984; Biernbaum and Bownds, 1985; Hamm and Bownds, 1986), and; (3) ability to correlate biochemical measurements with extensive electrophysiological data in the literature.

In this paper, we demonstrate that the frog 17 kDa homologue to the bovine  $\delta$  protein is expressed in frog retina, can bind to PDE, and releases it from the membrane *in vitro*. PDE solubilization by recombinant frog  $\delta$  is shown to directly correlate with uncoupling of transducin activation of PDE.  $\delta$  also has a significant effect on cGMP binding to the noncatalytic sites of PDE. However, quantitative analysis of the stoichiometry and localization of  $\delta$  in retina and in isolated ROS demonstrates that there is insufficient  $\delta$  to significantly affect the subcellular localization of PDE. Other  $\delta$ -immunoreactive proteins are present in retinal extracts and in purified ROS. A 36 kDa,  $\delta$ -immunoreactive protein that is released from disk membranes along with PDE was found to not interact with PDE with high affinity. These results cast doubt on the ability of  $\delta$  to regulate PDE during visual transduction.

## **Experimental Procedure**

*Materials*- Frogs (*Rana catesbeiana*) were obtained from Niles Biologicals, and maintained on a 12 h dark-light cycle for two weeks before use in experiments (Cote, 2000). Frozen bovine retinas were obtained from W.L. Lawson, and Ficoll-purified bovine ROS from freshly isolated retinas (Schnetkamp, 1981) were a kind gift of Dr. Paul Schnetkamp (University of Calgary). [<sup>3</sup>H]cGMP was from PerkinElmer Life Sciences. Membranes for filter binding assays and the polyvinylidene fluoride (PVDF) for immunoblotting were obtained from Millipore. Reagents and substrates for immunoblotting were from Pierce or from Bio-Rad. All other chemicals were obtained from Sigma. Bovine GST- $\delta$  expression plasmid was a kind gift from Drs. Terry Cook and Joe Beavo (University of Washington).

*Cloning and expression of frog  $\delta$* - A frog (*R. pipiens*) retinal cDNA library was prepared as described elsewhere (Li and Baehr, 1998). Frog  $\delta$  was cloned by screening the cDNA library using bovine  $\delta$  as a probe. The resulting clone, fpded1, contained a 2.7-kb cDNA insert in pBluescript SK. The 450 base pair coding region of  $\delta$  was PCR-amplified with primers 5'-GGATCCATGTCTAGTAATGAGCGA and 5'-GAATTCTCAAACATAAAACAGCCTG, containing Bam H1 and EcoR1 restriction sites. The resulting PCR product was inserted into the TOPO cloning vector and then transferred into the pGEX-KG expression plasmid. DNA sequencing of both strands confirmed the coding region to contain the authentic nucleotide sequence. The cloning of frog  $\delta$  was done by Ning Li and Wolfgang Baehr, University of Utah Health Center.



The pGEX-KG construct was transformed into the E.coli strain BL21 DE3. Overnight cultures were diluted 1:20 and grown at 37° until the OD<sub>600</sub> reached 0.7, at which point 1 mM isopropyl-β-D-thiogalactopyranoside was added to induce protein expression. Growth continued for 1 hour at 37°. Cells were pelleted by centrifugation, washed, and the resuspended cell pellet was sonicated. Centrifugation removed the membranes, and the extracted proteins were applied to a glutathione-agarose column, closely following established procedures. Bound GST-δ was eluted, concentrated by ultrafiltration (Millipore BioMax 15K MWCO filter) then cleaved with thrombin (4 hours at 37°). The thrombin was removed with the Thrombin Cleavage Capture Kit (Novagen). The δ was purified from GST by passage over a glutathione-agarose column, and the recombinant frog δ was concentrated by ultrafiltration (Millipore BioMax 5K MWCO filter). The concentration of δ was determined with a colorimetric protein assay (Smith et al., 1985) and agreed with spectrometric measurements at 280 nm. The purity of the protein was >95%, as judged by SDS-PAGE.

*Preparation of Rod Outer Segments (ROS)*- Osmotically intact frog ROS were purified on a discontinuous Percoll gradient exactly as described (Cote, 2000). Purified ROS were homogenized in a pseudointracellular medium [LIM: 77 mM KCl, 35 mM NaCl, 2.0 mM MgCl<sub>2</sub>, 1.0 mM CaCl<sub>2</sub>, 1 mM EGTA, 10 mM HEPES (pH 7.5), 2 mM dithiothreitol, 1 mM 4-(2-aminoethyl)benzenesulfonyl fluoride, 1 μM leupeptin, and 1 μM pepstatin]. Endogenous nucleotides were depleted by incubation of ROS homogenates in the dark at room temperature for 30 minutes. For ROS isolated from dark-adapted frogs, the rhodopsin concentration was determined using difference

spectroscopy (Bownds et al., 1971). The concentration of PDE in ROS from both dark-adapted and light-adapted frogs was determined by a cGMP filter binding assay (see below).

Bovine ROS from frozen retinas were purified in the dark on a discontinuous sucrose gradient as previously described (McDowell, 1993). In some cases, the sucrose-purified ROS were removed from the sucrose gradient, resuspended in Ringers, and then loaded on a discontinuous Percoll gradient for further purification. ROS were homogenized in LIM at 4° in the dark. The concentration of rhodopsin was determined by difference spectroscopy. PDE concentration was determined by measuring the maximum cGMP hydrolysis of the PDE upon limited trypsin proteolysis (see below).

Subcellular fractionation of ROS homogenates was performed by centrifugation for 3 minutes at  $110,000 \times g_{av}$  at room temperature using a Beckman Airfuge. The integral membrane protein, rhodopsin, was present in the supernatant at undetectable levels and >95% of the rhodopsin was recovered in the membrane pellet under this condition.

To hypotonically extract PDE, ROS homogenates were spun down to remove soluble proteins. The ROS membranes were washed in hypotonic buffer (5 mM Tris, 0.5 mM EDTA, 1 mM dithiothreitol) supplemented with 10 mM MgCl<sub>2</sub> to reduce the amount of peripheral membrane proteins. Three consecutive washes of the membranes with hypotonic buffer lacking MgCl<sub>2</sub> were done to extract the PDE from the membranes. The first wash included a 10 minute incubation on ice before centrifugation. To extract PDE using CHAPS detergent, ROS membranes were prepared as above, and then the membrane pellet was resuspended in LIM containing CHAPS (final concentration of 10

mM). This sample was incubated on ice for 10 minutes before centrifugation. Two more extractions of the membranes with 10 mM CHAPS were performed and the detergent-solubilized PDE pooled.

*Immunoblot analysis of the  $\delta$  protein in frog ROS-* Samples for immunoblot analysis were added to electrophoresis sample buffer, followed by SDS-PAGE on a 12% polyacrylamide gel. Proteins were transferred onto Immobilon-P<sup>SO</sup> polyvinylidene fluoride or nitrocellulose membranes. The membrane was blocked with 1% bovine serum albumin in TTBS (20 mM Tris pH 7.6, 137 mM NaCl, 0.5% Tween 20) prior to incubation with anti- $\delta$  antibodies. Anti- $\delta$  antibodies were generated in rabbits using the following immunogens: FL antibody: full-length bovine recombinant  $\delta$ ; FD antibody: a synthetic peptide consisting of a.a. 4-12 of the frog  $\delta$  sequence conjugated to KLH; BD antibody: a synthetic peptide consisting of a.a. 41-52 of the bovine  $\delta$  sequence. The antibodies were affinity purified over a  $\delta$ -Sepharose column, or by peptide-coupled beads. Antibodies to PDE catalytic subunits (NC; 1:10,000 dilution), and transducin  $\alpha$  subunit (Santa Cruz Biotech., 1:10,000 dilution) were also used. Antibody binding was detected using a goat anti-rabbit secondary antibody coupled to horseradish peroxidase (1:5000 dilution), followed by incubation of the membrane with peroxidase substrate (Pierce SuperSignal West Pico Chemiluminescent Light). For quantitative analysis of the  $\delta$  protein in frog and bovine ROS, a standard curve of known concentrations of recombinant frog or bovine  $\delta$  was run on the same gel as the sample of purified ROS. Quantitation of immunoreactive bands was performed with the image analysis program, Quantiscan (Biosoft).

*Immunocytochemistry*- Fresh bovine eyes were obtained from the slaughterhouse. The eyes were hemi-sected and the back portion of the eyecup was gently everted to expose the retina. This was immersed in 4% paraformaldehyde in 0.1 M phosphate buffer (pH 7.4). The eye was washed in ice-cold phosphate buffer and soaked in 30% buffered sucrose. Cryosectioning of the eye was performed, and the sections were exposed to primary antibody ( $\delta$ , FL). The sections were washed and a secondary antibody conjugated to a fluorescent marker was added. Digital images were acquired by a confocal microscope. Images were cropped, enlarged, and contrast-enhanced with Adobe Photoshop (Adobe Systems, San Jose, CA). Immunocytochemistry was performed by Dr. N. Vardi, University of Pennsylvania.

*cGMP binding and PDE activity assays*- The frog PDE concentration was routinely determined by quantitating [ $^3\text{H}$ ]cGMP binding to PDE under standard conditions where it has been established that 2 cGMP bind per PDE holoenzyme (Norton et al., 2000). In brief, PDE-containing samples were incubated for 10 min at room temperature with 1  $\mu\text{M}$  [ $^3\text{H}$ ]cGMP, 200  $\mu\text{M}$  zaprinast, and a 2-fold molar excess of  $\text{P}\gamma$ . Samples were filtered on pre-wet nitrocellulose filters, immediately followed by three 1-ml washes with ice cold LIM (Cote, 2000).

The rate of transducin-activated PDE hydrolysis was measured by a coupled-enzyme phosphate release assay (Cote, 2000).  $\text{GTP}\gamma\text{S}$  (equal in concentration to the amount of rhodopsin) was added to the PDE sample for 1 minute prior to the addition of 10 mM cGMP. For each experiment, rate measurements were obtained from at least 3 individual time points, during which time less than 30% of the substrate was consumed.

Measurements of the activity were made in the following buffer: 100 mM Tris (pH 7.5), 10 mM MgCl<sub>2</sub>, 0.5 mM EDTA, 2 mM dithiothreitol, and 0.5 mg/ml bovine serum albumin. This PDE enzyme assay was also used to determine the PDE content of various bovine ROS samples. In this instance, the bovine PDE was treated with trypsin to fully activate the enzyme ( $k_{\text{cat}} = 5600 \text{ s}^{-1}$ ) to estimate the enzyme concentration (Mou et al., 1999).

*Co-precipitation of PDE and  $\delta$*  - Four different antibodies were tested for their ability to immunoprecipitate  $\delta$  or  $\delta$ -like proteins. The FD, BD, and FL anti- $\delta$  antibodies were coupled to protein A beads prior to use. The ROS1 PDE antibody (Hurwitz et al., 1984) was coupled to Sulfolink beads (5 mg/ml). For immunoprecipitation, solubilized PDE was added to the antibody-coupled beads and incubated for 1-2 h at 4°. The beads were then washed with TMN buffer (10 mM Tris pH 7.5, 1 mM MgCl<sub>2</sub>, 300 mM NaCl, 1 mM dithiothreitol) three times, followed by elution of the bound proteins by boiling in 2X SDS-PAGE sample buffer. To minimize the elution of heavy or light antibody chains from the beads, 0.1 M glycine buffer pH 3 was also used to elute proteins from the beads.

To examine the binding of recombinant  $\delta$  to PDE by immunoprecipitation,  $\delta$  was added to ROS and incubated overnight to release PDE from the membrane. The supernatant was collected and incubated with ROS1 coupled to Sulfolink beads for at least 2 hours at 4° prior to washing and eluting the proteins bound to the beads. Alternatively, PDE binding to recombinant GST- $\delta$  and its release from its membrane-attached state was assayed by using glutathione-agarose beads to pull down GST- $\delta$  and any proteins to which it was bound.

*Gel filtration chromatography of hypotonic extracts of frog ROS-* Hypotonically extracted PDE was chromatographed on a Superdex 200 (Amersham Pharmacia Biotech) column equilibrated in: 5 mM Tris (pH 8), 0.5 mM EDTA, 10 mM NaCl, 1 mM dithiothriitol, 0.2 mM Pefabloc. 0.3 ml fractions were collected. PDE elution was determined by an activity assay. The protein-containing fractions were precipitated with 3.5% TCA, incubated for 5 minutes at room temperature, and then centrifuged. The pellets were resuspended in Laemmli gel sample buffer and heated to 80° for 10 minutes. The proteins in the fractions were examined by western analysis. A standard curve for the molecular weight calibration of the Superdex 200 was done using the Molecular Weight Marker Kit for gel filtration chromatography range 29,000-700,000 (Sigma).

### **Results and Discussion**

*Frog retina contains a 17 kDa protein homologous to the bovine rod photoreceptor  $\delta$  protein.* To identify the frog retinal homologue of the mammalian 17 kDa  $\delta$  protein, a *Rana pipiens* retinal cDNA library was screened using the bovine  $\delta$  nucleotide sequence as a probe. A clone containing the complete coding region (450 base-pairs) of frog  $\delta$  was identified and sequenced. The deduced amino acid sequence for frog  $\delta$  represents a protein of 149 amino acids, one shorter than mammalian  $\delta$  (Figure 3.1). The amino acid sequence of frog  $\delta$  is 80% identical (90% similarity) to known mammalian  $\delta$  sequences, indicating that this protein is highly conserved through vertebrate evolution. Substantial sequence homology (60-70% sequence

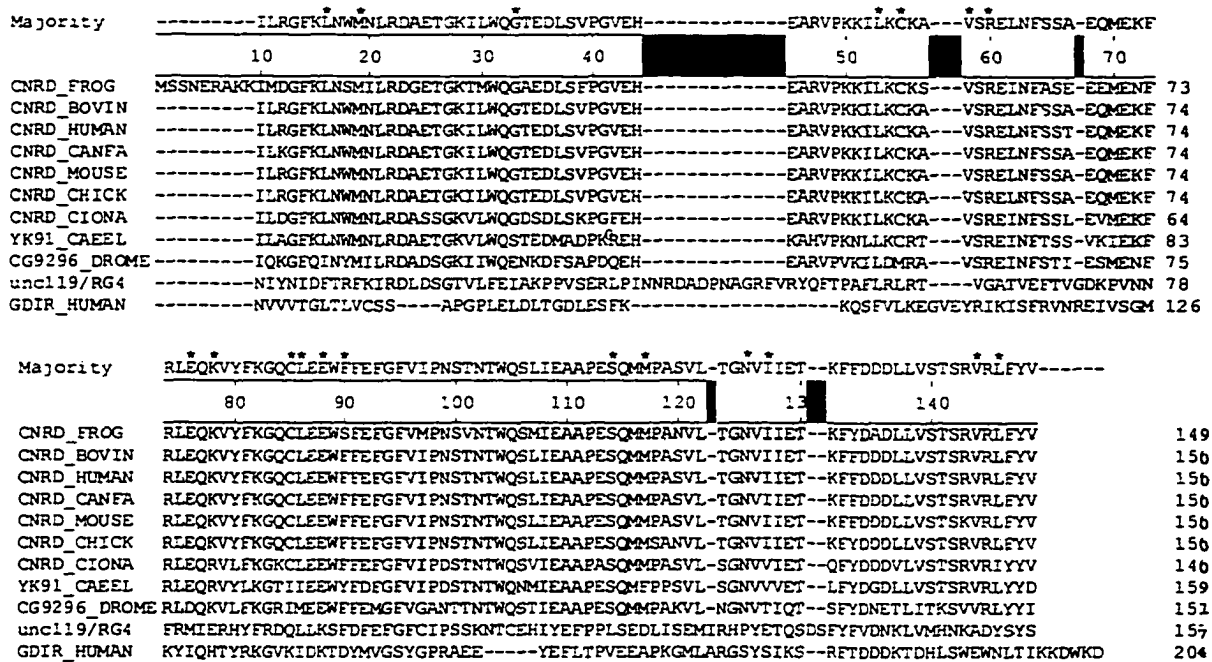


Figure 3.1. The frog  $\delta$  sequence is homologous to other  $\delta$  proteins. The deduced amino acid sequence of frog  $\delta$  was obtained from the nucleotide sequence (deposition Genbank AY044177). Multiple sequence alignment with known  $\delta$  and  $\delta$ -like proteins was performed using CLUSTALW (default options). The following  $\delta$  sequences were aligned for evaluation of the conserved amino acid residues: human  $\delta$ , Q43924; mouse  $\delta$ , AAC40094; dog  $\delta$ , AAD54058; bovine  $\delta$ , Q95142; *C. elegans*  $\delta$ , Q18268; *D. melanogaster*  $\delta$ , AC015134; chicken  $\delta$ , derived from EST AL588430, and *Ciona intestinalis*  $\delta$ , AB079881. The consensus sequence for uncl19/RG4 was obtained from analysis of 8 sequences currently available in GenBank. The RhoGDI sequence is GDIR\_HUMAN, and the residues forming the prenyl binding pocket (Hoffman et al., 2000) are indicated with \*.

identity) of frog  $\delta$  with three invertebrate orthologues of  $\delta$  is also evident when these sequences are aligned (Figure 3.1). Phylogenetic analysis indicates that sequence divergence of  $\delta$  agrees with the order of general evolutionary divergence, where amphibians diverged earlier in time than mammals and birds.

Other proteins closely related to  $\delta$  have been identified, namely uncl19/RG4 (Higashide et al., 1996) and RhoGDI (Nancy et al., 2002). Based on comparisons of the predicted secondary structure and the pattern of hydrophobic residues in the three

proteins, a structural homology model based on the isoprenyl binding domain of RhoGDI has been proposed (Nancy et al., 2002). This prenyl binding pocket consists of all but the extreme N-terminus of  $\delta$ , whereas the larger unc119/RG4 and RhoGDI proteins incorporate this domain in their C-terminal region. Figure 3.1 also include the consensus sequence for unc119/RG4 derived from alignment of 8 sequences available in GenBank, as well as the sequence for human RhoGDI.

Several residues of the RhoGDI prenyl binding pocket are conserved in the  $\delta$  protein sequence. Thus, secondary structural information of the  $\delta$  protein can be inferred by comparison to the RhoGDI crystal structure analysis (Hoffman et al., 2000). It was proposed that the  $\delta$  protein folds similar to the C-terminal immunoglobulin-like domain of RhoGDI, creating a hydrophobic pocket. In RhoGDI, this pocket is where the geranylgeranyl moiety of the small GDI protein inserts. The existence of this pocket in the  $\delta$  protein is consistent with several results (Marzesco et al., 1998; Linari et al., 1999b; Linari et al., 1999b), including the ability of  $\delta$  to release membrane-bound PDE (Florio et al., 1996). However,  $\delta$  interaction with non-prenylated proteins such as the retinitis pigmentosa GTPase regulator, RPGR (Linari et al., 1999b) and the Arf-like protein Arl3 (Linari et al., 1999a) that are localized to various tissues, may occur through a region (amino acids 44-52) that is not conserved in RhoGDI (Nancy et al., 2002).

The majority of the  $\delta$  sequence is involved in forming the isoprenyl binding domain. Unc119/RG4 is a 25 kDa protein that also contains sequence similarity in the isoprenyl binding domain. Thus, these three proteins RhoGDI, Unc119/RG4, and  $\delta$  may form a family of proteins whose role includes membrane trafficking of proteins through



interactions at this isoprenyl binding domain. The short sequence of  $\delta$  suggests that it may be the basic prototype for this family.

*Recombinant frog  $\delta$  binds to and releases frog PDE from ROS membranes.* To test whether frog  $\delta$  retains the biological activity reported for the mammalian homologue, we expressed recombinant frog  $\delta$  in *E. coli* as a GST-fusion protein. Purification of the fusion protein by glutathione-agarose affinity chromatography yielded 4 mg of GST- $\delta$  per liter of bacterial culture. The apparent molecular weight of the GST- $\delta$  was 43 kDa, running as a single band on SDS-PAGE. After cleavage of the GST portion with thrombin and re-purification, the resulting 17 kDa  $\delta$  was >95% pure, and migrated identically to native frog  $\delta$  on SDS-PAGE.

To test whether frog  $\delta$  retained the ability to solubilize membrane-bound PDE, we added increasing amounts of recombinant frog  $\delta$  to ROS homogenates. The soluble proteins were separated from the membranes by centrifugation. In contrast to bovine ROS where 20-30% of the total PDE is found in the soluble fraction (Gillespie et al., 1989), purified frog ROS have essentially no PDE in the soluble fraction ( $1.0\% \pm 0.2\%$ ;  $n = 5$ ). Addition of increasing amounts of frog  $\delta$  can release up to 100% of the PDE from ROS membranes in a dose-dependent manner (Figure 3.2). The effectiveness with which frog  $\delta$  releases frog PDE from the disk membrane is comparable to previously reported values for bovine PDE solubilization (Florio et al., 1996). In both cases, a 4-6-fold excess of  $\delta$  relative to PDE is needed to solubilize 50% of the total enzyme. The  $IC_{50}$  of frog

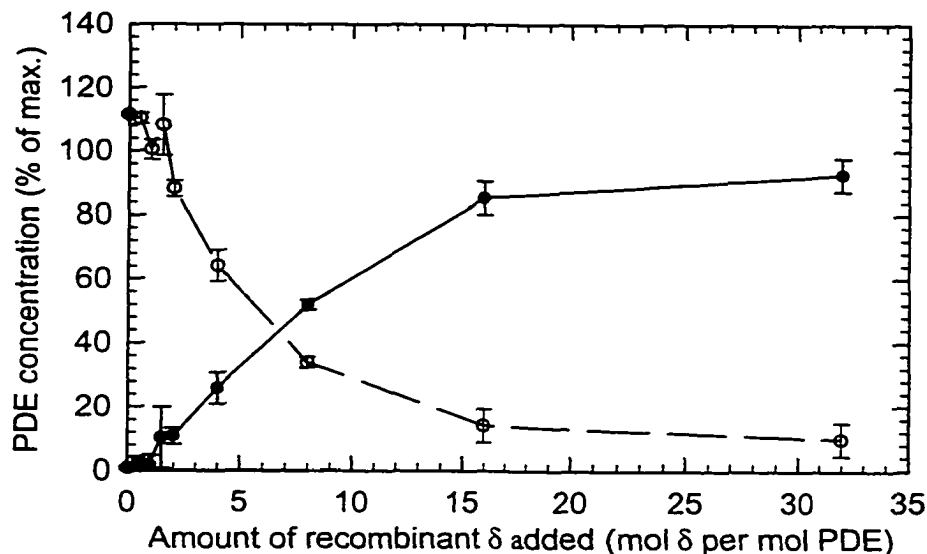


Figure 3.2. Frog  $\delta$  releases PDE from ROS membranes. Frog ROS homogenates (20–40 nM PDE) were incubated with increasing amounts of recombinant frog  $\delta$  overnight at 4°. Samples were centrifuged to separate solubilized (●) from membrane-associated (○) PDE. The amount of PDE in each sample was determined by the cGMP binding stoichiometry (see Methods). Data are mean  $\pm$  S.E.M. for 6 separate experiments.

PDE release from ROS membranes is  $128 \pm 11$  nM recombinant frog  $\delta$  (20–40 nM PDE, 4°). The time needed for  $\delta$  to exert its solubilizing effect on membrane-bound PDE is slow: only one-third of the total PDE is released after 5 h incubation of  $\delta$  with ROS at 4°, compared to 100% release after 24 h. The slow release of membrane-associated PDE by  $\delta$  is not explained by a slow incorporation of  $\delta$  into ROS membranes, since immunoblot analysis shows no increase in 17 kDa  $\delta$ -immunoreactivity in ROS membranes following addition of exogenous  $\delta$ . Thus, recombinant  $\delta$  does not bind to ROS membranes but rather slowly exerts a direct effect on PDE to solubilize this enzyme.

To test whether recombinant  $\delta$  remains bound to PDE following its release from the disk membranes,  $\delta$ -solubilized PDE was immunoprecipitated with the PDE catalytic

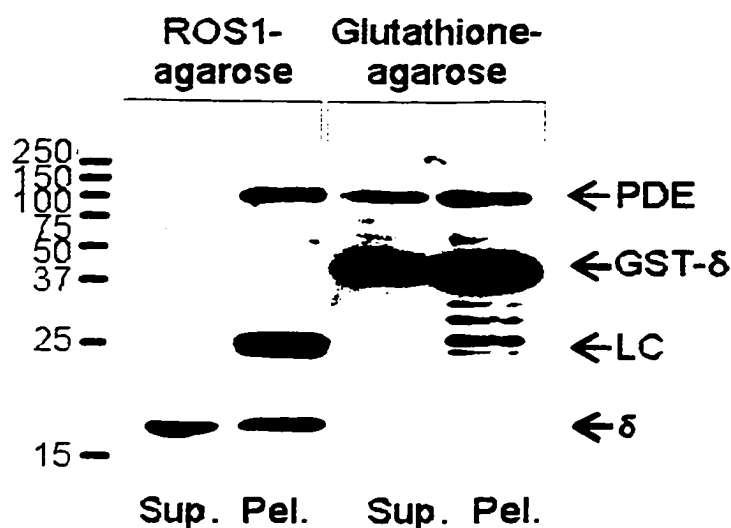


Figure 3.3. Frog  $\delta$  binds to PDE upon releasing it from the disk membranes. Frog ROS homogenates were incubated with either recombinant frog  $\delta$  or GST- $\delta$  overnight. PDE that was solubilized by treatment with 8  $\delta$  per PDE was immunoprecipitated with ROS1-agarose beads, while PDE incubated with 30 GST- $\delta$  per PDE was pulled down with glutathione-agarose beads. The supernatants and pellets were analyzed after a brief spin. The immunoblot was probed with antibodies to  $\delta$  (FD) and PDE (NC).

subunit antibody, ROS1 (Hurwitz et al., 1985). All of the solubilized PDE was pulled down with the PDE antibody, along with recombinant  $\delta$  (Figure 3.3). In a similar experiment, we incubated frog ROS membranes with recombinant GST- $\delta$ , which also solubilizes PDE effectively. After adding glutathione-agarose beads to the soluble PDE, we were able to co-precipitate PDE bound to the GST- $\delta$  (Figure 3.3). Thus,  $\delta$  does not act catalytically to release PDE from the membrane-associated state, but rather remains in a complex with PDE following solubilization.

*Effects of  $\delta$  on cGMP binding and transducin activation of frog PDE.* Membrane-associated bovine PDE contains two high affinity cGMP binding sites in its GAF domains, but one of these sites does not exchange its bound cGMP with free cGMP.

Addition of exogenous  $\delta$  to bovine rod PDE converts this nonexchangeable cGMP binding site to an exchangeable site, but the overall binding affinity for cGMP is unaltered by  $\delta$  binding (Mou et al., 1999). In comparison, frog PDE also has two high-affinity noncatalytic cGMP binding sites, but both of them readily exchange bound cGMP (Cote et al., 1994). To examine the effects of  $\delta$  on frog PDE GAF domains, binding of 1  $\mu$ M [ $^3$ H]cGMP was measured as a function of the amount of  $\delta$  added. No increase in the exchange rate of bound cGMP was observed following  $\delta$  addition. However, addition of recombinant  $\delta$  decreased by up to 25% the maximum binding of cGMP to the noncatalytic sites of frog PDE (data not shown). An 8-fold excess of  $\delta$  relative to PDE was needed to observe this 25% decrease in cGMP binding, consistent with the efficacy of  $\delta$  to solubilize frog PDE. Because of the positive cooperativity between cGMP binding and the  $P\gamma$  subunit interaction with PDE, we next examined whether  $\delta$  could influence  $P\gamma$  affinity for PDE. Addition of increasing amounts of  $\delta$  to nonactivated PDE had minor effects on the basal rate of PDE, suggesting little effect of  $\delta$  on the interaction of  $\gamma$  with the catalytic sites. However, the ability of  $\delta$  to affect cGMP binding to frog and bovine PDE suggests that the mechanism of  $\delta$  binding to the isoprenylated C-terminus induces an allosteric change in the catalytic subunit that is reflected in a local conformational change in the GAF domains. This significance of this effect is not clear at present.

A proposed role for  $\delta$  in phototransduction is to release PDE from the membrane, preventing its association with transducin, thereby causing a decrease in the maximum transducin activation of PDE (Cook et al., 2001). To test the relevance of this hypothesis for frog ROS, nonactivated frog ROS homogenates were incubated overnight with

recombinant  $\delta$ , and then assayed for the maximal PDE activation by transducin. A reduction in the maximum transducin-activated PDE rate correlated with the release of PDE from the membrane into the supernatant (Figure 3.4). We found that there was a 70% decrease in the maximum transducin-activated PDE rate with the addition of a large molar excess of  $\delta$ . The  $IC_{50}$  for suppression of transducin activation of PDE was similar to the  $IC_{50}$  for solubilization of PDE (Figure 3.4). This uncoupling of transducin

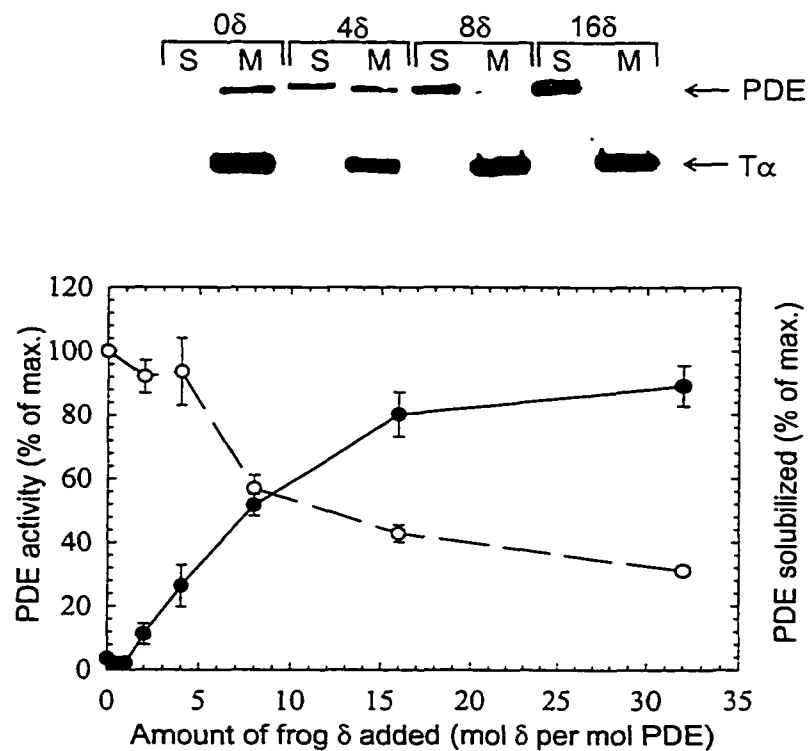


Figure 3.4.  $\delta$  decreases the ability of transducin to fully activate PDE. Light-exposed ROS homogenates (40 nM PDE) were incubated with increasing amounts of recombinant frog  $\delta$  overnight at 4°. GTP $\gamma$ S (12.8  $\mu$ M) was added to one portion to determine the maximum extent of PDE activation (o). The remainder (lacking GTP $\gamma$ S) was centrifuged to measure the extent of PDE solubilization ( $\bullet$ ). Western analysis of the nonactivated PDE samples shows that while the PDE is solubilized from the membranes by recombinant  $\delta$ , T $\alpha$  remains membrane-bound. The immunoblot was probed with a mixture of the PDE (NC) and transducin (T $\alpha$ ) antibodies. Graph shows the average  $\pm$  SEM for 3 separate experiments.

activation of PDE by  $\delta$  is not accompanied by solubilization of the transducin  $\alpha$  subunit, since immunoblots show no release of T $\alpha$  upon  $\delta$  addition (Figure 3.4), in agreement with previous results (Cook et al., 2001). We conclude that in order for there to be efficient activation of PDE, PDE must be attached to the membrane in proximity with the membrane-associated transducin. These *in vitro* results are consistent with the hypothesis that  $\delta$  could desensitize the phototransduction pathway by regulating the subcellular localization of PDE.

*Sub-stoichiometric levels of the  $\delta$  protein are found in frog ROS.* In order for  $\delta$  to solubilize the entire pool of PDE in the rod outer segment,  $\delta$  must be present in stoichiometric amounts relative to PDE. This is because  $\delta$  remains in a complex with PDE following solubilization (Figure 3.3). To determine the concentration of  $\delta$  in ROS, we performed immunoblot analysis using anti- $\delta$  antibodies. When frog retinal homogenates, crude ROS preparations, or Percoll-purified ROS were separated by SDS-PAGE, several  $\delta$ -immunoreactive bands were detected on immunoblots, including the expected  $\delta$  band at 17 kDa (Figure 3.5). In retinal homogenates and crude ROS, the most abundant  $\delta$ -immunoreactivity was seen with proteins of 17 and 33 kDa, with additional bands of lower intensity. However, purification of frog ROS on a Percoll gradient to obtain osmotically intact outer segments removes the majority of the 17 kDa immunoreactivity. This suggests that most of the  $\delta$ -immunoreactivity seen in retinal homogenates and crude ROS is of non-ROS origin.

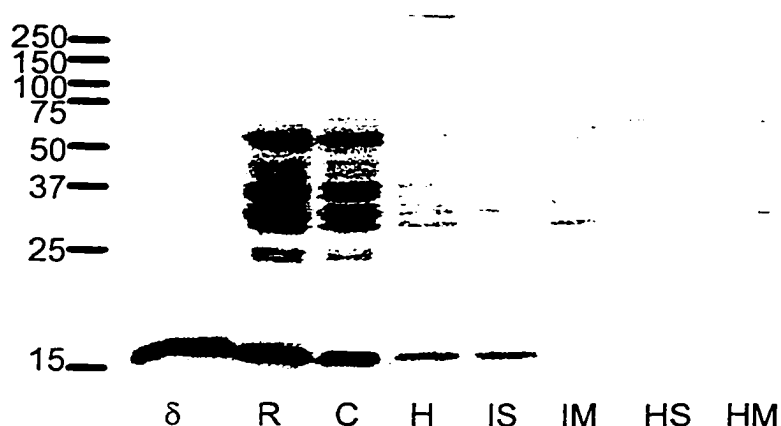


Figure 3.5. Little  $\delta$  co-purifies with intact frog ROS. Frog ROS were purified on a Percoll gradient to examine the localization of the 17 kDa  $\delta$  protein. Samples (1 pmol PDE per lane) tested were: R, retinal homogenate; C: crude ROS; H, purified ROS homogenate. Soluble proteins (IS) were separated from ROS membranes (IM) by high-speed centrifugation in the light. The membranes were resuspended with 10 mM  $MgCl_2$  and re-centrifuged to obtain a supernatant (MS) portion. PDE was released by a magnesium-free hypotonic solution (see Methods) and centrifuged to obtain a supernatant (HS) and membrane (HM) fraction. The affinity purified FL  $\delta$  antibody was used for the western analysis.

To quantify the amount of  $\delta$  present in ROS, we compared the amount of 17 kDa immunoreactivity in ROS samples to known amounts of recombinant, purified frog  $\delta$  applied to the same gel. We found only  $0.03 \pm 0.005$  mol  $\delta$  per mol PDE in purified frog ROS (Table 3.1). In contrast, the unpurified retinal homogenate contains  $0.62 \pm 0.05$  mol  $\delta$  per mol PDE. The small amount of  $\delta$  detected in ROS suggests that most of the 17 kDa protein in the frog retina is expressed in other cells of the retina or in a portion of the photoreceptor cell other than its outer segment.

Because >95% of PDE from frog ROS is membrane-bound (Norton et al., 2000), we next determined the subcellular localization of  $\delta$  by centrifugation. Fractionation of ROS homogenates in an isotonic medium demonstrates that most of the 17 kDa  $\delta$  protein is soluble (Figure 3.5, lane IS). The fact that most  $\delta$  is soluble, while PDE is membrane-

associated, indicates that the low levels of  $\delta$  present in intact frog ROS are not sufficient to solubilize a significant portion of the PDE. Other  $\delta$ -immunoreactive bands detected in ROS homogenates were found to localize to either the isotonic soluble or membrane fractions. A small amount of the  $\delta$  protein remains membrane-associated at all times including when PDE is extracted with hypotonic buffer or 10 mM CHAPS. When large amounts of the hypotonic extract are examined by western analysis, 36 kDa and 90 kDa  $\delta$ -immunoreactive proteins are seen (Figure 3.7B). However, a portion of each of these proteins is not extracted and can be found in the membrane fraction following hypotonic extraction.

We considered the possibility that different expression levels or sub-cellular localization of  $\delta$  might result from the light history of the retinas prior to isolation. No differences were observed in either the  $\delta$  content of frog ROS or its subcellular localization when comparing dark-adapted versus illuminated conditions or subjective day versus subjective night conditions (data not shown).

These results with frog ROS led us to re-evaluate whether the concentration of  $\delta$  in bovine ROS is similar to our results reported above. Quantitative immunoblot analysis using recombinant bovine  $\delta$  standards on the same gel as bovine ROS samples reveal low levels of  $\delta$  in sucrose-purified bovine ROS from frozen retinas (Table 3.1;  $0.05 \pm 0.001$  mol  $\delta$  per mol PDE;  $n = 3$ ). Bovine retinal homogenates contain ~10 fold greater amounts of  $\delta$  ( $0.44 \pm 0.044$  mol  $\delta$  per mol PDE;  $n = 8$ ), suggesting a non-ROS origin for much of the 17 kDa  $\delta$  protein in both amphibian and mammalian retinas. Overall, the number and relative intensity of  $\delta$ -immunoreactive bands in bovine ROS are qualitatively similar to



*Table 3.1: Content of  $\delta$  and PDE in purified ROS*

Source and purification	total [ $\delta$ ] ( $\delta$ /PDE)	% $\delta$ soluble	% PDE soluble
Fresh frog ROS/Percoll	$0.03 \pm 0.005$ n = 5	>80%	1%
Frozen bovine ROS/sucrose	$0.05 \pm 0.01$ n = 3	25%	4%
Fresh bovine ROS/sucrose	$0.07 \pm 0.001$ n = 2	67%	35%
Fresh bovine ROS/Ficoll	$0.1 \pm 0.008$ n = 3	70%	30%

Table 3.1. Quantitation of  $\delta$  in ROS. The amount of  $\delta$  in purified bovine and frog ROS was determined by western analysis. ROS samples were loaded on SDS-PAGE along with known amounts of  $\delta$ . The samples were transferred to PVDF membrane for immunoblot analysis (FL antibody 1:20,000). The amount of  $\delta$  in each ROS sample was determined by Quantiscan. Data represents mean  $\pm$  S. E. M. for n determinations. The concentration of PDE was determined by cGMP binding for frog PDE, and by activity measurements for bovine PDE.

those in frog ROS. (Unlike Figure 1A of Cook et al. (Cook et al., 2000), we did not observe these bands to be artifacts associated with the secondary antibody.)

The amount of  $\delta$  found in our purified bovine ROS from frozen bovine retinas was less than expected based on previously published results (Cook et al., 2000). To examine whether the results we obtained were due to the fact that the retina's were frozen prior to purification of the ROS, we obtained sucrose- and Ficoll-purified ROS from fresh bovine retinas (a kind gift of Dr. Paul Schnetkamp, University of Calgary) (Schnetkamp, 1981). Table 3.1 shows that the freshly isolated bovine ROS contained slightly more  $\delta$  than found in the frozen ROS samples, possibly due to disruption of photoreceptor cell integrity upon freezing and thawing the retinas. However, the overall amount of  $\delta$  in fresh bovine ROS is much lower than the amount of PDE present, consistent with our

original observations in both frog and bovine ROS. The subcellular location of the  $\delta$  in fresh bovine ROS is also similar to the data obtained from frog ROS. The main difference between the two species examined is the amount of soluble PDE from each preparation. The results obtained here suggest that the amount of membrane association is not due to the  $\delta$  protein, since the ratio between  $\delta$  and PDE in both species are similar and the effect seen by exogenous  $\delta$  also is consistent. It is possible that the PDE in bovine ROS contain a higher level of carboxymethylation than that in frog ROS. Cook et al. (2000), show that PDE that is released by the  $\delta$  protein contains a higher level of C-terminal carboxymethylation at the site of prenylation.

*Localization of  $\delta$  in the retina by immunocytochemistry.* Previous research showed the localization of the  $\delta$  protein in bovine retina exclusively to the rod outer segment portion of the retina (Florio et al., 1996). However, the antibody that was used for the immunocytochemistry results was not the same one presented in the paper showing  $\delta$  localization on immunoblots. Thus, it is possible that the immunocytochemistry results reflect some  $\delta$ -immunoreactive proteins other than  $\delta$ . The relative lack of  $\delta$  found in the outer segment of the frog and bovine retina convinced us to reexamine the localization of the  $\delta$  protein in the retina.

Figure 3.6A shows the results of immunocytochemistry of a bovine retina with the FL  $\delta$  antibody (red) used throughout this chapter for immunoblot analysis and double labeling with an antibody raised to red/green opsin antibody to which detects cone cells (COS; green). The scattered immunoreactivity in the outer segment layer (OS) of the retina is consistent with cone cells than the more abundant rod cells. The yellow

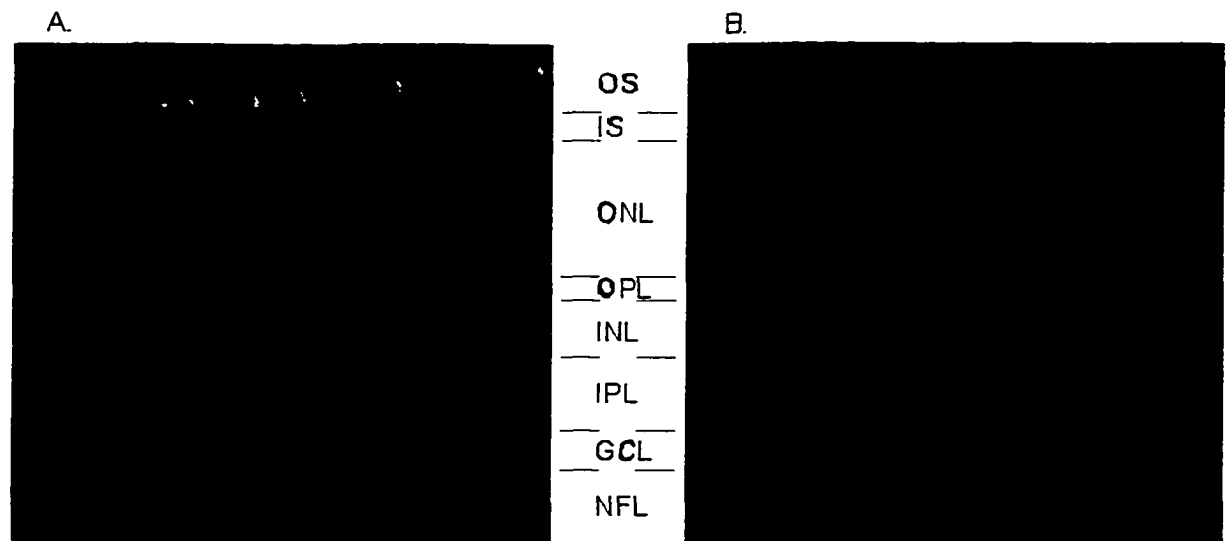


Figure 3.6. Localization of the  $\delta$  protein in bovine retina. Fresh bovine eyes were hemi-sectioned, everted and fixed in 4% paraformaldehyde. The eyes were washed in phosphate buffer, and incubated in buffered sucrose. Cryosections were performed, and the sections treated with primary antibody. Panel A was probed with FL ( $\delta$  antibody) and COS (cone opsin antibody). Panel B was probed with COS. The secondary antibody used was conjugated to a fluorescent marker. Pictures were taken on a confocal microscope. The layers of the retina are: outer segments (OS), inner segments (IS), outer nuclear layer (ONL), outer plexiform layer (OPL), inner nuclear layer (INL), inner plexiform layer (IPL), ganglion cell layer (GCL), and the neural fiber layer (NFL). This work was performed by N. Vardi, University of Pennsylvania.

fluorescence shows cells that contain both cone opsin and  $\delta$  protein. Figure 3.6B shows immunoreactivity of the cone cells alone by probing with COS. Interestingly, there are three other cell layers that show  $\delta$  immunoreactivity (red), the inner segments (IS), inner nuclear layer (INL) and ganglion cell layer (GCL). The wide distribution of  $\delta$  in various retinal cells is consistent with the quantitative immunoblot analysis we presented above. This suggests that the  $\delta$  we see in our frog ROS preparations could be a contaminant from either cone cells, or possibly the inner segment of rod cells. However, this

immunocytochemistry is a preliminary experiment and more needs to be done to examine  $\delta$  localization, including controls for nonspecific labeling and co-localization of  $\delta$ -immunoreactivity with photoreceptor-specific antibodies. Specificity of the antibody will be examined by blocking the retina with recombinant  $\delta$  prior to the antibody incubation. We also need to repeat the immunocytochemical localization of  $\delta$  in the frog retina to ensure that the results for the two species are the same.

*Co-purification of  $\delta$ -immunoreactive proteins with PDE in frog ROS.* There was more  $\delta$  immunoreactivity seen in higher molecular weight proteins than with the 17 kDa band in purified frog ROS (Figure 3.5). We therefore questioned whether PDE was interacting with other  $\delta$ -like proteins present in frog ROS. We started by examining whether any  $\delta$ -immunoreactive proteins co-purified with PDE when it is released from the membrane by hypotonic extraction. Treating washed ROS membranes with a hypotonic buffer extracts ~60% of the PDE, but the very small amount of 17 kDa  $\delta$  remains membrane-associated under this condition (Figure 3.5). Detergent extraction of washed ROS membranes with 10 mM CHAPS releases 90% of the PDE, but not  $\delta$  (data not shown). However, a 36 kDa protein which is membrane-bound under isotonic conditions can be co-extracted with PDE upon treatment of ROS membranes with a hypotonic buffer (Figure 3.5, HS). Immunoblots with other anti- $\delta$  antibodies were consistent with the results in Figure 3.5 with the FL  $\delta$  antibody.

Due to the co-solubilization of PDE and the 36 kDa  $\delta$ -immunoreactive protein observed in frog ROS, we sought to determine whether this protein binds to PDE. When

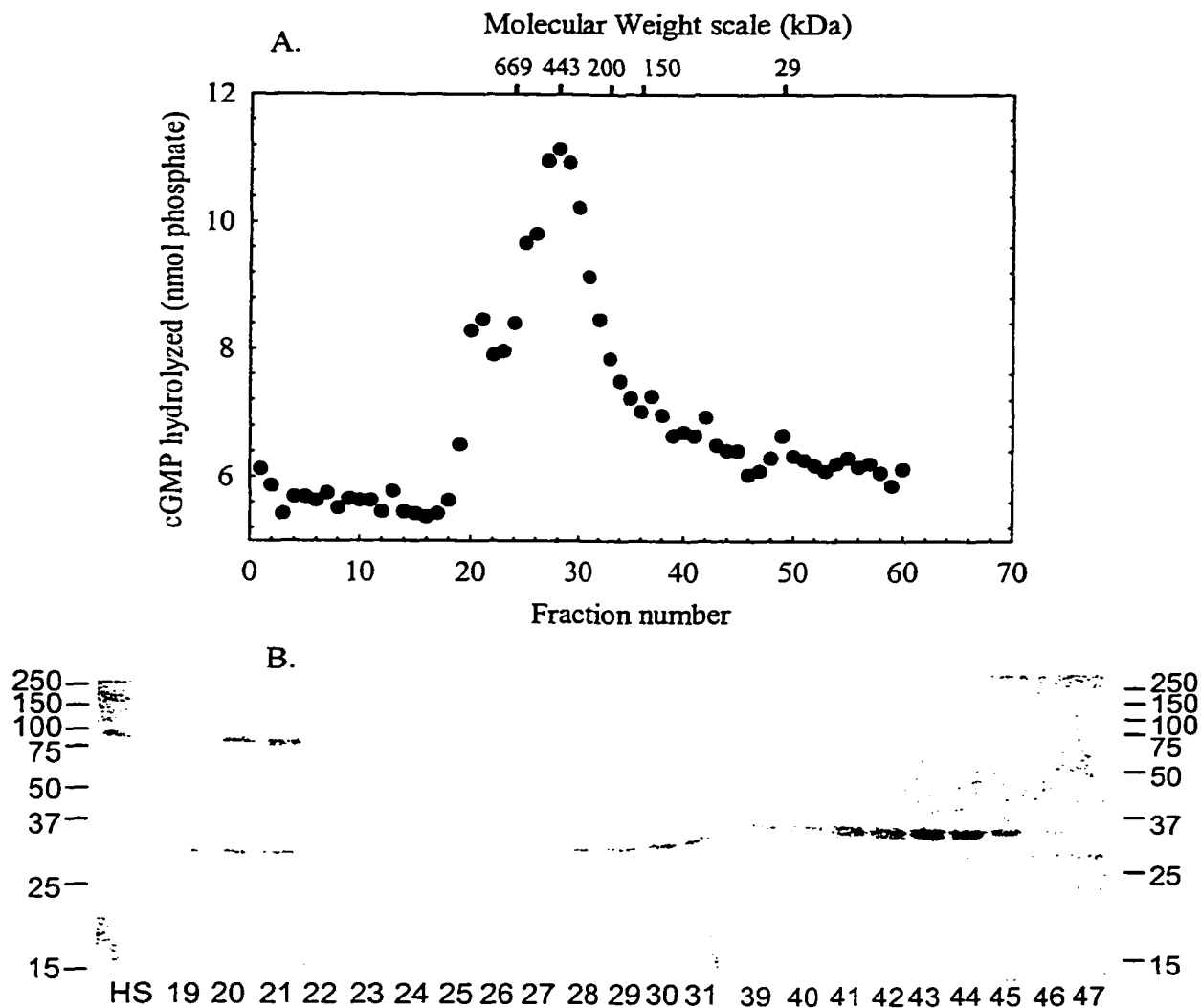


Figure 3.7. PDE does not associate with the 36 kDa  $\delta$ -immunoreactive protein. Frog PDE was hypotonically extracted from purified ROS (HS) and 29 pmol were loaded on a gel filtration chromatography column. 0.3 ml fractions were collected and portions assayed for PDE activity (panel A). The remainder was concentrated, proteins separated by SDS-PAGE, and immunoblots probed with FL antibodies (panel B).

we hypotonically extracted PDE and the 36 kDa protein from ROS membranes, and immunoprecipitated PDE with ROS1-Sulfolink beads, PDE was quantitatively precipitated while the 36 kDa protein remained in the supernatant (data not shown). To further investigate whether a  $\delta$ -immunoreactive protein was binding to PDE, gel filtration

chromatography was performed using hypotonically extracted PDE. The fractions were analyzed by a PDE activity assay to determine where the PDE eluted (Figure 3.7). The apparent  $M_r$  for hypotonically extracted frog PDE on the Superdex 200 column was 410 kDa. This suggests that either PDE does not behave as a globular protein on the column, or that the PDE holoenzyme ( $M_r$  220,000) exists in a complex with other ROS proteins under these conditions. The latter possibility is supported by Coomassie staining of the PDE peak revealing additional, unidentified proteins co-eluting with PDE (data not shown). Most of the 36 kDa  $\delta$ -immunoreactivity eluted at  $\sim$ 60 kDa.

Gel filtration of PDE solubilized from ROS membranes by exogenous  $\delta$  showed a similar apparent molecular weight to that seen in Figure 3.7. The majority of the  $\delta$  and PDE co-eluted from the column, demonstrating that the PDE- $\delta$  interaction was of sufficient affinity to remain in a complex during gel filtration. In contrast, PDE released from ROS membranes by trypsin proteolysis had an apparent  $M_r$  of 196 kDa. The failure to detect significant binding of  $\delta$ -immunoreactive proteins by either ROS1 immunoprecipitation or gel filtration chromatography makes it unlikely that PDE is regulated by binding of  $\delta$  or a  $\delta$ -like protein to the C-terminal, isoprenylated catalytic subunits of PDE.

### **Conclusions**

The results presented here suggest that  $\delta$  is not a subunit of PDE due to its low abundance and lack of binding to PDE in rod photoreceptor cells. Preliminary evidence from immunocytochemistry suggests that  $\delta$  may be localized to cone and other retinal cells, but not the rod outer segments. The wide tissue distribution of the  $\delta$  protein

suggests a more wide-spread role as a prenyl binding protein, possibly directing intracellular targeting of prenylated proteins.  $\delta$  also interacts with non-prenylated proteins (Linari et al., 1999b; Linari et al., 1999a), so additional contact sites besides the prenyl binding pocket are likely. The PDZ recognition sequence at its extreme C-terminus also presents the possibility of serving to dock prenylated proteins into signaling complexes.

Our comparative analysis of frog and bovine ROS samples suggests that the presence and abundance of  $\delta$  in amphibian and mammalian retina are similar, consistent with the high degree of conservation of other phototransduction components. It is likely that the designation of the  $\delta$  protein as a subunit of PDE was premature, and if it has a role in visual transduction, it is likely to be limited to cone cells.

## CHAPTER 4

### **BINDING OF ROD OUTER SEGMENT PROTEINS TO PHOSPHODIESTERASE: POTENTIAL ROLES IN REGULATING VISUAL TRANSDUCTION**

#### Summary

Phosphodiesterase (PDE) is the central enzyme of visual transduction. Proteins such as  $\gamma$ ,  $\delta$  and GARP have all been shown to bind to PDE, and besides the well-studied  $\gamma$  subunit, other proteins may also serve to regulate the enzyme *in vivo*. We found that the interaction between  $\gamma$  and  $P\alpha\beta$  is very strong, such that a fragment of  $\gamma$  remains bound to trypsin-proteolyzed frog PDE after dilution and purification by gel filtration chromatography. Limited trypsin proteolysis of the  $\gamma$  subunit at 0.02 nM PDE resulted in a catalytic rate of  $7870 \pm 150$  mol cGMP/PDE/sec for frog PDE, about twice the transducin-activated rate. Due to the fact that proteolysis could cause an increased rate of hydrolysis, a method to nonenzymatically remove  $\gamma$  was developed. The rate by this method was  $7000 \pm 180$  mol cGMP/PDE/sec, demonstrating that trypsin did not significantly alter the enzymatic properties of PDE during limited proteolysis.

It has been proposed that phosphorylation of the  $\gamma$  subunit can regulate PDE during phototransduction. To test this, we developed a method to extract and purify  $\gamma$  from rod outer segments. Cell homogenates incubated in 30% acetonitrile/0.1% TFA and then heated to 75° for 5 minutes were able to release 100% of  $\gamma$  for subsequent analysis. Solid phase purification on a Sep-Pak column eluted the  $\gamma$  at 40% acetonitrile/0.1% TFA.



Besides  $\gamma$ , other proteins in ROS bind to PDE. Gel filtration chromatography of solubilized frog PDE showed co-elution of a number of different proteins with PDE, suggesting that PDE may exist in a multi-protein signaling complex. Specific proteins that eluted in the PDE-containing fractions ran at 74 kDa, 65 kDa, 55 kDa, 50 kDa, and 43 kDa.

One candidate protein that could serve as a scaffold to form protein complexes with PDE is the  $\delta$  protein. Co-precipitation of ROS extracts with immobilized  $\delta$  pulled down PDE and several other proteins, providing support for the idea that PDE exists in a multi-component signaling complex in ROS. One of these proteins may also serve as a direct target for  $\delta$  in ROS, since the large excess of PDE over  $\delta$  makes it unlikely that the major function of  $\delta$  is to directly regulate PDE.

## **Introduction**

### *1. Mechanism of transducin activation of PDE*

PDE is a heterotetramer composed of two catalytic subunits,  $P\alpha$  and  $P\beta$ , as well as two identical inhibitory subunits,  $\gamma$ . In the dark-adapted state,  $\gamma$  maintains PDE inactivity by physically blocking the active site (Takemoto et al., 1993; Artemyev et al., 1998). Upon light exposure, activated transducin ( $T\alpha$ -GTP) binds to  $\gamma$  and  $P\alpha\beta$ , pulling  $\gamma$  away from the catalytic site, allowing cGMP to enter and become hydrolyzed. The stoichiometry of  $T\alpha$  binding to PDE upon activation is controversial. It was widely accepted that there were two binding sites for  $T\alpha$  on PDE (Clerc and Bennett, 1992; Pagès et al., 1993). However, in order to obtain complete activation of PDE, a large excess of  $T\alpha$ -GTP must be added for reconstituted systems, or activated for ROS

membrane experiments (Wensel and Stryer, 1986; Bennett and Clerc, 1989; Malinski and Wensel, 1992). This suggests that there could be a heterogeneity in the  $T\alpha$  activation of PDE, possibly due to the membrane binding of  $T\alpha$  as this is correlated to activation (Fung and Nash, 1983; Melia et al., 2000). The large excess of  $T\alpha$  necessary to obtain complete activation has made it difficult to determine both the stoichiometry of  $T\alpha$  binding to PDE, as well as the stoichiometry of  $T\alpha$  required for complete activation of PDE. One possibility is that there is cooperative binding of two  $T\alpha$  to PDE for full activation of PDE (Whalen and Bitensky, 1989; Bruckert et al., 1994). It is also possible that full activation of PDE requires only one  $T\alpha$ -GTP and the second PDE catalytic site remains inactive. Melia et al. (Melia et al., 2000) showed that complete activation of bovine PDE in reconstituted membranes occurs upon stoichiometric levels of  $T\alpha$  and PDE.

In order to understand the activation of PDE by transducin, we first must have a complete understanding of the behavior of the catalytic dimer ( $P\alpha\beta$ ) lacking the inhibitory  $\gamma$  subunits. Limited trypsin proteolysis of the  $\gamma$  subunits will be examined, but there is a concern that the proteolysis could alter the catalytic or regulatory properties of  $P\alpha\beta$  (Hurley and Stryer, 1982). Thus, these results will be compared to  $P\alpha\beta$  prepared nonenzymatically, although there are limitations to this approach since previous attempts have not released all of the  $\gamma$  (Yamazaki et al., 1990). The high affinity interaction between  $\gamma$  and  $P\alpha\beta$  has made it difficult to get a complete characterization of the catalytic dimer  $P\alpha\beta$ , as well as an accurate measurement for the binding affinity of  $\gamma$  for  $P\alpha\beta$  (Yamazaki et al., 1990; Yamazaki et al., 1996b; Arshavsky et al., 1992). Indeed, there is some question as to whether or not  $\gamma$  is released from mammalian PDE, or whether it is

simply displaced from the active site of  $P\alpha\beta$  (Whalen and Bitensky, 1989; Whalen et al., 1990).

*2. Extracting  $\gamma$  from cell extracts to evaluate the significance of post-translational modifications of  $\gamma$*

Based on sequence analysis of  $\gamma$ , it has been proposed that phosphorylation or ADP-ribosylation of the inhibitory  $\gamma$  subunit may regulate the activity of PDE in vivo. Visual transduction is a highly regulated process, and these reversible modifications could occur during times of adaptation when the rod cell is completely saturated or exposed to a low level of background light.

To address the physiological significance of post-translational modification of the  $\gamma$  subunit, we had to extract the  $\gamma$  from purified ROS for chemical analysis. Previous approaches to extracting  $\gamma$  from purified mammalian PDE or from bovine ROS membranes used heat, acetic acid, or a combination of heat and formic acid to release  $\gamma$  (Hurley and Stryer, 1982; Wensel and Stryer, 1986; Hayashi et al., 1991). To extract  $\gamma$  from illuminated amphibian ROS homogenates, washes with GTP were done to release  $T\alpha$ -GTP in a complex with  $\gamma$ , followed by reverse-phase HPLC to purify the  $\gamma$  (Yamazaki et al., 1980; Yamazaki et al., 1983; Yamazaki et al., 1990). For the purpose of examining light-induced modification of the  $\gamma$  subunit, methods to extract the  $\gamma$  directly from dark-adapted frog ROS had to be developed. There are many proteins that are soluble in frog ROS, and others that may be released under the conditions of  $\gamma$  extraction. Thus, it would be helpful to enrich for  $\gamma$  prior to MS-fingerprinting. One common method that is used to

further purify and concentrate proteins is to use a solid phase matrix. It is also easily combined with reverse-phase HPLC which can further purify the desired protein.

### *3. Identifying proteins which associate with PDE to form a signaling complex*

The  $\gamma$  subunit is not the only protein believed to regulate PDE. Photoreceptor PDE is unique in having C-terminal isoprenyl modifications that bind it to the disk membranes.  $P\alpha$  contains a farnesyl group while  $P\beta$  has a geranylgeranyl group (Anant et al., 1992). This membrane association makes it difficult to determine proteins that bind to PDE. Previous research has examined the role of some key PDE-binding proteins and the situations under which they bind to PDE. It has been found that  $T\alpha$  in its non-activated state is capable of binding to PDE, although with lower affinity (Gray-Keller et al., 1990; Kutuzov and Pfister, 1994). It is possible that PDE exists in a complex with several proteins, allowing for an accelerated response to light activation. Indeed, the interaction of PDE with several proteins may be dependent on light exposure (Maftei et al., 2000). For example, GARP2 (glutamic acid-rich protein) is believed to bind to PDE during bleaching adaptation, to prevent cGMP hydrolysis when the rod cells are completely saturated (Körschen et al., 1999).

There are several different ways to characterize PDE binding proteins. Extraction of PDE from the membranes could disrupt protein-protein interactions under some conditions, so a comparison of several methods should be examined. PDE can be released from ROS membranes using a hypotonic buffer (Emeis et al., 1982), or with 10 mM CHAPS detergent (Maftei, 2000). An alternate way to release PDE from the membrane is to incubate overnight with a 15-fold excess of  $\delta$  protein over PDE (Norton

and Cote, 2001). Varying the method of extraction (hypotonic, detergent, or  $\delta$  protein) will help identify artifacts that might occur with any one extraction method. Alternate methods of PDE purification should also be examined. Immunoprecipitation, gel filtration, and pull-down assays can all be used for separating PDE from proteins that are in solution but not associated with PDE. Once proteins have been identified by protein staining, they can be characterized by western analysis or by mass spectroscopy.

#### 4. *Investigation of $\delta$ binding proteins in ROS*

In mammalian retinas, ~30% of the PDE exists in a soluble form bound to a protein called  $\delta$  (Gillespie et al., 1989; Florio et al., 1996). It is believed that  $\delta$  binds to PDE at its C-terminus, releasing it from the disk membranes of the rod outer segment where transducin is localized, and preventing the enzyme from being activated upon light exposure (Cook et al., 2000; Cook et al., 2001; Norton and Cote, 2001). Recently, several published studies have proposed that  $\delta$  may play a general role in signal transduction due to its wide tissue distribution (Florio et al., 1996; Marzesco et al., 1998). The majority of  $\delta$  expression is found in the retina, but its presence in the brain and adrenal glands suggests that the role of the  $\delta$  protein exists in all nerve cells, and not specifically as a regulator of PDE in photoreceptor cells (Florio et al., 1996). The C-terminus of the  $\delta$  protein encodes for a putative PDZ binding domain (Marzesco et al., 1998) which could bind to many different proteins. PDZ-containing proteins are often located to microdomains on a specific plasma membrane (Marzesco et al., 1998). It was found that deletion of the PDZ domain of  $\delta$  destroys the membrane localization of  $\delta$  in epithelial cells (Marzesco et al., 1998).

Alignment of the  $\delta$  sequence with RhoGDI, a protein involved in regulating membrane association of Rho and Rab GTPases (Hoffman et al., 2000), shows 24% sequence identity in the known prenyl binding domain (Nancy et al., 2002). This is consistent with the observation of that  $\delta$  has been shown to solubilize Rab13, a geranylgeranylated Ras-related protein, in addition to  $P\alpha\beta$  (Marzesco et al., 1998). The ability of  $\delta$  to solubilize RPGR (Linari et al., 1999b) and Arl3 (Linari et al., 1999a), two non-prenylated proteins, could occur through the PDZ-binding domain of  $\delta$  or possibly in a region of  $\delta$  that diverges significantly from RhoGDI (Marzesco et al., 1998; Nancy et al., 2002). The large variety of proteins that bind to  $\delta$  also suggest that  $\delta$  may play a role in scaffolding by allowing proteins to come together as a complex.

Chapter 4 addresses the regulation of PDE by PDE-binding proteins, with a strong focus on the  $\gamma$  subunit. Several experimental results encouraged us that further analysis was necessary to fully understand the interaction of  $\gamma$  with  $P\alpha\beta$ . First of all, the literature contained no convincing measurements for the maximum catalytic activity of frog rod  $P\alpha\beta$  and whether the activity of transducin and trypsin activated PDE are equal. Our results demonstrate that one of the  $\gamma$  subunits is not displaced from the catalytic site upon transducin activation of frog PDE. Second, in pilot experiments to investigate the phosphorylation of  $\gamma$  we developed a method by which *in vivo* levels of  $P\gamma$  phosphorylation could be measured. Third, we carried out preliminary experiments to identify possible regulatory interactions of PDE with other proteins using gel filtration chromatography. Finally, to examine the potential role of  $\delta$  in rod photoreceptors, the chapter concludes with studies of  $\delta$  binding proteins that are present in ROS.

## **Materials and Methods**

*Materials.* Frogs (*Rana catesbeiana*) were purchased from Niles Biologicals.

Membranes for filter binding assays were obtained from Millipore. [<sup>3</sup>H]cGMP was purchased from PerkinElmer Life Sciences. Immunoblotting reagents, substrates and nitrocellulose and PVDF membranes were purchased from Pierce or BioRad. All other chemicals were obtained from Sigma.

*Preparation of purified rod outer segments (ROS).* *Rana catesbeiana* were decapitated in the dark and the eyes were dissected under infrared light. The retinas were removed and osmotically intact ROS were purified on a discontinuous Percoll density gradient as previously reported (Cote, 2000). The cells were homogenized with a mortar and pestle at 4° (Dumke et al., 1994). Pseudointracellular medium (LIM) was used for most cell preparations: 77 mM KCl, 35 mM NaCl, 2.0 mM MgCl<sub>2</sub>, 1.0 mM CaCl<sub>2</sub>, 10 mM HEPES (pH 7.5), 2 mM dithiothreitol, 1 mM 4-(2-aminoethyl)benzenesulfonyl fluoride, 5 μM leupeptin, and 1 μg/ml pepstatin. The concentration of rhodopsin was measured by difference spectroscopy (Bownds et al., 1971). An alternative buffer was used when PDE activity measurements were done (see below). Endogenous nucleotides were eliminated by incubation of the homogenized ROS in the dark for 30 minutes at room temperature. The amount of PDE in the sample was determined by a cGMP binding assay (see below).

Bovine ROS from frozen retinas were purified under infrared light on a discontinuous sucrose gradient (McDowell, 1993). ROS were homogenized at 4° in an isotonic medium (25 mM Tris pH 7.5, 30 mM NaCl, 60 mM KCl, 2 mM MgCl<sub>2</sub>, 1 mM

DTT, mammalian protease inhibitor cocktail) . The amount of PDE was determined by an activity assay.

*Preparation of recombinant  $\gamma$ .* Bovine recombinant  $\gamma$  was expressed in *Escherichia coli* and purified as previously reported (Granovsky et al., 2000). The final purity of the  $\gamma$  protein was found to be >97% by Coomassie staining on acrylamide gels. The concentration of the  $\gamma$  subunit was determined by spectroscopy and correlated with its ability to inhibit trypsinized PDE activity upon addition of 2 mol  $\gamma$  per mol PDE (Cote, 2000). The activity assays and spectroscopy results agreed to within 10% for all of the experiments in these studies.

*Preparation of recombinant frog GST- $\delta$ .* Recombinant frog  $\delta$  was prepared as described in the Methods section of Chapter 3. The protein was produced in *E. coli* as a GST-fusion protein. The GST was removed from  $\delta$  using a thrombin cleavage kit, followed by purification on a glutathione column. The final sample was concentrated by ultrafiltration and stored in 50% glycerol at  $-20^{\circ}$ .

*PDE activity assays.* The amount of cGMP hydrolyzed by trypsinized, transducin-activated, and  $\gamma$ -depleted  $P\alpha\beta$  was measured by a phosphate release assay as previously described (Cote, 2000). The buffer used for this assay (TEM) contained: 20 mM Tris (pH 7.5), 10 mM  $MgCl_2$ , 0.5 mg/ml bovine serum albumin. The assay was done in a 96 well plate by addition of 10 mM cGMP to the activated PDE-containing samples. The



measurements were taken at a time when less than 30% of the total cGMP was consumed.

*cGMP binding assays.* PDE binds cGMP with high affinity to two noncatalytic cGMP binding sites. Since it is the only photoreceptor protein to bind cGMP with high affinity, measurements of [<sup>3</sup>H]cGMP binding to frog PDE allow estimates of the active PDE concentration (Cote, 2000). 1 μM [<sup>3</sup>H]cGMP was added to PDE preparations in the presence of 200 μM zaprinast (to prevent cGMP hydrolysis) and incubated for 10 min at room temperature. 10 μl portions were then filtered through a pre-wet 0.45 μm nitrocellulose filter and washed with ice-cold pseudointracellular medium. Filters were shaken in scintillation fluid (Ultima Gold) for 20 minutes and radioactivity was measured in a Packard scintillation counter.

*Gel filtration of frog PDE.* Purified frog ROS homogenates were pelleted by centrifugation (3 minutes; 110,000  $g_{av}$ ). Isotonic soluble proteins were removed and the pellet was washed in hypotonic buffer containing 10 mM MgCl<sub>2</sub> (Hypotonic buffer: 5 mM Tris-HCl (pH 8), 0.5 mM ethylenediamine-tetraacetic acid, 1.0 mM dithiothreitol, and mammalian protease inhibitor cocktail) to remove any remaining soluble proteins. The membranes were then extracted three consecutive times with hypotonic buffer lacking Mg<sup>2+</sup> to release PDE from the membranes. The first extraction included a 10 minute incubation on ice prior to pelleting the membranes. The concentration of PDE in the hypotonic extract was determined by cGMP binding and cGMP hydrolysis. The PDE-containing extract was then chromatographed on a Superdex 200 gel filtration

column at 0.5 ml/min equilibrated in 5 mM Tris-HCl (pH 8), 0.5 mM ethylenediamine-tetraacetic acid, 10 mM NaCl, 1 mM DTT and mammalian protease inhibitor cocktail. 0.3 ml fractions were collected for analysis. PDE-containing fractions were determined by measuring cGMP hydrolysis of a portion of the fraction that had been exposed to trypsin on ice for 10 minutes. To concentrate the proteins in the fraction, the desired fractions were precipitated with 3.5% TCA. The TCA was added for 5 minutes at room temperature then centrifuged (3 min at 12,000 rpm) to pellet precipitated proteins. The supernatant was removed and the pellet resuspended in gel sample buffer. The samples were neutralized using 1 M Tris-HCl (pH 8).

*Preparation of P $\alpha\beta$ .* For these experiments, P $\alpha\beta$  was made by trypsin proteolysis or by nonenzymatic removal of the inhibitory  $\gamma$  subunits. For trypsin proteolysis, a time course of trypsin addition was used to determine the amount of trypsin and the length of time of proteolysis needed for each preparation (Figure 4.1). PDE was added to TEM buffer and incubated on ice. Trypsin was added, the sample was mixed and remained on ice throughout proteolysis. The trypsin proteolysis was quenched by the addition of soybean trypsin inhibitor, either by addition of a small amount of the PDE to the trypsin inhibitor, or by adding a 6-fold excess (compared to trypsin amount) to a large amount of trypsinized PDE. The samples were then brought to room temperature prior to cGMP addition. To ensure accurate results, three time points of cGMP hydrolysis were measured for each of the trypsinized PDE samples.

For non-enzymatic preparations of P $\alpha\beta$ , several different methods were examined for their ability to release  $\gamma$  from P $\alpha\beta$  (See Results, Table 4.1). Purified, nucleotide-

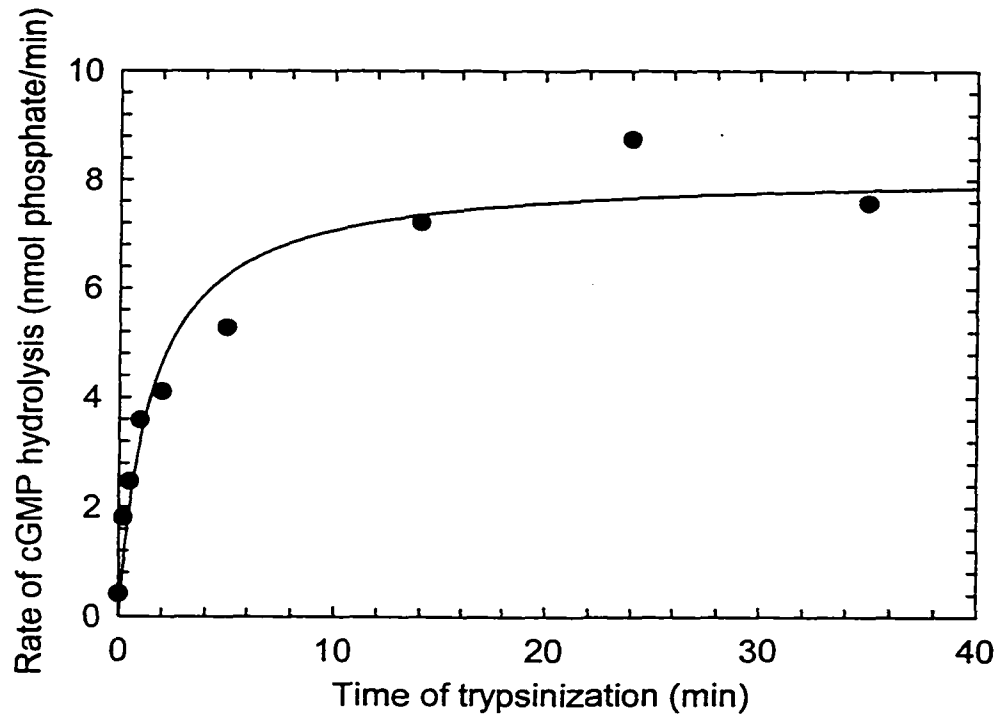


Figure 4.1. Time course of frog PDE trypsinization. Trypsin (50  $\mu\text{g/ml}$ ) was added to purified frog ROS (114.1 nM PDE) on ice. Trypsin activity was quenched by adding 10  $\mu\text{l}$  PDE into 90  $\mu\text{l}$  of soybean trypsin inhibitor (50  $\mu\text{g/ml}$ ). Samples were diluted with TEM and brought to room temperature. cGMP was added and three time points were taken for each of the different trypsin proteolysis lengths. The rate values plotted correspond to the linear regression of the cGMP incubation time points.  $V_{\text{max}}$  for the experiment was 4770 cGMP/PDE/sec ( $[\text{PDE}_{\text{final}}] = 10.3 \text{ nM}$ ).

depleted frog ROS were exposed to light in LIM. GTP $\gamma$ S was added for a 1 hour incubation at 4 $^{\circ}$  to allow  $\gamma$  to be released from P $\alpha\beta$ . Membranes were pelleted in the centrifuge at 110,000  $\times g_{\text{av}}$ . The supernatant was discarded, and the process was repeated to release more  $\gamma$  from P $\alpha\beta$ . The amount of  $\gamma$  remaining on PDE was determined by its ability to bind [ $^3\text{H}$ ]cGMP, since the P $\alpha\beta$  lacking  $\gamma$  do not bind cGMP in the noncatalytic sites. The total concentration of PDE in the sample was determined by measuring [ $^3\text{H}$ ]cGMP binding in the presence of a molar excess of recombinant  $\gamma$ .

*Purification of  $\gamma$  using the Sep-Pak column.* The cartridge was solvated in 10 ml of acetonitrile, then flushed with 10 ml of 10 mM Tris, pH 7.5. Next, the  $\gamma$ -containing sample was loaded on the cartridge and washed with 5 ml of 10 mM Tris. The  $\gamma$  was eluted with 0.2 ml fractions of the following solvents: 10 % acetonitrile/0.1% TFA, 40% acetonitrile/0.1% TFA, and 100% acetonitrile/0.1% TFA. This procedure was routinely used in the lab for purification of  $\gamma$ . The amount of  $\gamma$  recovered from the column was determined by spectrophotometry (OD<sub>277</sub>) or by its ability to inhibit trypsinized PDE.

*Pull-down assay of proteins binding to immobilized  $\delta$ .* To measure the binding of ROS proteins to  $\delta$ , two similar methods were used to immobilize  $\delta$  to beads. In the first approach, 67  $\mu$ g of GST- $\delta$  was added to 20  $\mu$ l of glutathione-agarose beads. The sample mixed at 4° for 1.5 hours before centrifuging the beads (5 min. at 12,000 rpm). The beads were washed with TMN buffer (TMN buffer: 50 mM Tris pH 7.5, 0.1 M NaCl, 0.5 mM MgCl<sub>2</sub>) prior to the addition of ROS extracts (extracted using 10 mM CHAPS or hypotonic buffer). After incubating at 4°, samples were centrifuged and the supernatants were collected (unbound fraction). The beads were washed with TMN buffer three times and then the  $\delta$ -binding proteins were eluted with 10 mM reduced glutathione in 10 mM Tris (pH 8). The samples were TCA precipitated, resuspended in Laemmli gel sample buffer, neutralized, and heated to 80° for 10 minutes prior to being analyzed by SDS-PAGE. Any proteins remaining on the beads were collected by adding Laemmli SDS-PAGE gel sample buffer and heating the sample to 80° for 10 minutes. The specificity of protein binding to immobilized  $\delta$  protein was determined in two ways. First, ROS

extracts were incubated with beads lacking bound  $\delta$ . Second, an excess of GST- $\delta$  was added to the ROS sample during the incubation to compete with the  $\delta$ -beads.

A second set of experiments utilized  $\delta$  covalently coupled to beads.  $\delta$  (cleaved from its fusion partner by thrombin proteolysis) was coupled to CNBr-activated beads following the manufacturer's instructions. Untreated sites were blocked by incubating the beads with 0.1 M ethanolamine for an hour at room temperature. The beads were then washed and stored in 0.02% sodium azide. These beads were then used in the same manner as described above to pull down  $\delta$  binding proteins from ROS extracts. To eliminate nonspecific binding of proteins to the  $\delta$ -beads more completely, 0.1% Triton X-100 was added to the sample during incubation and to the wash buffer (wash buffer: 50 mM Tris-HCl pH 8, 0.1% Triton X-100, 0.5 M NaCl).

For experiments testing bovine ROS extracts, bovine PDE was hypotonically extracted from purified ROS membranes as described above for frog PDE hypotonic extraction. Detergent extraction of PDE resulted from addition of 10 mM CHAPS to resuspended bovine ROS membranes in isotonic buffer. This was repeated 3 times and the extracts from each were pooled together as one sample.

## **Results and Discussion**

*The conditions of trypsin proteolysis of  $\gamma$  greatly affects the maximum PDE activity.* To better understand  $\gamma$  binding to  $P\alpha\beta$ , the catalytic dimer itself must be studied. One common method for preparing  $P\alpha\beta$  is by trypsin proteolysis of the enzyme (Hurley and Stryer, 1982). When the PDE holoenzyme ( $P\alpha\beta\gamma\gamma$ ) is exposed to trypsin, the  $\gamma$  subunits

are cleaved ( $P\alpha\beta$ ) and the C-terminus of PDE is also cleaved, causing PDE to be released from the disk membrane (Oppert et al., 1991; Catty et al., 1992). The maximum rate measurements for trypsin-activated PDE were found to be greater than for transducin activation (Norton et al., 2000). There is wide variation in the literature for the  $k_{cat}$  value for trypsinized and transducin-activated PDE, although generally trypsin activates PDE to a greater extent than transducin activation (Pugh, Jr. and Lamb, 1993).

While examining trypsin proteolysis of PDE (tPDE) as a method of preparing  $P\alpha\beta$ , we found that the concentration of PDE at the time of the trypsin proteolysis greatly affected the activity of the enzyme, such that the lower the concentration of the PDE at the time of trypsinization, the higher the maximal catalytic activity. However, if the PDE was trypsinized at a high concentration ( $>100$  nM PDE) and subsequently diluted prior to assaying the activity, an increase in maximum activity was also seen (Figure 4.2). The fact that the proteolysis and assay conditions alter the catalytic rate obtained may account for the variation seen in the literature for the maximum catalytic rate of trypsinized frog PDE (Whalen and Bitensky, 1989; Whalen et al., 1990; Yamazaki et al., 1996a; D'Amours and Cote, 1999). Interestingly, the maximum activity observed by trypsinization was about 7500 cGMP/PDE/sec. The maximum  $k_{cat}$  for transducin-activated PDE (taPDE) was found to be 4400 cGMP/PDE/sec (D'Amours and Cote, 1999; Norton et al., 2000).

These differing values for the maximal rate of tPDE and taPDE could arise from a number of different circumstances. First, it could be that transducin is only activating one of the two catalytic sites on PDE. However, trypsinization of PDE should result in a

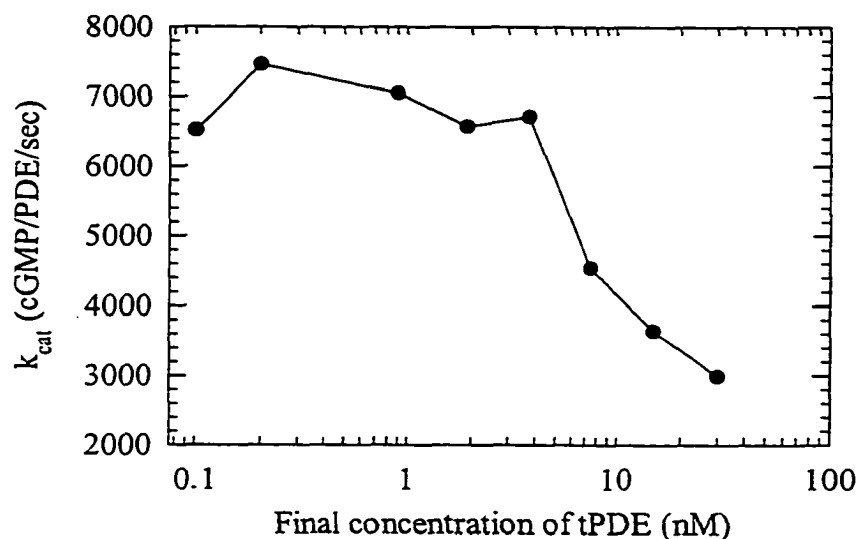


Figure 4.2. Dilution of trypsinized PDE gives a higher maximum catalytic activity. Frog ROS homogenates (120 nM PDE) were trypsinized on ice with 0.2 mg/ml trypsin for 10 minutes. The reaction was quenched with 1.25 mg/ml STI. The trypsinized PDE was diluted to the indicated concentrations. Three time points of cGMP incubation were used to obtain the  $P\alpha\beta$  rate measurements. This graph is representative of 2 separate experiments.

$k_{cat}$  exactly twice the  $k_{cat}$  of tPDE, which is not the case. It is possible that transducin activation of PDE completely activates one catalytic site, and slightly (10-20%) activates the second site.

An alternate scenario could be that  $T\alpha$ -GTP activates each catalytic site equally, but not to 100%. This would result in any ratio of activation by transducin, including a maximal observed rate of 60% the tPDE  $k_{cat}$ . Thus, equal activation of each catalytic site agrees with the results we obtained.

Alternatively, negative cooperativity could also account for the result, if activation at one site makes activation of the second site less likely. We also cannot rule out from our studies the presence of diverse populations of PDE ( $P\alpha\beta$ ,  $P\alpha\alpha$ ,  $P\beta\beta$ ). This

scenario could provide the exact maximum rates we found, with each population contributing differently to the final value.

One hypothesis is that the maximum rate for trypsin-proteolyzed PDE should be 8800 cGMP/PDE/sec, and that not all of the  $\gamma$  inhibition was abolished. Figure 4.1 shows that the PDE has been trypsinized to its maximal activity. However, it is possible that a fragment of the  $\gamma$  subunit remains after trypsin proteolysis of PDE that would inhibit catalysis to some extent. Analysis of the trypsin cleavage sites (using Protein Parameters in EXPASY) predicts that a fragment (aa 45/46-87) containing the inhibitory C-terminus is formed. To test this, the different samples of diluted tPDE used in Figure 4.2 were subsequently transducin activated by addition of GTP $\gamma$ S, but no further increase in activity was seen. However, results presented in Chapter 3 would suggest that PDE released from the membrane upon trypsinization removes it from the vicinity of T $\alpha$ -GTP.

The C-terminus of  $\gamma$  is the primary region involved in inhibition of cGMP catalysis. Addition of a  $\gamma$  antibody to the C-terminal region of  $\gamma$  might be expected to compete with P $\alpha\beta$  for  $\gamma$  binding and subsequently activate the enzyme. However, when trypsinized PDE was incubated with an excess of C-terminal  $\gamma$  antibody, no increase in tPDE activity was observed (data not shown).

*Upon trypsinization, frog PDE retains a fragment of  $\gamma$  that is not removed by dilution of the sample.* To examine whether there was truly a tryptic fragment (specifically 45/46-87) of  $\gamma$  that did not dissociate from P $\alpha\beta$  upon trypsin proteolysis, we tried purifying the trypsinized PDE by ultrafiltration or gel filtration. Due to the results shown above



(Figure 4.2), we suspected that the concentration of the tPDE may alter the affinity of the  $\gamma$  fragment for the  $P\alpha\beta$ . Thus, two different concentrations were tested. Figure 4.3

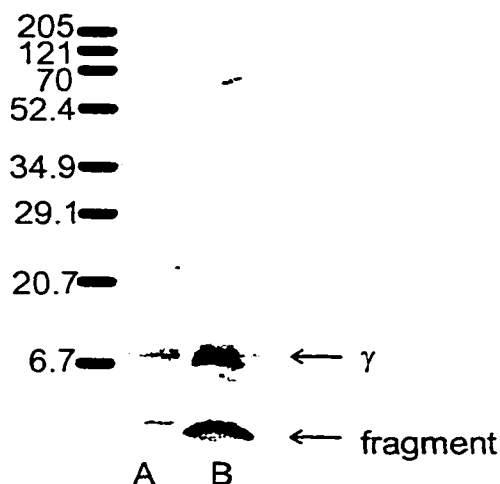


Figure 4.3. Trypsinized PDE binds a fragment of  $\gamma$  even after gel filtration chromatography. Frog ROS homogenates at two different concentrations (concentrated: 100 nM PDE, A; and diluted 2 nM PDE, B) were trypsinized to 60% of their maximum activity. Membranes were removed by centrifugation (3 min,  $110,000 \times g_{av}$ ). The trypsinized PDE-containing supernatants were purified by gel filtration chromatography on Superdex 200. PDE-containing fractions were pooled and concentrated by ultrafiltration (Millipore Biomax 30K MWCO filter). Western analysis was done using the antibody to the C-terminal region of  $\gamma$  (UNH-9710, 1:30,000).

shows that a 4.5 kDa fragment of  $\gamma$  was not completely removed upon gel filtration when the sample was trypsinized at either a high concentration or a low PDE concentration.

Full length  $\gamma$  is observed at ~11 kDa on SDS-PAGE. Figure 4.3 shows a loss of the 11 kDa band and an appearance of a 4.5 kDa proteolytic band that co-elutes with PDE catalytic subunits during gel filtration chromatography. If the  $\gamma$  fragment had dissociated from  $P\alpha\beta$ , then it would have eluted from the Superdex 200 in the included volume for this column (~25 ml), not at an apparent MW of 300,000 kDa. The fragment was also observed bound to tPDE when treated with two consecutive dilutions followed by

ultrafiltration prior to gel filtration (data not shown). This method was used to increase the likelihood that the low MW fragment would separate from  $P\alpha\beta$  and enter the filtrate, while  $P\alpha\beta$  would remain in the retentate. The co-purification of  $P\alpha\beta$  with the 4.5 kDa  $\gamma$  fragment under these conditions suggests that the fragment of the  $\gamma$  subunit remains associated with  $P\alpha\beta$  upon trypsinization, even at low PDE concentrations. Thus, this fragment could be limiting the maximum activity of the trypsinized PDE. Dilution of the sample to sub-nanomolar PDE concentrations may induce dissociation of the 4.5 kDa fragment, thereby further increasing the apparent  $k_{cat}$ .

*Developing alternative methods to prepare  $P\alpha\beta$  lacking  $\gamma$ .* It is possible that the higher catalytic activity of trypsinized PDE compared to transducin activated PDE could arise from a proteolytic artifact resulting from cleaving a portion of  $P\alpha\beta$ . Therefore, we searched for an alternative method to remove the  $\gamma$  subunits from the PDE holoenzyme. Upon transducin activation,  $T\alpha$ -GTP binds to  $\gamma$  and releases some of it from its association with  $P\alpha\beta$  (Yamazaki et al., 1990). Yamazaki et al. (Yamazaki et al., 1996b) found that the release of  $\gamma$  from  $P\alpha\beta$  with  $T\alpha$ -GTP was higher in the presence of salt. Unfortunately, none of the conditions we tested were able to remove all of the  $\gamma$  from  $P\alpha\beta$ . We found that the best method for preparing  $P\alpha\beta$  was to centrifuge nucleotide-depleted frog ROS homogenates after two consecutive one-hour incubations in the presence of either GTP $\gamma$ S or GTP (Table 4.1). To compare the catalytic activity of this  $\gamma$ -depleted  $P\alpha\beta$  to that of trypsinized PDE, we determined the amount of  $\gamma$  remaining on the  $P\alpha\beta$  using a cGMP binding assay (see Methods).  $P\alpha\beta$  lacking  $\gamma$  subunits cannot bind cGMP with high affinity to the noncatalytic cGMP binding sites

**Table 4.1**

**Summary of P $\alpha$  $\beta$  preparations**

Concentration of NaCl	pH	GTP $\gamma$ S	Number of spins	Amount of $\gamma$ remaining (mol $\gamma$ per mol PDE)
200mM NaCl	7.5	GTP $\gamma$ S = 2 $\times$ [rho]	2	0.25
300 mM NaCl	7.5	0	1	0.25
600 mM NaCl	7.5	0	1	0.24
300 mM NaCl	8.5	0	1	0.25
600 mM NaCl	8.5	0	1	0.27
300 mM NaCl	9.5	0	1	0.33
600 mM NaCl	9.5	0	1	0.35
600 mM NaCl	6.5	0	5	0.26
0	7.5	GTP $\gamma$ S = 2 $\times$ [rho]	3	0.16

Table 4.1. Nonenzymatic preparation of P $\alpha$  $\beta$ . ROS homogenates were treated with varying levels of salt, pH and GTP $\gamma$ S to remove the  $\gamma$  subunit of PDE. The  $\gamma$  was removed by centrifugation for 3 min (110,000  $g_{av}$ ). The amount of  $\gamma$  remaining was determined using a cGMP binding assay. Filter binding was done on the P $\alpha$  $\beta$  sample with and without recombinant  $\gamma$  to indirectly estimate the amount of  $\gamma$  bound to the depleted P $\alpha$  $\beta$  samples.

(Arshavsky et al., 1992; Cote et al., 1994). Thus, the amount of cGMP binding to  $\gamma$ -depleted P $\alpha$  $\beta$  represents a 1:1 relationship with the amount of  $\gamma$  remaining bound to P $\alpha$  $\beta$ . By comparing this value with the binding of the same PDE sample supplemented with excess recombinant  $\gamma$ , the amount of endogenous  $\gamma$  still bound to P $\alpha$  $\beta$  can be determined.

We then measured the maximal activity of the P $\alpha$  $\beta$  preparation and extrapolated the value to determine the catalytic rate we would obtain if no  $\gamma$  was bound. By this method, the  $k_{cat}$  for P $\alpha$  $\beta$  was estimated to be  $7000 \pm 180$  cGMP/PDE/sec. The similarity of this result to the  $k_{cat}$  obtained with trypsinized PDE demonstrates that trypsin proteolysis of PDE does not alter significantly the maximum catalytic activity of the P $\alpha$  $\beta$

dimer. Also it supports the hypothesis that transducin-activated PDE only activates PDE to 50%-60% of the maximum possible rate, most likely by activating primarily 1 active site.

The fact that not all of the  $\gamma$  could be removed from the catalytic dimer suggests that not all  $P\alpha\beta$  molecules are behaving identically. PDE heterogeneity is also suggested by the observation that only 60%-70% of the total frog PDE can be released from the disk membrane by hypotonic extraction. In an effort to discover whether the tight association of  $\gamma$  to  $P\alpha\beta$  is related to the tight membrane association of PDE, we hypotonically extracted our  $\gamma$ -depleted  $P\alpha\beta$  sample. We found that there was no direct correlation between membrane association and  $\gamma$  association of PDE. Measurements of the  $P\alpha\beta$  released from the disk membranes by hypotonic extraction showed that the released PDE still contained the same ratio of  $\gamma$  to  $P\alpha\beta$  as was seen prior to extraction (data not shown).

These observations were used as a basis for examining the activation of frog PDE by transducin, focusing specifically on the role of the  $\gamma$  subunit. The results of this detailed investigation are presented in Chapter 3 of this thesis.

*The  $\gamma$  subunit of PDE can be extracted from purified, intact frog ROS for analysis of post-translational modifications.* The tight association between  $P\alpha\beta$  and  $\gamma$  heightens the need for understanding how this interaction is regulated *in vivo*. It has been suggested that phosphorylation of  $\gamma$  plays a role in adaptation of the cell by increasing or decreasing the affinity of  $\gamma$  for either  $P\alpha\beta$  or  $T\alpha$  (Hayashi et al., 1991; Udovichenko et al., 1993; Xu et al., 1998; Tsuboi et al., 1994; Matsuura et al., 2000; Hayashi et al., 2000). To examine the occurrence of post-translational modifications of the  $\gamma$  subunit *in vivo*, we developed a

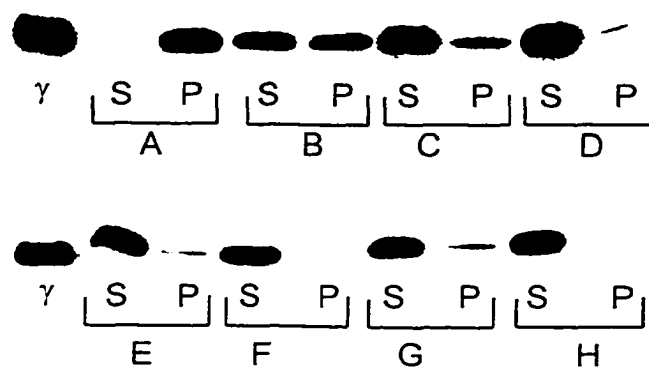


Figure 4.4. Extraction of endogenous  $\gamma$  from frog ROS. Frog ROS homogenates (0.2 nmol of rhodopsin) were treated to remove soluble proteins. The ROS membrane pellets were treated in the following ways: TEM+ (A), TEM+ boiled for 5 min (B), 10% acetonitrile/0.1% TFA (C), 10% acetonitrile/0.1% TFA heated to 75° for 5 min. (D), 20% acetonitrile/0.1% TFA (E), 20% acetonitrile/0.1% TFA heated to 75° for 5 min (F), 30% acetonitrile/0.1% TFA (G), and 30% acetonitrile/0.1% TFA heated to 75° for 5 min (H). The samples were spun in the Airfuge at 30 psi for 5 minutes as soon as possible. Supernatants were collected and the pellets were resuspended in TEM+. The results were analyzed by western analysis using the C-terminal  $\gamma$  antibody.

method for quantitating and partially purifying  $\gamma$  from ROS extracts. Several conditions were tested and it was found that heating the sample for 5 minutes at 75° in 30% acetonitrile/0.1% TFA released all of the  $\gamma$  from ROS homogenates (Figure 4.4). For samples where we wanted to extract  $\gamma$  from intact ROS, we obtained better recovery of endogenous  $\gamma$  if the whole cells were first treated with acetonitrile, then sonicated or disrupted by a freeze-thaw cycle prior to heating to 75°.

After extraction, the  $\gamma$  was purified on a solid reverse phase C-18 Sep Pak cartridge in order to avoid loading large amounts of impurities from frog ROS extracts on an HPLC column (see Methods). This method was first optimized using purified recombinant  $\gamma$ . Figure 4.5 shows the elution profile of the recombinant  $\gamma$  measured by absorbance ( $OD_{277}$ ) as a function of the acetonitrile concentration. Elution of  $\gamma$  from the

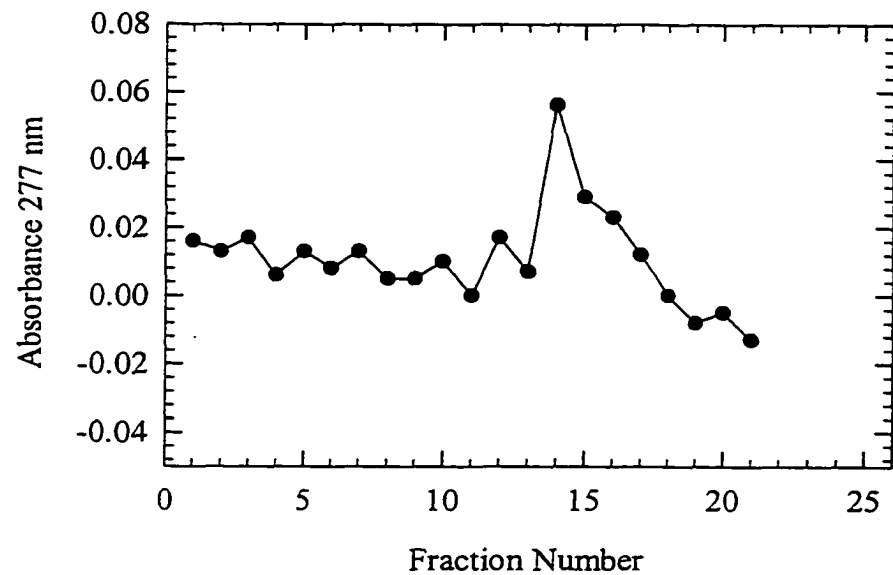


Figure 4.5. Purification of recombinant  $\gamma$  on reverse phase Sep Pak cartridges. 27  $\mu\text{g}$  of recombinant bovine  $\gamma$  was loaded on the Sep Pak cartridge (WAT023501) equilibrated in 10 mM Tris, pH 7.5. The sample was washed with 10 mM Tris. The sample was then eluted with 0.1 ml of each of the following buffers: 10% acetonitrile/0.1% TFA (fractions 1-5), 20% acetonitrile/0.1% TFA (fractions 6-9), 30% acetonitrile/0.1% TFA (fractions 10-13), 40% acetonitrile/0.1% TFA (fractions 14-17), and 50% acetonitrile/0.1% TFA (fractions 18-22). The elution of  $\gamma$  was measured by absorbance ( $\text{OD}_{277}$ ), as well as by the ability of the  $\gamma$  to inhibit trypsinized PDE(not shown).

Sep Pak cartridge occurred at 40% acetonitrile/0.1% TFA. Fraction 14 showing the highest absorbance at 277 nm also had the greatest inhibitory potency for trypsinized PDE. The amount recovered was 67% (18  $\mu\text{g}$ ) of the  $\gamma$  protein loaded on the column (27  $\mu\text{g}$ ).

Once this simple enrichment procedure for  $\gamma$  was developed, ROS samples could be tested under different illumination conditions to examine whether changes in  $\gamma$  phosphorylation serve as a regulatory mechanism of visual transduction. These initial

experiments were the basis for work performed by Michael Paglia in the lab (Paglia et al., 2002).

*Identifying novel PDE binding proteins.* The  $\gamma$  subunit is only one protein that binds to PDE. Other proteins that are known to interact with PDE are transducin, GARP2 and  $\delta$ . However, understanding the role of each of these PDE-binding proteins, and when they each may bind *in vivo* has not been well established. It is also likely that there are some yet unidentified proteins that bind to PDE *in vivo*, possibly contributing to the regulation of visual transduction. We chose to analyze PDE solubilized from ROS membranes using gel filtration chromatography.

Nonactivated PDE from frog ROS was hypotonically extracted from washed ROS membranes. This extracted frog PDE was applied to a Superdex 200 gel filtration chromatography column, and the PDE-containing fractions were identified by a cGMP hydrolysis assay (Figure 4.6A). As seen in panel B of Figure 4.6, the PDE-containing fractions have other protein bands besides  $P\alpha$  and  $P\beta$ . Proteins of lower molecular weight that elute in these fractions must be in a protein complex or form oligomers. Bands of particular interest are those that appear solely in the fractions containing the majority of the PDE activity (fractions 30 and 31). A doublet arises at about 50 kDa which is not seen on the gel prior to fraction 30. Other protein bands that could be important are ~74, 65, 55, and 43 kDa. However, just because they elute at the same molecular weight as PDE does not mean that they are bound to PDE, as they could be in a completely different protein complex, or in association with another protein that

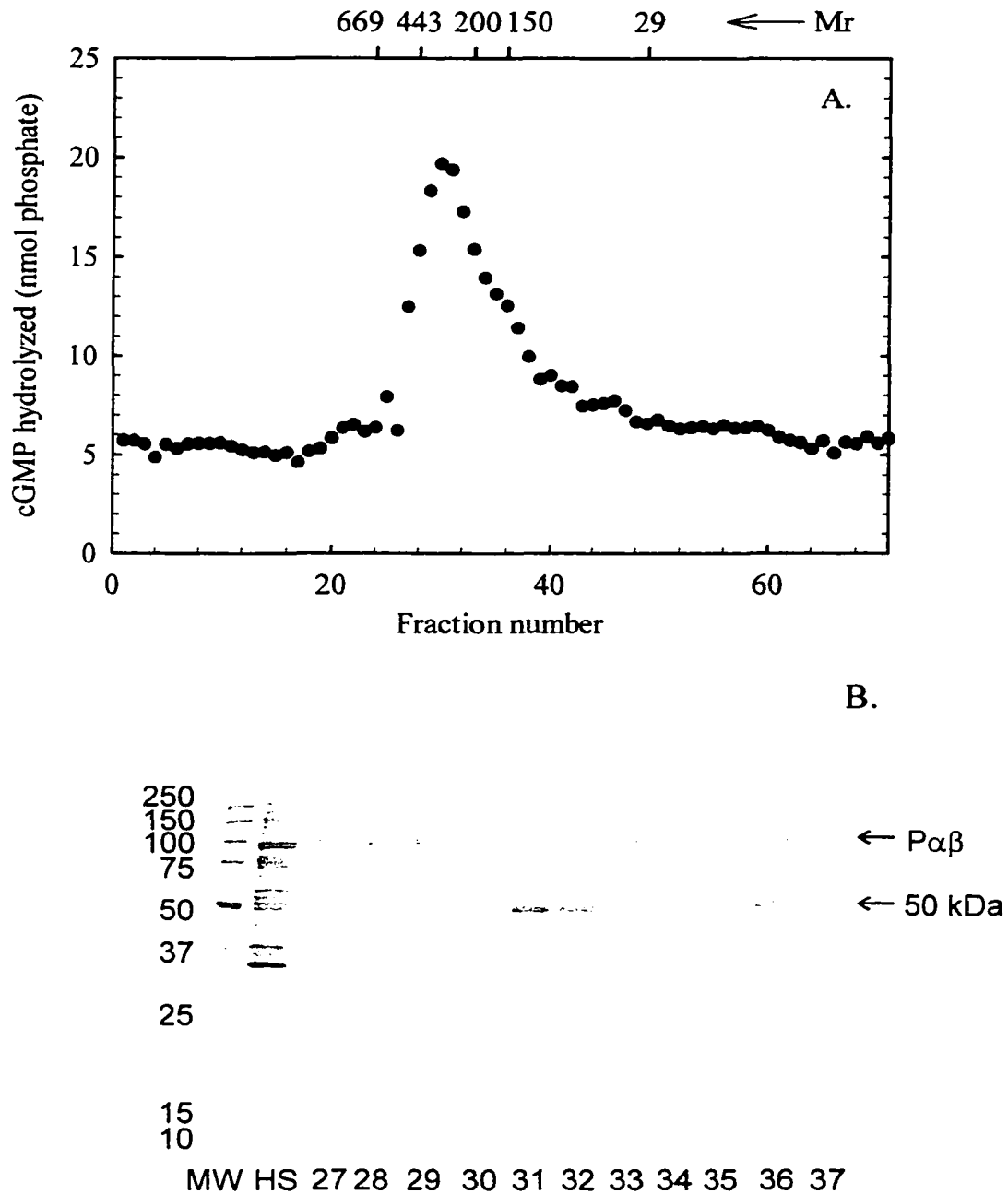


Figure 4.6. Gel filtration of hypotonically extracted proteins from frog ROS membranes. 9 pmol of hypotonically extracted frog PDE was run at 0.5 ml/min on a Superdex 200 gel filtration column. 0.3 ml fractions were collected. A PDE activity assay was done to measure the elution profile of PDE from the column (panel A). The top axis shows the corresponding molecular weight standards. The fractions were TCA precipitated, suspended in gel sample buffer, and then run on a 12% SDS-PAGE gel and stained with Coomassie (panel B). The starting material (HS; 1 pmol PDE) was included on the gel to show the total proteins run over the column.



binds to PDE. Thus, by this method alone, it is difficult to discern what proteins are bound to PDE. However, comparisons of this method with others such as immunoprecipitation of PDE, and western analysis of known ROS proteins would allow for the identification of some of the proteins on the Coomassie-stained gel. Although  $\gamma$  is associated with  $P\alpha\beta$  during gel filtration chromatography, it cannot be detected under these conditions.

These results show preliminary evidence for novel PDE binding proteins. Releasing PDE from its membrane-associated state may retain some of the protein interactions that exist on the disk membrane. One hypothesis is that there is a complex of visual transduction proteins that associate to allow for the rapid response time of visual excitation. A protein complex may also facilitate regulation of visual transduction during bleaching and light adaptation. The PDE signaling complex may mirror the *Drosophila* invertebrate phototransduction system, where a PDZ-containing InaD protein organizes phototransduction components on the rhabdomeric membrane (Tsunoda et al., 1997; Bahner et al., 2000; Tsunoda et al., 2001).

*Several ROS proteins in addition to PDE bind to  $\delta$  in vitro.* Chapter 3 of this thesis presents a detailed study of the  $\delta$  protein in frog ROS. This project evolved from previously published work done with bovine photoreceptor cells (Florio et al., 1996; Cook et al., 2000; Cook et al., 2001) and from our interest in proteins binding to PDE. The hypothesis that  $\delta$  may be involved in membrane binding of numerous proteins in a variety of cells led us to examine the possibility that there are other proteins in ROS that

could be associating with this protein. Many proteins involved in signal transduction use prenylation as a means to reduce signaling pathways to a 2-dimensional process by binding the important proteins to membranes. The putative PDZ and prenyl binding domains of the  $\delta$  protein suggests a scaffolding role for  $\delta$  that brings various proteins closer to one another in the cell. Figure 4.7 examines solubilized proteins from purified frog ROS that can be precipitated by GST- $\delta$  bound to glutathione beads. For each of the

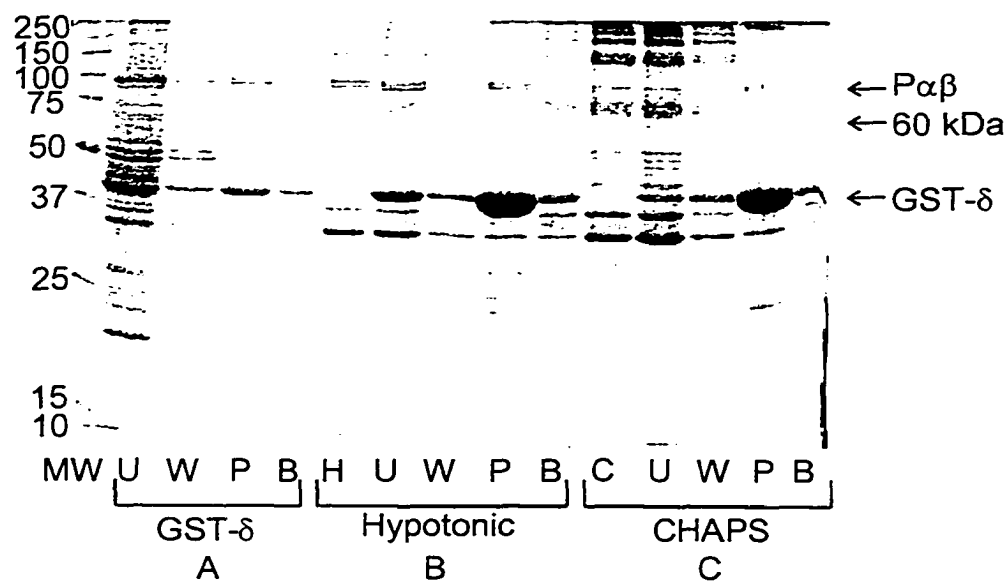


Figure 4.7.  $\delta$  binding proteins from various ROS extracts. A. Frog ROS homogenates (19 pmol PDE) were incubated overnight with recombinant frog GST- $\delta$  (0.4 nmol  $\delta$ ). The sample was centrifuged at 30 psi for 3 min in the Airfuge. GST- $\delta$  released PDE (6 pmol PDE) was incubated with 20  $\mu$ l of glutathione agarose beads for 1 hour at 4°. B. and C. Hypotonically extracted PDE (H, 4 pmol) or CHAPS extracted PDE (C, 5 pmol) were incubated with 20  $\mu$ l of glutathione-agarose beads with 1.5 nmol GST- $\delta$  bound for 1.5 hour at 4°. The samples from all three extractions were centrifuged 5 min at 12,000 rpm to remove unbound proteins in the supernatant (U). The beads were then washed with 50  $\mu$ l of TMN buffer (W). Proteins that bound to the beads were eluted (P) with 10 mM reduced glutathione in 10 mM Tris (pH 8). The glutathione beads were heated in Laemmli sample buffer to 80° to remove any residual proteins that were not released by glutathione treatment (B).

extraction methods, a portion of the PDE exists bound to the GST- $\delta$  beads. A few other bands could be bound to PDE or  $\delta$  in this experiment, such as the band at 60 kDa in the hypotonic and CHAPS extracted samples. In the sample where the ROS membranes were incubated with GST- $\delta$  overnight, two very interesting bands are bound to the beads at  $\sim$  50 and 48 kDa. These are possibly proteins binding directly to  $\delta$  as they are not found in the samples extracted with CHAPS or hypotonic buffer. This experiment has several limitations that control the amount of information we can obtain. One problem consistently observed is the breakdown of the GST from the GST- $\delta$ . Thus any bands on the Coomassie gel that are less than 43 kDa could be from GST- $\delta$  breakdown in the sample, and not ROS proteins bound to the beads. Second, the interaction of GST- $\delta$  with the glutathione beads is not very strong, so a portion of GST- $\delta$  is found in the unbound samples and the remainder is eluted from the beads and found in the precipitated sample on the Coomassie gel. Thus, if there are any proteins running around 43 kDa they would be overshadowed by the GST- $\delta$  that is in the sample.

To overcome these limitations of doing pull-down with glutathione-agarose, we coupled purified bovine  $\delta$  to CNBr-activated Sepharose (See Methods). Figure 4.8 presents  $\delta$  binding proteins found in bovine ROS. For this experiment, three different samples were incubated overnight with  $\delta$ -beads. PDE is found to bind to  $\delta$  as expected. It was verified by western analysis that PDE and  $\gamma$  both exist bound to the  $\delta$ -beads (data not shown). The hypotonically extracted proteins show the highest number of proteins precipitated with the  $\delta$ -beads. Proteins at 50 kDa, 48 kDa, 40 kDa, and 10 kDa are specifically bound to the  $\delta$ -beads. It is important to note that the precipitated proteins

may be directly binding to  $\delta$ , or bound to protein that is itself bound to  $\delta$  (such as PDE). Although CHAPS removed more of the proteins from the membrane, the CHAPS extracted sample shows less proteins precipitating with  $\delta$ , possibly due to disruption of protein-protein interactions by the detergent.

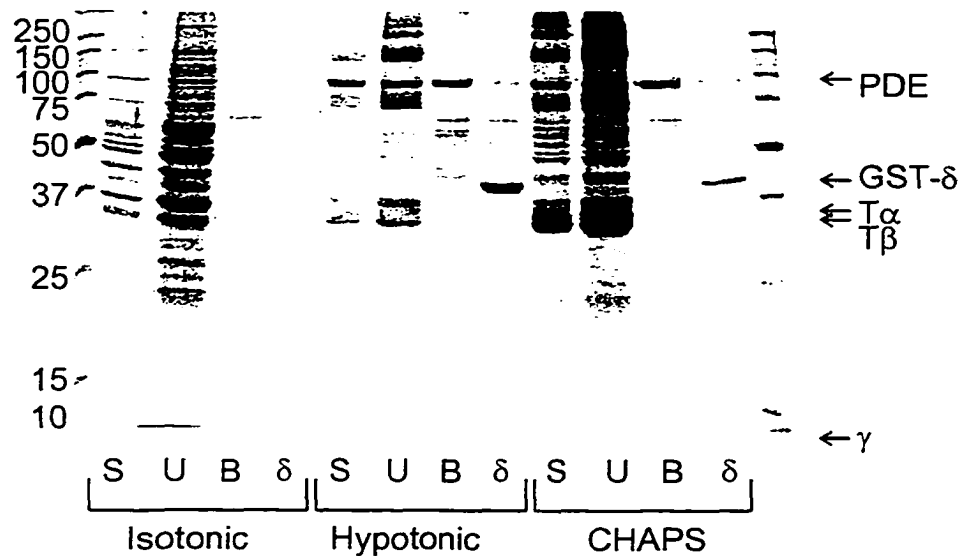


Figure 4.8.  $\delta$  binding proteins in bovine ROS extracts. Isotonic soluble proteins (0.59 pmol PDE), hypotonically extracted proteins (8.25 pmol PDE), and CHAPS extracted proteins (11.3 pmol PDE) were incubated with 30  $\mu$ l of  $\delta$ -beads overnight at 4 $^{\circ}$  in the presence of 0.1% Triton X-100. The unfractionated sample (S) is shown for each condition. Nonspecific binding was estimated by the addition of 0.9 nmol bovine GST- $\delta$  to each sample prior to the incubation ( $\delta$ ). The beads were precipitated by centrifugation (5 min at 12,000 rpm). Unbound proteins were collected (U). The samples were washed 3 times with 50  $\mu$ l of wash buffer (see Methods). Proteins were eluted from the beads by heating to 80 $^{\circ}$  in 2 $\times$  Laemmli sample buffer (B).

An important reason for examining the proteins other than PDE that are co-precipitating with  $\delta$  is the low level of  $\delta$  in ROS compared to that of PDE. Quantitative analysis of the  $\delta$  protein (presented in Chapter 3), shows that there is a large excess of PDE in the outer segment compared to  $\delta$ . This suggests that PDE may not be the major

target of  $\delta$  in the outer segment of the photoreceptor cell. It would be very difficult for  $\delta$  to regulate PDE at such low quantities. The other proteins that are pulled down with the  $\delta$  protein would be more likely to be the candidate for  $\delta$  action *in vivo* as they may exist in similar quantities.

Some of the protein bands stained here could be the same as those observed bound to PDE after gel filtration chromatography (Figure 4.7). Specifically, both the  $\delta$ -precipitation reaction and the gel filtration showed several bands in the 37-50 kDa range on the Coomassie gel.  $T\alpha$  and  $T\beta$  are known to run in this range, and it would not be unexpected to find some  $T\alpha$  bound to PDE, as some  $T\alpha$ -GDP can bind to PDE, though with a lower affinity than  $T\alpha$ -GTP (Gray-Keller et al., 1990; Kutuzov and Pfister, 1994). At the same time the  $T\gamma$  subunit is bound to the photoreceptor cell disk membranes by a farnesyl group similar to  $P\alpha$ . Previously published results suggest that  $T\gamma$  and  $T\beta$  would not be precipitated, as they are not released from the disk membranes with  $\delta$  (Cook et al., 2001).

There is still work that needs to be done to identify the proteins binding to PDE or the  $\delta$  protein *in vivo*. Western analysis of the gel filtration and  $\delta$ -precipitation samples with antibodies to known ROS proteins will give more information about some of the protein bands found on the Coomassie gels. Other proteins can be purified from the SDS-PAGE and sequenced by MS-fingerprinting. These results can be compared to experiments that examine  $\delta$  binding proteins in retinal extracts. There may be a common protein that has yet to be identified that serves as the primary  $\delta$  target in several cell types.

## Conclusions

The results presented in this chapter represent pilot studies for future projects related to rod PDE regulation by novel proteins, as well as preliminary experiments that formed the foundation for the published work presented in Chapters 2 and 3.

The inability to extract all of the PDE from ROS membranes, along with the incomplete removal of  $\gamma$  from PDE by non-enzymatic methods both suggest a heterogeneity in the PDE population in rod outer segments. Heterogeneity with respect to post-translational modification of the  $\gamma$  subunit was one avenue that was partially explored in this chapter in our efforts to develop methods to enrich for  $\gamma$  from complex protein extracts of rod outer segments. It is possible that  $\alpha\alpha$  or  $\beta\beta$  homodimers may exist in addition to the  $\alpha\beta$  catalytic dimer that is assumed to predominate, serving as a sub-population of PDE that with different  $\gamma$ -binding or membrane-binding properties. The observation that the  $k_{cat}$  of activated PDE was not significantly different when catalytic dimers were prepared by trypsin proteolysis of the  $\gamma$  subunit versus extraction of  $\gamma$  by transducin activation and centrifugal fractionation demonstrated that the proteolytic treatment did not create artificially high catalytic rates for cGMP hydrolysis.

The role of the 17 kDa  $\delta$  protein remains unclear. The preliminary work in this chapter provides a new approach to identifying proteins that bind to  $\delta$  in photoreceptor cells. This is an important first step to understand the role  $\delta$  plays to potentially organize proteins that bind to  $\delta$  in photoreceptor cells. The strategy of immobilizing potential PDE binding proteins to identify novel proteins that interact with PDE and its known associated proteins may lead to characterization of a multi-protein signaling complex on the disk membrane where PDE is activated, inactivated and allosterically regulated.

## SUMMARY

The research presented here examined the regulation of rod photoreceptor PDE upon transducin activation. In order to observe the mechanisms of PDE regulation, we first had to characterize the basic properties of transducin activation. We found that transducin activation of frog rod PDE reached half the maximal activation rate of the catalytic dimer ( $P\alpha\beta$ ), prepared by trypsin proteolysis or by a nonenzymatic method of  $\gamma$  extraction. The  $\gamma$  subunit plays an important part in regulating visual excitation by inhibiting PDE activity. The interaction of  $\gamma$  with  $P\alpha\beta$  is correlated with cGMP binding to the noncatalytic sites of  $P\alpha\beta$ , such that when cGMP is bound,  $\gamma$  is more tightly associated. Indeed, we found that the release of cGMP from the noncatalytic cGMP binding sites directly correlates with  $\gamma$  release from  $P\alpha\beta$ .

A result that we continually observed in our studies of PDE regulation was a heterogeneity in protein and ligand binding to PDE. First, upon transducin activation of PDE, there was heterogeneity in the dissociation of cGMP from the noncatalytic binding sites. The effect of transducin activation at the noncatalytic sites could be overcome by the addition of excess  $\gamma$ . However, heterogeneity also existed in the binding of  $\gamma$  to  $P\alpha\beta$ , as two distinct classes of  $\gamma$  binding sites were seen when titrating  $P\alpha\beta$  with  $\gamma$  in the presence of cGMP.

When transducin activation of PDE is prolonged, such as during light adaptation, additional regulatory mechanisms are believed to take place. One protein hypothesized to be involved in PDE regulation during light adaptation is the 17 kDa  $\delta$  protein. We

examined the role of the  $\delta$  protein in regulating frog PDE. Biochemical experiments on the effect of  $\delta$  on frog PDE agreed with previously published results done on mammalian PDE, showing  $\delta$  releasing PDE from the membrane and decreasing the maximal transducin activated rate of PDE. However, quantitative analysis resulted in less than 0.1 mol  $\delta$  per mol PDE in frog and bovine retinas localized to ROS. Consistent with this finding, increased purification of ROS showed a decrease in the amount of  $\delta$  compared to the entire retina. This suggests that  $\delta$  binding to rod PDE may be an artifact resulting from  $\delta$  entering the outer segment during the purification process. Previous immunocytochemical experiments were done with a  $\delta$  antibody that was not shown to identify the 17 kDa  $\delta$  protein on immunoblots. Due to the low levels of  $\delta$  measured in outer segments by immunoblot analysis, we chose to reexamine  $\delta$  localization in the retina by immunocytochemistry. Preliminary evidence observed with the  $\delta$  antibody that we developed resulted in localization of  $\delta$  to several cells in the retina, but not to rod outer segments.

These results suggest that the designation of the  $\delta$  protein as a subunit of PDE was premature. Recently published work on RhoGDI (Nancy et al., 2002) suggests that  $\delta$  may be one of a family of proteins that is involved in the trafficking of prenylated proteins to distinct membranes, due to the sequence similarity of  $\delta$  and RhoGDI. The small amount of  $\delta$  in the rod outer segment suggests that PDE is not the central target for  $\delta$ . Preliminary experiments using immobilized  $\delta$  protein show that several different proteins in the rod outer segment are capable of binding to  $\delta$ , or alternatively, form a



complex with a protein that does bind to  $\delta$ . One hypothesized role for the  $\delta$  protein could be to form a scaffold for a group of interacting proteins.

The highly specialized role of photoreceptor cells presents a unique model system where the majority of the protein and membrane components are involved in the same process. Numerous interactions of the proteins in the rod outer segment are likely to work in concert to regulate visual transduction. Understanding the details of how the visual transduction pathway is regulated will allow us to determine the cause of diseases leading to the loss of vision. Using this information, drugs can be developed to combat vision loss in patients suffering from these diseases, allowing them to maintain a more independent and fulfilling life.

## LIST OF REFERENCES

1. Adams, M.D., et al. (2000). The genome sequence of *Drosophila melanogaster*. *Science* 287, 2185-2195.
2. Anant, J.S., Ong, O.C., Xie, H., Clarke, S., O'Brien, P.J., and Fung, B.K.K. (1992). *In vivo* differential prenylation of retinal cyclic GMP phosphodiesterase catalytic subunits. *J. Biol. Chem.* 267, 687-690.
3. Aravind, L. and Ponting, C.P. (1997). The GAF domain: an evolutionary link between diverse phototransducing proteins. *Trends Biochem. Sci.* 22, 458-459.
4. Arshavsky, V.Y. and Bownds, M.D. (1992). Regulation of deactivation of photoreceptor G protein by its target enzyme and cGMP. *Nature* 357, 416-417.
5. Arshavsky, V.Y., Dumke, C.L., and Bownds, M.D. (1992). Noncatalytic cGMP binding sites of amphibian rod cGMP phosphodiesterase control interaction with its inhibitory  $\gamma$ -subunits. A putative regulatory mechanism of the rod photoresponse. *J. Biol. Chem.* 267, 24501-24507.
6. Arshavsky, V.Y., Lamb, T.D., and Pugh, E.N., Jr. (2002). G proteins and phototransduction. *Annu. Rev. Physiol.* 64, 153-187.
7. Arshavsky, V.Y. and Pugh, E.N., Jr. (1998). Lifetime regulation of G protein-effector complex: Emerging importance of RGS proteins. *Neuron* 20, 11-14.
8. Artemyev, N.O., Arshavsky, V.Y., and Cote, R.H. (1998). Photoreceptor phosphodiesterase: Interaction of inhibitory  $\gamma$  subunit and cyclic GMP with specific binding sites on catalytic subunits. *Methods* 14, 93-104.
9. Artemyev, N.O. and Hamm, H.E. (1992). Two-site high-affinity interaction between inhibitory and catalytic subunits of rod cyclic GMP phosphodiesterase. *Biochem. J.* 283, 273-279.
10. Bahner, M., Sander, P., Paulsen, R., and Huber, A. (2000). The Visual G Protein of Fly Photoreceptors Interacts with the PDZ Domain Assembled INAD Signaling Complex via Direct Binding of Activated Galpha q to Phospholipase Cbeta. *J. Biol. Chem.* 275, 2901-2904.
11. Bennett, N. and Clerc, A. (1989). Activation of cGMP phosphodiesterase in retinal rods: mechanism of interaction with the GTP-binding protein (transducin). *Biochem.* 28, 7418-7424.

12. Bennett,N., Ildfonse,M., Crouzy,S., Chapron,Y., and Clerc,A. (1989). Direct activation of cGMP-dependent channels of retinal rods by the cGMP phosphodiesterase. *Proc. Natl. Acad. Sci. U. S. A.* *86*, 3634-3638.
13. Berger,A.L., Cerione,R.A., and Erickson,J.W. (1999). Delineation of two functionally distinct gammaPDE binding sites on the bovine retinal cGMP phosphodiesterase by a mutant gammaPDE subunit. *Biochemistry* *38*, 1293-1299.
14. Biernbaum,M.S. and Bownds,M.D. (1985). Frog rod outer segments with attached inner segment ellipsoids as an *in vitro* model for photoreceptors on the retina. *J. Gen. Physiol.* *85*, 83-105.
15. Bownds,D., Gordon-Walker,A., Gaide Huguenin,A.C., and Robinson,W. (1971). Characterization and analysis of frog photoreceptor membranes. *J. Gen. Physiol.* *58*, 225-237.
16. Brown,R.L. and Stryer,L. (1989). Expression in bacteria of functional inhibitory subunit of retinal rod cGMP phosphodiesterase. *Proc. Natl. Acad. Sci. U. S. A.* *86*, 4922-4926.
17. Bruckert,F., Catty,P., Deterre,P., and Pfister,C. (1994). Activation of phosphodiesterase by transducin in bovine rod outer segments: Characteristics of the successive binding of two transducins. *Biochem.* *33*, 12625-12634.
18. Burns,F., Rodger,I.W., and Pyne,N.J. (1992). The catalytic subunit of protein kinase A triggers activation of the type V cyclic GMP-specific phosphodiesterase from guinea-pig lung. *Biochem. J.* *283*, 487-491.
19. Burns,M.E. and Baylor,D.A. (2001). Activation, deactivation, and adaptation in vertebrate photoreceptor cells. *Annu. Rev. Neurosci.* *24*, 779-805.
20. Calvert,P.D., Govardovskii,V.I., Arshavsky,V.Y., and Makino,C.L. (2002). Two temporal phases of light adaptation in retinal rods. *J. Gen. Physiol.* *119*, 129-146.
21. Calvert,P.D., Ho,T.W., LeFebvre,Y.M., and Arshavsky,V.Y. (1998). Onset of feedback reactions underlying vertebrate rod photoreceptor light adaptation. *J. Gen. Physiol.* *111*, 39-51.
22. Catty,P. and Deterre,P. (1991). Activation and solubilization of the retinal cGMP-specific phosphodiesterase by limited proteolysis--Role of the C-terminal domain of the  $\beta$ -subunit. *Eur. J. Biochem.* *199*, 263-269.
23. Catty,P., Pfister,C., Bruckert,F., and Deterre,P. (1992). The cGMP phosphodiesterase-transducin complex of retinal rods. Membrane binding and subunits interactions. *J. Biol. Chem.* *267*, 19489-19493.

24. Charbonneau,H., Prusti,R.K., Letrong,H., Sonnenburg, W.K., Mullaney,P.J., Walsh,K.A., and Beavo,J.A. (1990). Identification of a noncatalytic cGMP-binding domain conserved in both the cGMP-stimulated and photoreceptor cyclic nucleotide phosphodiesterase. *Proc. Natl. Acad. Sci. U. S. A.* 87, 288-292.
25. Clerc,A. and Bennett,N. (1992). Activated cGMP phosphodiesterase of retinal rods. A complex with transducin  $\alpha$  subunit. *J. Biol. Chem.* 267, 6620-6627.
26. Clerc,A., Catty,P., and Bennett,N. (1992). Interaction between cGMP-phosphodiesterase and transducin  $\alpha$ -subunit in retinal rods. A cross-linking study. *J. Biol. Chem.* 267, 19948-19953.
27. Cook,T.A., Ghomashchi,F., Gelb,M.H., Florio,S.K., and Beavo,J.A. (2000). Binding of the delta subunit to rod phosphodiesterase catalytic subunits requires methylated, prenylated C-termini of the catalytic subunits. *Biochemistry* 39, 13516-13523.
28. Cook,T.A., Ghomashchi,F., Gelb,M.H., Florio,S.K., and Beavo,J.A. (2001). The  $\delta$  subunit of type 6 phosphodiesterase reduces light-induced cGMP hydrolysis in rod outer segments. *J. Biol. Chem.* 276, 5248-5255.
29. Corbin,J.D., Turko,I.V., Beasley,A., and Francis,S.H. (2000). Phosphorylation of phosphodiesterase-5 by cyclic nucleotide-dependent protein kinase alters its catalytic and allosteric cGMP-binding activities. *Eur. J. Biochem.* 267, 2760-2767.
30. Cote,R.H. (2000). Kinetics and regulation of cGMP binding to noncatalytic binding sites on photoreceptor phosphodiesterase. *Methods Enzymol.* 315, 646-672.
31. Cote,R.H. (2002). Structure, function, and regulation of photoreceptor phosphodiesterase (PDE6). In *Handbook of Cell Signaling*, R.Bradshaw and E.Dennis, eds. (San Diego: Academic Press), p. *in press*.
32. Cote,R.H., Biernbaum,M.S., Nicol,G.D., and Bownds,M.D. (1984). Light-induced decreases in cGMP concentration precede changes in membrane permeability in frog rod photoreceptors. *J. Biol. Chem.* 259, 9635-9641.
33. Cote,R.H., Bownds,M.D., and Arshavsky,V.Y. (1994). cGMP binding sites on photoreceptor phosphodiesterase: Role in feedback regulation of visual transduction. *Proc. Natl. Acad. Sci. U. S. A.* 91, 4845-4849.
34. Cote,R.H. and Brunnock,M.A. (1993). Intracellular cGMP concentration in rod photoreceptors is regulated by binding to high and moderate affinity cGMP binding sites. *J. Biol. Chem.* 268, 17190-17198.

35. D'Amours,M.R. and Cote,R.H. (1999). Regulation of photoreceptor phosphodiesterase catalysis by its noncatalytic cGMP binding sites. *Biochem. J.* *340*, 863-869.
36. D'Amours,M.R., Granovsky,A.E., Artemyev,N.O., and Cote,R.H. (1999). The potency and mechanism of action of E4021, a PDE5-selective inhibitor, on the photoreceptor phosphodiesterase depends on its state of activation. *Mol. Pharmacol.* *55*, 508-514.
37. Deterre,P., Bigay,J., Forquet,F., Robert,M., and Chabre,M. (1988). cGMP phosphodiesterase of retinal rods is regulated by two inhibitory subunits. *Proc. Natl. Acad. Sci. U. S. A.* *85*, 2424-2428.
38. Dumke,C.L., Arshavsky,V.Y., Calvert,P.D., Bownds,M.D., and Pugh,E.N., Jr. (1994). Rod outer segment structure influences the apparent kinetic parameters of cyclic GMP phosphodiesterase. *J. Gen. Physiol.* *103*, 1071-1098.
39. Emeis,D., Kuhn,H., Reichert,J., and Hofmann,K.P. (1982). Complex formation between metarhodopsin II and GTP-binding protein in bovine photoreceptor membranes leads to a shift of the photoproduct equilibrium. *FEBS Lett.* *143*, 29-34.
40. Fain,G.L., Matthews,H.R., Cornwall,M.C., and Koutalos,Y. (2001). Adaptation in vertebrate photoreceptors. *Physiol. Rev.* *81*, 117-151.
41. Fawcett,L., Baxendale,R., Stacey,P., McGrouther,C., Harrow,I., Soderling,S., Hetman,J., Beavo,J.A., and Phillips,S.C. (2000). Molecular cloning and characterization of a distinct human phosphodiesterase gene family: PDE11A. *Proc. Natl. Acad. Sci. U. S. A.* *97*, 3702-3707.
42. Florio,S.K., Prusti,R.K., and Beavo,J.A. (1996). Solubilization of membrane-bound rod phosphodiesterase by the rod phosphodiesterase recombinant  $\delta$  subunit. *J. Biol. Chem.* *271*, 1-12.
43. Fong,D.S. (2000). Age-related macular degeneration: update for primary care. *Am. Fam. Physician* *61*, 3035-3042.
44. Forget,R.S., Martin,J.E., and Cote,R.H. (1993). A centrifugal separation procedure detects moderate affinity cGMP binding sites in membrane-associated proteins and permeabilized cells. *Anal. Biochem.* *215*, 159-161.
45. Fung,B.K.K. and Nash,C. (1983). Characterization of transducin from bovine retinal rod outer segments: Evidence for distinct binding sites and conformational changes revealed by limited proteolysis with trypsin. *J. Biochem.* *258*, 10503-10510.

46. Fung,B.K.K., Young,J.H., Yamane,H.K., and Griswold-Prenner,I. (1990). Subunit stoichiometry of retinal rod cGMP phosphodiesterase. *Biochem.* 29, 2657-2664.
47. Gallagher,S. (1998). Immunoblot detection. In *Current Protocols in Protein Science*, J.E.Coligan, B.M.Dunn, H.L.Ploegh, D.W.Speicher, and P.T.Wingfield, eds. (New York: John Wiley & Sons, Inc.), p. 10.10.1-10.10.12.
48. Gillespie,P.G. and Beavo,J.A. (1988). Characterization of a bovine cone photoreceptor phosphodiesterase purified by cyclic GMP-Sepharose chromatography. *J. Biol. Chem.* 263, 8133-8141.
49. Gillespie,P.G., Prusti,R.K., Apel,E.D., and Beavo,J.A. (1989). A soluble form of bovine rod photoreceptor phosphodiesterase has a novel 15 kDa subunit. *J. Biol. Chem.* 264, 12187-12193.
50. Granovsky,A.E., Muradov,K.G., and Artemyev,N.O. (2000). Inhibition of photoreceptor cGMP phosphodiesterase by its  $\gamma$  subunit. *Methods Enzymol.* 315, 635-646.
51. Granovsky,A.E., Natochin,M., and Artemyev,N.O. (1997). The  $\gamma$  subunit of rod cGMP-phosphodiesterase blocks the enzyme catalytic site. *J. Biol. Chem.* 272, 11686-11689.
52. Gray-Keller,M.P., Biernbaum,M.S., and Bownds,M.D. (1990). Transducin activation in electroporated frog rod outer segments is highly amplified, and a portion equivalent to phosphodiesterase remains membrane-bound. *J. Biol. Chem.* 265, 15323-15332.
53. Gutfreund,H. (1995). *Kinetics for the Life Sciences: Receptors, Transmitters and Catalysts*. Cambridge University Press).
54. Hamm,H.E. and Bownds,M.D. (1986). Protein complement of rod outer segments of frog retina. *Biochem.* 25, 4512-4523.
55. Hayashi,F., Lin,G.Y., Matsumoto,H., and Yamazaki,A. (1991). Phosphatidylinositol-stimulated phosphorylation of an inhibitory subunit of cGMP phosphodiesterase in vertebrate rod photoreceptors. *Proc. Natl. Acad. Sci. U. S. A.* 88, 4333-4337.
56. Hayashi,F., Matsuura,I., Kachi,S., Maeda,T., Yamamoto,M., Fujii,Y., Liu,H., Yamazaki,M., Usukura,J., and Yamazaki,A. (2000). Phosphorylation by cyclin-dependent protein kinase 5 of the regulatory subunit of retinal cGMP phosphodiesterase: II. Its role in the turnoff of phosphodiesterase in vivo. *J. Biol. Chem.* 275, 32958-32965.
57. He,W., Cowan,C.W., and Wensel,T.G. (1998). RGS9, a GTPase accelerator for phototransduction. *Neuron* 20, 95-102.

58. Helmreich, E.J.M. and Hofmann, K.P. (1996). Structure and function of proteins in G-protein-coupled signal transfer. *Biochim. Biophys. Acta* *1286*, 285-322.
59. Higashide, T., Murakami, A., McLaren, M.J., and Inana, G. (1996). Cloning of the cDNA for a novel photoreceptor protein. *J. Biol. Chem.* *271*, 1797-1804.
60. Hoffman, G.R., Nassar, N., and Cerione, R.A. (2000). Structure of the Rho family GTP-binding protein Cdc42 in complex with the multifunctional regulator RhoGDI. *Cell* *100*, 345-356.
61. Hulme, E.C. and Birdsall, N.J.M. (1992). Strategy and tactics in receptor-binding studies. In *Receptor-Ligand Interactions: A Practical Approach*, E.C. Hulme, ed. (Oxford: Oxford University Press), pp. 63-176.
62. Hurley, J.B. and Stryer, L. (1982). Purification and characterization of the gamma regulatory subunit of the cyclic GMP phosphodiesterase from retinal rod outer segments. *J. Biol. Chem.* *257*, 11094-11099.
63. Hurwitz, R.L., Bunt Milam, A.H., Chang, M.L., and Beavo, J. (1985). cGMP phosphodiesterase in rod and cone outer segments of the retina. *J. Biol. Chem.* *260*, 568-573.
64. Hurwitz, R.L., Hanson, R.S., Harrison, S.A., Martins, T.J., Mumby, M.C., and Beavo, J.A. (1984). Immunologic approaches to the study of cyclic nucleotide phosphodiesterases. *Adv. Cyclic Nucleotide Protein Phosphorylation Res.* *16*, 89-106.
65. Körschen, H.G., Beyermann, M., Müller, F., Heck, M., Vantler, M., Koch, K.W., Kellner, R., Wolfrum, U., Bode, C., Hofmann, K.P., and Kaupp, U.B. (1999). Interaction of glutamic-acid-rich proteins with the cGMP signalling pathway in rod photoreceptors. *Nature* *400*, 761-766.
66. Kutuzov, M. and Pfister, C. (1994). Activation of the retinal cGMP-specific phosphodiesterase by the GDP-loaded  $\alpha$ -subunit of transducin. *Eur. J. Biochem.* *220*, 963-971.
67. Laemmli, U.K. (1970). Cleavage of structural proteins during the assembly of the head of bacteriophage T4. *Nature* *227*, 680-685.
68. Li, N. and Baehr, W. (1998). Expression and characterization of human PDE $\delta$  and its *Caenorhabditis elegans* ortholog CE $\delta$ . *FEBS Lett.* *440*, 454-457.
69. Li, N., Florio, S.K., Pettenati, M.J., Rao, P.N., Beavo, J.A., and Baehr, W. (1998). Characterization of human and mouse rod cGMP phosphodiesterase  $\delta$  subunit (PDE6D) and chromosomal localization of the human gene. *Genomics* *49*, 76-82.

70. Linari,M., Hanzal-Bayer,M., and Becker,J. (1999a). The delta subunit of rod specific cyclic GMP phosphodiesterase, PDE  $\delta$ , interacts with the Arf-like protein Arl3 in a GTP specific manner. *FEBS Lett.* 458, 55-59.
71. Linari,M., Ueffing,M., Manson,F., Wright,A., Meitinger,T., and Becker,J. (1999b). The retinitis pigmentosa GTPase regulator, RPGR, interacts with the delta subunit of rod cyclic GMP phosphodiesterase. *Proc. Natl. Acad. Sci. U. S. A.* 96, 1315-1320.
72. Lorenz,B., Migliaccio,C., Lichtner,P., Meyer,C., Strom,T.M., D'Urso,M., Becker,J., Ciccodicola,A., and Meitinger,T. (1998). Cloning and gene structure of the rod cGMP phosphodiesterase delta subunit gene (*PDED*) in man and mouse. *Eur. J. Hum. Genet.* 6, 283-290.
73. Loughney,K., Martins,T.J., Harris,E.A.S., Sadhu,K., Hicks,J.B., Sonnenburg,W.K., Beavo,J.A., and Ferguson,K. (1996). Isolation and characterization of cDNAs corresponding to two human calcium, calmodulin-regulated, 3',5'-cyclic nucleotide phosphodiesterases. *J. Biol. Chem.* 271, 796-806.
74. Maftai, C. G. Solubilization of membrane-associated PDE for studies of its activation during visual transduction. 1-93. 2000. University of New Hampshire, Durham, NH.
75. Maftai, C. G., D'Amours, M. R., Hebert, T. L., and Cote, R. H. Subcellular localization of frog rod photoreceptor phosphodiesterase (PDE) subunits. *Investigative Ophthalmology and Visual Science* 41, S606. 2000.
76. Makino,E.R., Handy,J.W., Li,T.S., and Arshavsky,V.Y. (1999). The GTPase activating factor for transducin in rod photoreceptors is the complex between RGS9 and type 5 G protein  $\beta$  subunit. *Proc. Natl. Acad. Sci. U. S. A.* 96, 1947-1952.
77. Malinski,J.A. and Wensel,T.G. (1992). Membrane stimulation of cGMP phosphodiesterase activation by transducin: Comparison of phospholipid bilayers to rod outer segment membranes. *Biochem.* 31, 9502-9512.
78. Manganiello,V.C. and Degerman,E. (1999). Cyclic nucleotide phosphodiesterases: Diverse regulators of cyclic nucleotide signals and inviting molecular targets for novel therapeutic agents. *Thromb. Haemost.* 82, 407-411.
79. Martins,T.J., Mumby,M.C., and Beavo,J.A. (1982). Purification and characterization of a cyclic GMP-stimulated cyclic nucleotide phosphodiesterase from bovine tissues. *J. Biol. Chem.* 257, 1973-1979.



80. Marzesco,A.M., Galli,T., Louvard,D., and Zahraoui,A. (1998). The rod cGMP phosphodiesterase delta subunit dissociates the small GTPase Rab13 from membranes. *J. Biol. Chem.* 273, 22340-22345.
81. Matsuura,I., Bondarenko,V.A., Maeda,T., Kachi,S., Yamazaki,M., Usukura,J., Hayashi,F., and Yamazaki,A. (2000). Phosphorylation by cyclin-dependent protein kinase 5 of the regulatory subunit of retinal cGMP phosphodiesterase: I. Identification of the kinase and its role in the turnoff of phosphodiesterase in vitro. *J. Biol. Chem.* 275, 32950-32957.
82. McAllister-Lucas,L., Sonnenburg,W.K., Kadlecck,A., Seger,D., Le Trong,H., Colbran,J.L., Thomas,M.K., Walsh,K.A., Francis,S.H., Corbin,J.D., and Beavo,J.A. (1993). The structure of a bovine lung cGMP-binding, cGMP-specific phosphodiesterase deduced from a cDNA clone. *J. Biol. Chem.* 268, 22863-22873.
83. McDowell,J.H. (1993). Preparing rod outer segment membranes, regenerating rhodopsin, and determining rhodopsin concentration. P.A.Hargrave, ed. (San Diego: Academic Press), pp. 123-130.
84. Melia,T.J., Jr., Cowan,C.W., Angleson,J.K., and Wensel,T.G. (1997). A comparison of the efficiency of G protein activation by ligand-free and light-activated forms of rhodopsin. *Biophys. J.* 73, 3182-3191.
85. Melia,T.J., Malinski,J.A., He,F., and Wensel,T.G. (2000). Enhancement of phototransduction protein interactions by lipid surfaces. *J. Biol. Chem.* 275, 3535-3542.
86. Mendez,A., Burns,M.E., Sokal,I., Dizhoor,A.M., Baehr,W., Palczewski,K., Baylor,D.A., and Chen,J. (2001). Role of guanylate cyclase-activating proteins (GCAPs) in setting the flash sensitivity of rod photoreceptors. *Proc. Natl. Acad. Sci. U. S. A.*
87. Mou,H. and Cote,R.H. (2001). The catalytic and GAF domains of the rod cGMP phosphodiesterase (PDE6) heterodimer are regulated by distinct regions of its inhibitory  $\gamma$  subunit. *J. Biol. Chem.* 276, 27527-27534.
88. Mou,H., Grazio,H.J., Cook,T.A., Beavo,J.A., and Cote,R.H. (1999). cGMP binding to noncatalytic sites on mammalian rod photoreceptor phosphodiesterase is regulated by binding of its  $\gamma$  and  $\delta$  subunits. *J. Biol. Chem.* 274, 18813-18820.
89. Nancy,V., Callebaut,I., El Marjou,A., and de Gunzburg,J. (2002). The  $\delta$  subunit of retinal rod cGMP phosphodiesterase regulates the membrane association of Ras and Rap GTPases. *J. Biol. Chem.* *in press*.

90. Natochin, M. and Artemyev, N.O. (1996). An interface of interaction between photoreceptor cGMP phosphodiesterase catalytic subunits and inhibitory gamma subunits. *J. Biol. Chem.* 271, 19964-19969.
91. Norton, A. W. and Cote, R. H. Solubilization of the membrane-associated frog phosphodiesterase (PDE) in vitro by the frog homologue of the bovine 17 kDa delta protein. *Investigative Ophthalmology and Visual Science* 42, S186. 2001.
92. Norton, A.W., D'Amours, M.R., Grazio, H.J., Hebert, T.L., and Cote, R.H. (2000). Mechanism of transducin activation of frog rod photoreceptor phosphodiesterase: allosteric interactions between the inhibitory  $\gamma$  subunit and the noncatalytic cGMP binding sites. *J. Biol. Chem.* 275, 38611-38619.
93. Ong, O.C., Ota, I.M., Clarke, S., and Fung, B.K.K. (1989). The membrane binding domain of rod cGMP phosphodiesterase is posttranslationally modified by methyl esterification at a C-terminal cysteine. *Proc. Natl. Acad. Sci. U. S. A.* 86, 9238-9242.
94. Oppert, B., Cunnick, J.M., Hurt, D., and Takemoto, D.J. (1991). Identification of the retinal cyclic GMP phosphodiesterase inhibitory gamma-subunit interaction sites on the catalytic  $\alpha$ -subunit. *J. Biol. Chem.* 266, 16607-16613.
95. Otto-Bruc, A., Antonny, B., Vuong, T.M., Chardin, P., and Chabre, M. (1993). Interaction between the retinal cyclic GMP phosphodiesterase inhibitor and transducin. Kinetics and affinity studies. *Biochem.* 32, 8636-8645.
96. Pagès, F., Deterre, P., and Pfister, C. (1993). Enhancement by phosphodiesterase subunits of the rate of GTP hydrolysis by transducin in bovine retinal rods. Essential role of the phosphodiesterase catalytic core. *J. Biol. Chem.* 268, 26358-26364.
97. Paglia, M.J., Mou, H., and Cote, R.H. (2002). Regulation of photoreceptor phosphodiesterase (PDE6) by phosphorylation of its inhibitory  $\gamma$  subunit re-evaluated. *J. Biol. Chem.* 277, 5017-5023.
98. Phelan, J.K. and Bok, D. (2000). A brief review of retinitis pigmentosa and the identified retinitis pigmentosa genes. *Mol. Vis.* 6, 116-124.
99. Pugh, E.N., Jr. and Lamb, T.D. (1993). Amplification and kinetics of the activation steps in phototransduction. *Biochim. Biophys. Acta* 1141, 111-149.
100. Pugh, E.N., Jr. and Lamb, T.D. (2000). Phototransduction in vertebrate rods and cones: molecular mechanisms of amplification, recovery and light adaptation. In *Molecular Mechanisms in Visual Transduction*, D.G. Stavenga, W.J. DeGrip, and E.N. Pugh, Jr., eds. (New York: Elsevier Science B.V.), pp. 183-255.

101. Schnetkamp,P.P.M. (1981). Isolation and characterization of osmotically sealed bovine rod outer segments. *Methods Enzymol.* *81*, 110-116.
102. Smith,P.K., Krohn,R.I., Hermanson,G.T., Mallia,A.K., Gartner,F.H., Provenzano,M.D., Fujimoto,E.K., Goeke,N.M., Olson,B.J., and Klenk,D.C. (1985). Measurement of protein using bicinchoninic acid. *Anal. Biochem.* *150*, 76-85.
103. Soderling,S.H. and Beavo,J.A. (2000). Regulation of cAMP and cGMP signaling: new phosphodiesterases and new functions. *Curr. Opin. Cell Biol.* *12*, 174-179.
104. Stryer,L. (1991). Visual excitation and recovery. *J. Biol. Chem.* *266*, 10711-10714.
105. Takemoto,D.J., Gonzalez,K., Udovichenko,I., and Cunnick,J. (1993). Cyclic GMP-regulated cyclic nucleotide phosphodiesterases. *Cell. Signal.* *5*, 549-553.
106. Tsang,S.H., Gouras,P., Yamashita,C.K., Kjeldbye,H., Fisher,J., Farber,D.B., and Goff,S.P. (1996). Retinal degeneration in mice lacking the gamma subunit of the rod cGMP phosphodiesterase. *Science* *272*, 1026-1029.
107. Tsuboi,S., Matsumoto,H., Jackson,K.W., Tsujimoto,K., Williams,T., and Yamazaki,A. (1994). Phosphorylation of an inhibitory subunit of cGMP phosphodiesterase in *Rana catesbiana* rod photoreceptors. I. Characterization of the phosphorylation. *J. Biol. Chem.* *269*, 15016-15023.
108. Tsunoda,S., Sierralta,J., Sun,Y., Bodner,R., Suzuki,E., Becker,A., Socolich,M., and Zuker,C.S. (1997). A multivalent PDZ-domain protein assembles signalling complexes in a G- protein-coupled cascade. *Nature* *388*, 243-249.
109. Tsunoda,S., Sun,Y.M., Suzuki,E., and Zuker,C. (2001). Independent anchoring and assembly mechanisms of INAD signaling complexes in *Drosophila* photoreceptors. *J. Neurosci.* *21*, 150-158.
110. Turko,I.V., Francis,S.H., and Corbin,J.D. (1998). Binding of cGMP to both allosteric sites of cGMP-binding cGMP-specific phosphodiesterase (PDE5) is required for its phosphorylation. *Biochem. J.* *329*, 505-510.
111. Udovichenko,I.P., Cunnick,J., Gonzales,K., and Takemoto,D.J. (1993). Phosphorylation of bovine rod photoreceptor cyclic GMP phosphodiesterase. *Biochem. J.* *295*, 49-55.
112. Udovichenko,I.P., Cunnick,J., Gonzalez,K., and Takemoto,D.J. (1994). Functional effect of phosphorylation of the photoreceptor phosphodiesterase inhibitory subunit by protein kinase C. *J. Biol. Chem.* *269*, 9850-9856.

113. Wang,W.Q., Zhang,Q., Acland,G.M., Mellersh,C., Ostrander,E.A., Ray,K., and Aguirre,G.D. (1999). Molecular characterization and mapping of canine cGMP-phosphodiesterase delta subunit (*PDE6D*). *Gene* 236, 325-332.
114. Wensel,T.G. and Stryer,L. (1986). Reciprocal control of retinal rod cyclic GMP phosphodiesterase by its gamma subunit and transducin. *Prot. Struct. Funct. Genet.* 1, 90-99.
115. Wensel,T.G. and Stryer,L. (1990). Activation mechanism of retinal rod cyclic GMP phosphodiesterase probed by fluorescein-labeled inhibitory subunit. *Biochem.* 29, 2155-2161.
116. Whalen,M.M. and Bitensky,M.W. (1989). Comparison of the phosphodiesterase inhibitory subunit interactions of frog and bovine rod outer segments. *Biochem. J.* 259, 13-19.
117. Whalen,M.M., Bitensky,M.W., and Takemoto,D.J. (1990). The effect of the gamma-subunit of the cyclic GMP phosphodiesterase of bovine and frog (*Rana catesbiana*) retinal rod outer segments on the kinetic parameters of the enzyme. *Biochem. J.* 265, 655-658.
118. Xu,L.X., Tanaka,Y., Bondarenko,V.A., Matsuura,I., Matsumoto,H., Yamazaki,A., and Hayashi,F. (1998). Phosphorylation of the gamma subunit of the retinal photoreceptor cGMP phosphodiesterase by the cAMP-dependent protein kinase and its effect on the gamma subunit interaction with other proteins. *Biochemistry* 37, 6205-6213.
119. Yamamoto,T., Manganiello,V.C., and Vaughan,M. (1983). Purification and characterization of cyclic GMP-stimulated cyclic nucleotide phosphodiesterase from calf liver. *J. Biol. Chem.* 258, 12526-12533.
120. Yamazaki,A., Bartucci,F., Ting,A., and Bitensky,M.W. (1982). Reciprocal effects of an inhibitory factor on catalytic activity and noncatalytic cGMP binding sites of rod phosphodiesterase. *Proc. Natl. Acad. Sci. U. S. A.* 79, 3702-3706.
121. Yamazaki,A., Bondarenko,V.A., Dua,S., Yamazaki,M., Usukura,J., and Hayashi,F. (1996a). Possible stimulation of retinal rod recovery to dark state by cGMP release from a cGMP phosphodiesterase noncatalytic site. *J. Biol. Chem.* 271, 32495-32498.
122. Yamazaki,A., Hayashi,F., Tatsumi,M., Bitensky,M.W., and George,J.S. (1990). Interactions between the subunits of transducin and cyclic GMP phosphodiesterase in *Rana catesbeiana* rod photoreceptors. *J. Biol. Chem.* 265, 11539-11548.

123. Yamazaki,A., Sen,I., Bitensky,M.W., Casnellie,J.E., and Greengard,P. (1980). Cyclic GMP-specific, high affinity, noncatalytic binding sites on light-activated phosphodiesterase. *J. Biol. Chem.* 255, 11619-11624.
124. Yamazaki,A., Stein,P.J., Chernoff,N., and Bitensky,M.W. (1983). Activation mechanism of rod outer segment cyclic GMP phosphodiesterase: release of inhibitor by the GTP/GTP binding protein. *J. Biol. Chem.* 258, 8188-8194.
125. Yamazaki,A., Yamazaki,M., Bondarenko,V.A., and Matsumoto,H. (1996b). Discrimination of two functions of photoreceptor cGMP phosphodiesterase gamma subunit. *Biochem. Biophys. Res. Commun.* 222, 488-493.
126. Yuasa,K., Kotera,J., Fujishige,K., Michibata,H., Sasaki,T., and Omori,K. (2000). Isolation and characterization of two novel phosphodiesterase PDE11A variants showing unique structure and tissue-specific expression. *J. Biol. Chem.* 275, 31469-31479.